POLITECNICO DI TORINO

Collegio di Ingegneria Chimica e dei Materiali

Corso di laurea magistrale in

Ingegneria Chimica e dei Processi Sostenibili

Tesi di Laurea Magistrale

Analysis and improvement of the hydrogen liquefaction process' flexibility

Relatore

Prof.ssa Stefania Specchia

Candidato

Stefano Minellono

Dicembre 2021

Sommario

S1. Introduzione

S1.1. Contesto

Nell'ambito dell'obiettivo di decarbonizzazione fissato per l'Europa dall'European Green Deal per il 2050, l'idrogeno è indicato come uno dei maggiori attori della transizione energetica ed uno degli strumenti principali che possono permettere il raggiungimento di questo obiettivo. L'idrogeno, infatti, può essere utilizzato come mezzo di stoccaggio dell'energia, soprattutto di quella rinnovabile. Quest'ultima forma di energia, infatti, risulta spesso essere di natura intermittente (come, ad esempio, l'energia solare ed eolica), il che si traduce in una produzione di elettricità non costante sul lungo periodo. Un sistema basato esclusivamente sull'utilizzo dell'energia rinnovabile intermittente porterebbe quindi a periodi di mancanza di energia e periodi di surplus di produzione energetica. La possibilità di stoccare questo surplus permetterebbe di sopperire ai periodi di bassa produzione energetica mantenendo una migliore efficienza energetica del sistema. L'idrogeno si configura quindi come una delle soluzioni ai sistemi di stoccaggio tradizionali dell'energia, fungendo da ottimo vettore energetico. L'elettricità prodotta attraverso l'utilizzo di energie rinnovabili può essere sfruttata nel sistema di elettrolisi dell'acqua per la produzione di idrogeno, il quale può essere stoccato sotto diverse forme, tra cui quella gassosa (la più comune) o liquida, della quale si interessa questo lavoro.

S1.2. Interesse dell'idrogeno liquido

Come sottolineato in precedenza, l'aumento dell'interesse e dello sviluppo delle energie rinnovabili si è "scontrato" con la problematica dello stoccaggio energetico. Per quanto riguarda le energie rinnovabili a natura intermittente, la cui produzione energetica risulta essere dipendente da numerosi fattori, quali la posizione geografica, la stagionalità e il meteo stesso, questo risulta particolarmente vero. L'utilizzo dell'idrogeno come vettore energetico può rappresentare una soluzione a questa problematica, grazie alla possibilità di produrlo attraverso l'elettrolisi dell'acqua utilizzando le sopracitate fonti di energia.[10]

Uno dei maggiori problemi legati allo stoccaggio dell'energia attraverso l'idrogeno è rappresentato dalla sua bassa densità, pari a 0.09 kg/m^3, che si traduce di conseguenza anche in una bassa densità energetica, di circa 0.003 kWh/l, nonostante esso sia caratterizzato da una elevata energia specifica (33 kWh/kg) [11]. Se rapportato ad altri combustibili convenzionali, come ad esempio la benzina, la quale possiede una densità energetica di circa 10 kWh/l, è chiara la necessità di trovare metodi che permettano di migliorare questo parametro per quanto riguarda lo stoccaggio di idrogeno, dato che per quanto riguarda il trasporto esso permette di ottenere una diminuzione dei costi grazie a minori volume e minor peso.

L'idrogeno può essere stoccato attraverso diversi metodi, come presentato nella figura S1, con il più comune metodo rappresentato dall'idrogeno compresso. Anche ad alta pressione, purtroppo, la densità energetica rimane comunque limitata (1.3 kWh/l a 700 bar), aggiungendo lo svantaggio legato ai costi di investimenti relativi alla compressione e allo stoccaggio in recipienti che possano sostenere tale pressione. La tecnologia dell'idrogeno liquido permette di aumentare questa densità energetica a circa 2.4 kWh/l, con una domanda energetica che si attesta, per gli impianti industriali, tra 8-15 kWh/kg$_{LH2}$ di elettricità. Questo dato è pari a circa il 24-45% del contenuto energetico dell'idrogeno. Il risultato è però la possibilità di stoccare l'idrogeno in serbatoi a bassa pressione (intorno ai 2 bar), fornendo in questo modo la possibilità di utilizzo di grandi sistemi di stoccaggio a più elevata densità energetica. La principale problematica ad oggi è rappresentata dal costo ancora elevato del processo di liquefazione dell'idrogeno, il quale è previsto di essere abbattuto nei prossimi anni grazie allo sviluppo di nuove tecnologie che permetterebbero di rendere questo sistema di stoccaggio energetico competitivo.

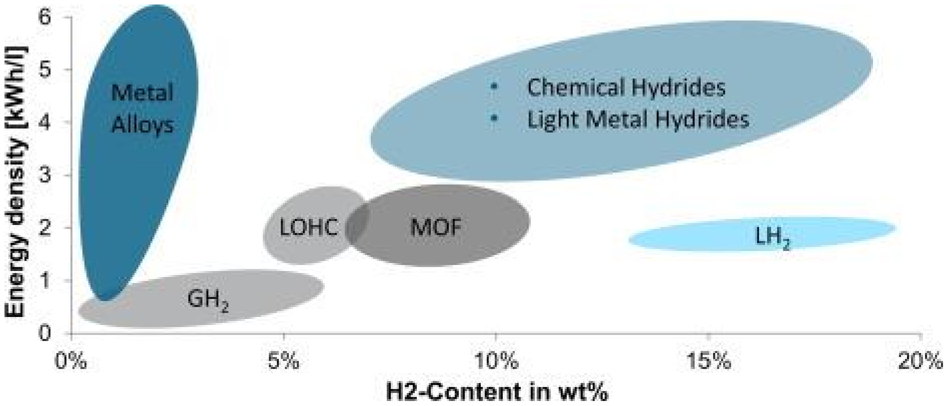

Figura S1. Confronto tra diversi sistemi di stoccaggio dell'idrogeno [11]

S1.2. Principio del processo di liquefazione dell'idrogeno

I processi di liquefazione dell'idrogeno possono essere schematizzati come in figura S2. Essi generalmente includono tre "fasi" principali: la fase di compressione, dove la pressione dei liquidi refrigeranti viene aumentata prima che essi raggiungano le altre due fasi; la fase di preraffreddamento, dove un fluido refrigerante viene utilizzato per raffreddare l'idrogeno gassoso a circa 80K; e la fase di raffreddamento, dove l'idrogeno raggiunge una temperatura di circa 21K, per poi essere espanso in una valvola Joule-Thomson e liquefatto.

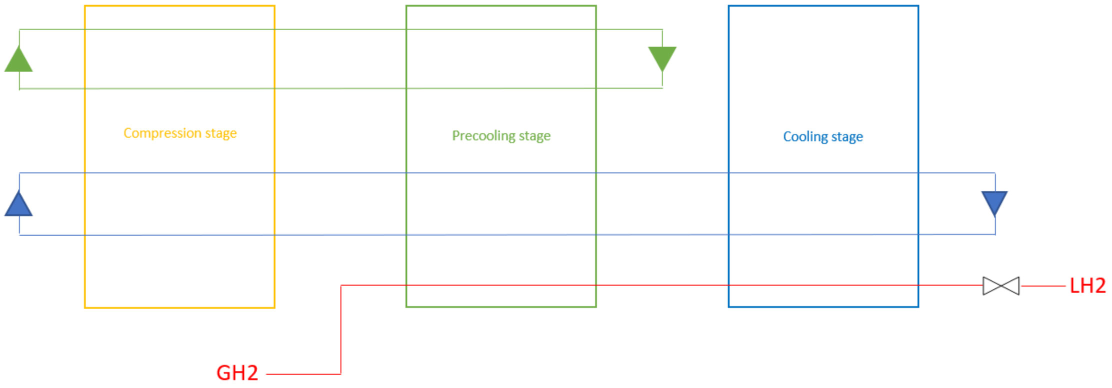

Figura S2. Schema semplificato del processo di liquefazione dell'idrogeno

Diversi sono i tipi di ciclo utilizzabili per quanto riguarda la liquefazione dell'idrogeno. I maggiormente utilizzati nelle applicazioni industriali sono i cicli Brayton e Claude. Maggiori dettagli sui diversi cicli utilizzati industrialmente possono essere trovati nella sezione 3.4 dell'elaborato.

S1.3. Conversione orto-para idrogeno

L'idrogeno esiste in natura sotto due diverse forme isomeriche: orto-idrogeno (o-H_2) e para-idrogeno (p-H_2). La prima presenta una configurazione elettronica avente spin nucleari paralleli, mentre la seconda ha una configurazione elettronica avente spin antiparalleli. Le due configurazioni possono essere osservate nella figura S3.

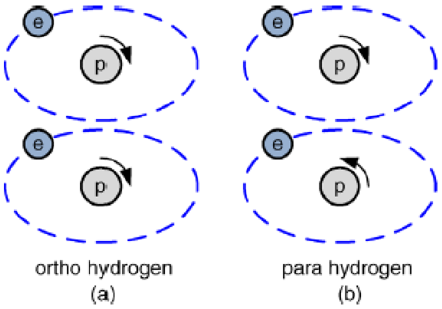

Figura S3. Gli allotropi dell'idrogeno [2]

La composizione di una miscela orto-para in equilibrio è dipendente dalla temperatura, come può essere osservato nella figura S4. A 0K, solo p-H_2 esiste, mentre a temperature più elevate, come ad esempio la temperatura ambiente, la composizione è limitata con un rapporto 3:1 tra orto-idrogeno e para-idrogeno. Questa composizione è generalmente chiamata normal-idrogeno. La conversione dalla forma orto alla forma para è esotermica, ma è generalmente lenta, soprattutto a basse temperature, se non catalizzata correttamente. Non esistono molte differenze tra le due forme da un punto di vista chimico-fisico. Esistono solo leggere differenze tra le temperature di fusione e di ebollizione, le quali hanno una variazione intorno a 0.1-0.2K ad ogni pressione. Le maggiori differenze possono essere osservate nel calore specifico e nelle sue proprietà correlate, come ad esempio la conduttività termica. [1]

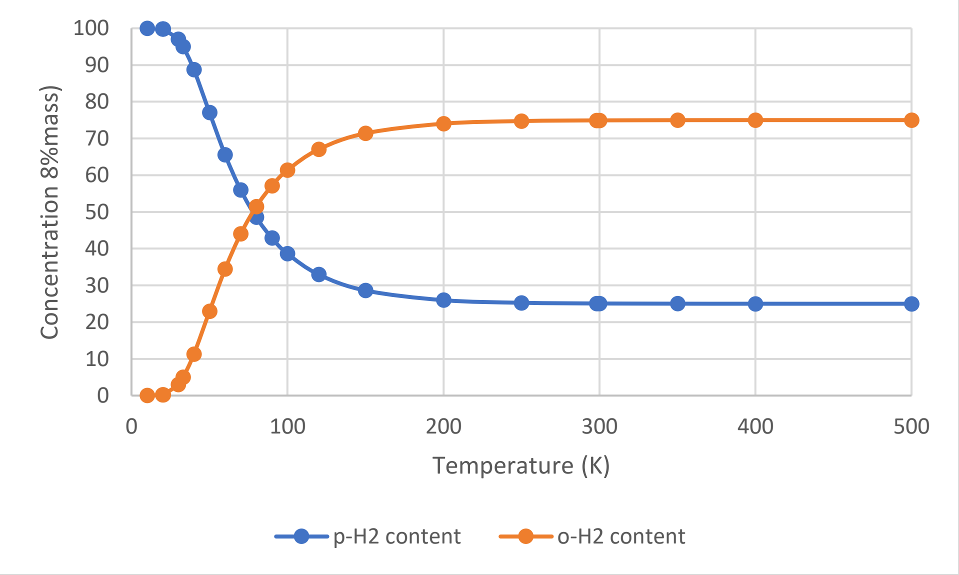

Figura S4. Evoluzione della concentrazione orto-para a diverse temperature [4]

Uno dei maggiori problemi relativi a questa conversione è dovuto al fatto che l'entalpia di conversione della reazione orto-para risulta essere maggiore dell'entalpia di vaporizzazione dell'idrogeno liquido. Ad esempio, a 20K, l'entalpia di conversione risulta essere pari a 520 kJ/kg, mentre l'entalpia di vaporizzazione risulta essere pari a 454 kJ/kg [2]. Per questo motivo, se l'idrogeno liquido è stoccato per lunghi periodi senza che abbia raggiunto la sua concentrazione di equilibrio, l'orto-idrogeno si convertirà in para-idrogeno, producendo un quantitativo non trascurabile di energia che porterà alla vaporizzazione di parte del liquido. È stato stimato che, per una composizione di idrogeno normale stoccata a 20K, la conversione orto-para può causare perdite fino a 18% della massa di idrogeno liquido nelle 24 ore successive alla liquefazione.

Per evitare questa problematica, l'idrogeno è generalmente convertito attraverso l'utilizzo di catalizzatori durante il processo di liquefazione nella sua forma para. Impianti industriali lavorano generalmente con un contenuto di p-idrogeno nel prodotto superiore al 95% [4]. Questa reazione è generalmente effettuata negli scambiatori di calore stessi, i quali risultano essere riempiti con materiali catalitico. $Fe(OH)_3$ e Fe_2O_3 sono i catalizzatori maggiormente usati nel processo.

S1.4. Produzione dell'idrogeno

Oggigiorno l'idrogeno può essere prodotto attraverso diversi processi. In questo momento la maggior parte dell'idrogeno (circa il 96%) viene prodotto a partire da risorse di tipo fossile, le quali partecipano ad un processo conosciuto come steam reforming. Esso permette la trasformazione del gas naturale (e altri componenti più pesanti, come ad esempio la nafta) in idrogeno [5],[6]. La restante parte della produzione di idrogeno deriva dall'elettrolisi dell'acqua, come mostrato nella seguente figura S5. Sebbene questo metodo di produzione occupi solo una minima parte della produzione totale di idrogeno, l'interesse nei suoi confronti è cresciuto negli ultimi anni grazie al possibile impatto ambientale positivo che esso potrebbe avere nell'industria dell'idrogeno [7].

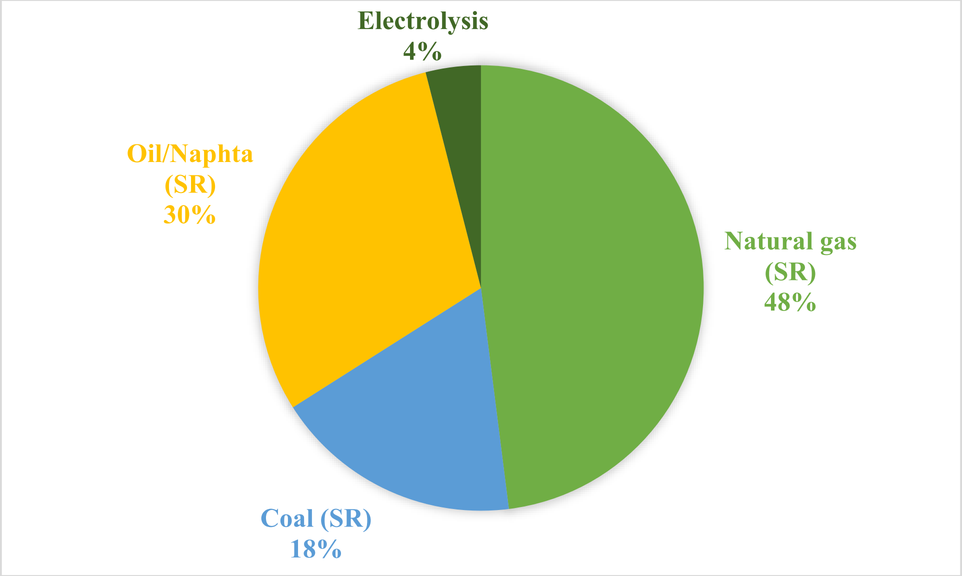

Figura S5. Ripartizione della produzione di idrogeno [5]

Questo interesse è supportato da numerose pubblicazioni che evidenziano il ruolo dell'idrogeno come vettore di energia rinnovabile nelle applicazioni PtG (Power to Gas) [8]. L'idrogeno avrà un impatto vantaggioso nello sviluppo di queste tecnologie grazie alle differenti possibilità di utilizzo che esso offre, come conversione in elettricità nelle pile a combustibile e un più semplice trasporto come carburante [9].

S1.5. Problematica della "flessibilità di processo"

Oltre alla problematica legata allo stoccaggio delle energie rinnovabili, queste ultime sono soggette anche ad una difficoltà di penetrazione all'interno dei processi chimici. Questo è dovuto al fatto che generalmente i processi di tipo fisico-chimico sono progettati e funzionano in maniera continua in stato stazionario, con una richiesta costante di energia [23]. Queste operazioni potrebbero essere incompatibili con la natura intermittente di alcune energie rinnovabili. Per questo motivo, negli ultimi anni, è cresciuto l'interesse riguardante l'analisi e lo studio della cosiddetta “flessibilità di processo”, ovvero lo studio di soluzioni tecniche che permettano di rendere un processo “adattabile” a diverse condizioni di processo senza che la qualità del prodotto sia compromessa e mantenendo i costi di progetto e produzione accettabili. In letteratura esistono due tipi di analisi: la prima si concentra nella definizione dei range di operabilità di un processo esistente, mentre la seconda ha come obiettivo il design di un processo “flessibile” ipotizzando possibili variazioni in alcuni parametri chiave.

Per quanto riguarda lo studio della flessibilità del processo di liquefazione dell’idrogeno verde, il secondo approccio è stato utilizzato in questo lavoro. In questo caso la variabilità dei parametri è soprattutto dovuta alla quantità di idrogeno in entrata al processo, legato alla sua produzione sulla base dell’utilizzo delle energie rinnovabili nel processo di elettrolisi dell’acqua. Questo ovviamente non accade nel caso in cui l’idrogeno utilizzato nella liquefazione provenga dal processo di steam reforming, dove la produzione risulta costante. Una soluzione tipica con l’obiettivo di limitare le variazioni di feed all’entrata di processo è l’installazione di u sistema di stoccaggio esterno dell’idrogeno gassoso. Nei periodi di surplus di produzione, questo viene compresso e stoccato, mentre nei periodi di sottoproduzione si ha l’utilizzo di questo idrogeno stoccato. Questa soluzione è stata adottata anche da altri processi di produzione in cui l’idrogeno risulta essere una delle materie prime, come ad esempio la produzione di ammoniaca e metanolo [23],[24],[28],[29]. Sebbene questa risulti essere un’interessante possibilità, un lavoro interno svolto da Engie ha evidenziato come i costi associati all’installazione di un tale sistema, capace di “assorbire” tutte le variazioni durante l’anno, abbia dei costi non compatibili con gli obiettivi aziendali [30].

Risulta quindi necessario studiare diversi metodi che possano migliorare la flessibilità del processo a permettere di mitigare l’impatto delle suddette variazioni sull’operabilità del processo.

S.2. Obiettivo

L’obiettivo del presente elaborato è quello di determinare l’impatto energetico ed economico dell’utilizzo di idrogeno proveniente da fonti intermittenti nel processo di produzione dell’idrogeno liquido. Risulta quindi necessario prima di tutto determinare la possibilità tecnica di liquefare un’alimentazione non costante nel tempo. Per far ciò, uno studio delle principali unità utilizzate nel processo di liquefazione, in particolare compressori e scambiatori di calore, deve essere effettuato. La possibilità di operare il processo in condizioni che si discostano da quelle previste dal design iniziale, con l’obiettivo di gestire eventuali variazioni nel processo, è stata investigata.

L’obiettivo di questo lavoro è quindi quello di definire i range di operabilità del processo, attraverso lo studio della letteratura scientifica e le simulazioni del processo in questione, e di definire l’impatto economico ed energetico delle suddette variazioni sul processo considerato. In aggiunta a questo, possibili soluzioni che permettano di migliorare la flessibilità di processo saranno proposte ed investigate, con l’obiettivo di determinare un processo che permetta di meglio gestire la liquefazione dell’idrogeno verde senza subire degli incrementi inaccettabili dei vari costi legati alla produzione dell’idrogeno liquido.

S.3. Metodologia di studio

L'analisi della problematica è stata affrontata sia attraverso uno studio bibliografico sia utilizzando un programma di simulazione di processo, ovvero Aspen Hysys versione 8.6. Sia la modalità stazionaria che la modalità dinamica sono state sfruttate per poter analizzare l'impatto delle variazioni di portata di idrogeno gassoso in entrata al processo.

Per quanto riguarda il ciclo di liquefazione considerato nelle analisi e nelle simulazioni, quello sviluppato da Linde nel suo stabilimento in Leuna, Germania, è stato utilizzato. Il PFD del processo può essere osservato nella sezione 6.1 dell'elaborato. Questo processo prevede principalmente tre operazioni principali: la compressione, il preraffreddamento e il raffreddamento e liquefazione. Il feed di idrogeno gassoso entra nel processo a circa 290K e 21 bar. Passa attraverso otto scambiatori di calore e viene raffreddato a 21K, dopodiché l'espansione attraverso una valvola di Joule-Thomson a circa 1.5 bar permette di ottenere l'idrogeno liquido. Nei primi due scambiatori viene effettuato il preraffreddamento, che porta l'idrogeno gassoso a circa 80K grazie all'utilizzo di azoto liquido fornito da un ciclo aperto, mentre il raffreddamento viene effettuato utilizzando come refrigerante un'altra corrente di idrogeno, la quale si trova in ciclo chiuso e viene compressa fino a circa 30 bar nella fase di compressione. L'idrogeno refrigerante passa anch'esso negli scambiatori di calore dove viene raffreddato, subisce un'espansione isentropica in tre turbine che permettono di recuperare una parte di energia, che può essere utilizzata per alimentare parzialmente i compressori, ed è anch'esso espanso in una valvola J-T che permette la sua liquefazione e la sua utilizzazione come refrigerante nel ciclo.

S3.1. Definizione del compressore in condizioni di off-design

Il compressore rappresenta una delle più importanti unità di processo della liquefazione dell'idrogeno e il suo funzionamento è critico per l'operabilità dell'impianto. Inoltre, esso rappresenta l'unità più costosa sia in termini di OPEX che in termini di CAPEX, come può essere osservato dalla figura S6. Esso rappresenta il 75% dell'investimento totale del processo di liquefazione; quindi, il suo studio diventa cruciale per limitare un drammatico aumento dei costi del processo.

Nell'ambito di questo studio, i compressori sono stati studiati nel loro funzionamento in condizioni di off-design. A differenza di altre unità, queste condizioni hanno un impatto fortemente negativo sulla loro efficienza e sul loro funzionamento. Infatti, l'efficienza diminuisce in maniera significativa allontanandosi dalle condizioni di design, risultando in un aumento importante dei costi, ed inoltre queste condizioni possono avere un impatto negativo sulle parti meccaniche dell'unità favorendo fenomeni negativi come la fatica, riducendo di fatto la vita del compressore [39].

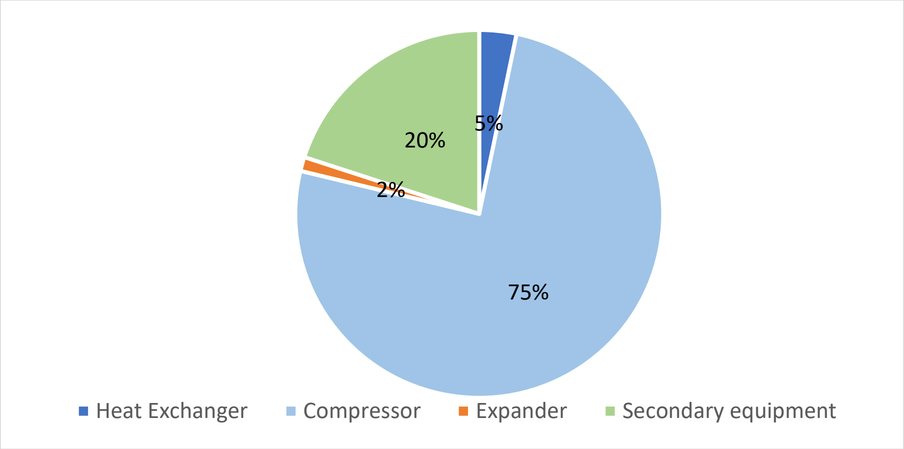

Figura S6. Ripartizione del CAPEX del processo Linde Leuna

Uno studio della letteratura ha permesso di investigare l'utilizzo di tecnologie di compressione differenti che meglio si adatterebbero a sistemi in cui esistono variazioni significative di portata. Un esempio è rappresentato dall'utilizzo di compressori a velocità variabile, i quali vengono evidenziati come una delle maggiori soluzioni per migliorare la flessibilità del processo di liquefazione [40], [41]. Sulla base di questi studi, le performance di questi tipi di compressori a diverse portate sono state investigate [42], [43]. Questo ha permesso di ottenere una correlazione tra l'efficienza del compressore a vite dotato di tecnologia a velocità variabile, utilizzata successivamente nelle simulazioni, e la frazione di portata in entrata rispetto alla portata di design del compressore. La correlazione ottenuta è mostrata nella seguente figura.

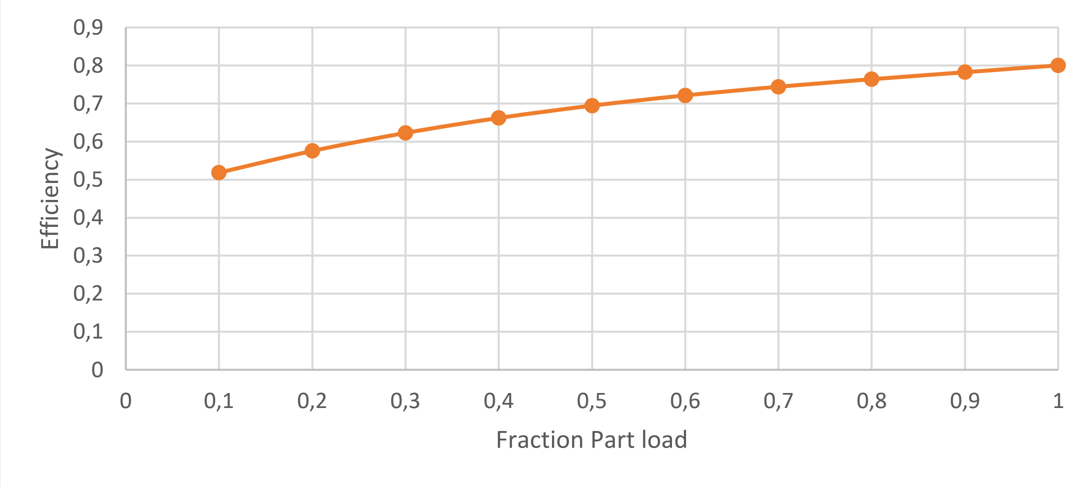

Figura S7. Efficienza del compressore con tecnologia a velocità variabile (correlazione da [43])

S3.2. Studio comportamento scambiatori di calore

In parallelo allo studio dei compressori, anche l'analisi degli scambiatori di calore è stata necessaria per poter simulare correttamente il processo nella sua interezza. Gli scambiatori di calori utilizzati nel processo di liquefazione dell'idrogeno sono generalmente degli scambiatori multi-stream in serie. In questo caso, la letteratura scientifica riguardante il loro funzionamento off-design è quasi inesistente. Per questo motivo i risultati sono stati ottenuti effettuando delle simulazioni affiancando ad Aspen Hysys il programma Aspen Exchanger Design & Rating, il quale permette di dimensionare e simulare rigorosamente gli scambiatori di calore. L'obiettivo di questa analisi è stato quello di ottenere delle relazioni tra la variazione della portata dell'idrogeno in entrata al processo e la variazione delle portate delle correnti di refrigerante (azoto e idrogeno) affinché il processo risulti operante in condizioni accettabili. Il parametro scelto per questa valutazione è stato la temperatura minima di approccio negli scambiatori, parametro che viene usato internamente per determinarne il funzionamento e l'efficienza. Il processo è quindi stato simulato facendo variare le diverse portate con l'obiettivo di mantenere il parametro in esame tra 2 e 4K, valore ritenuto accettabile a seguito di studi condotti internamente.

Le relazioni tra le variazioni di portata che permettono di mantenere il valore nel range accettabile sono mostrate nella seguente figura S8.

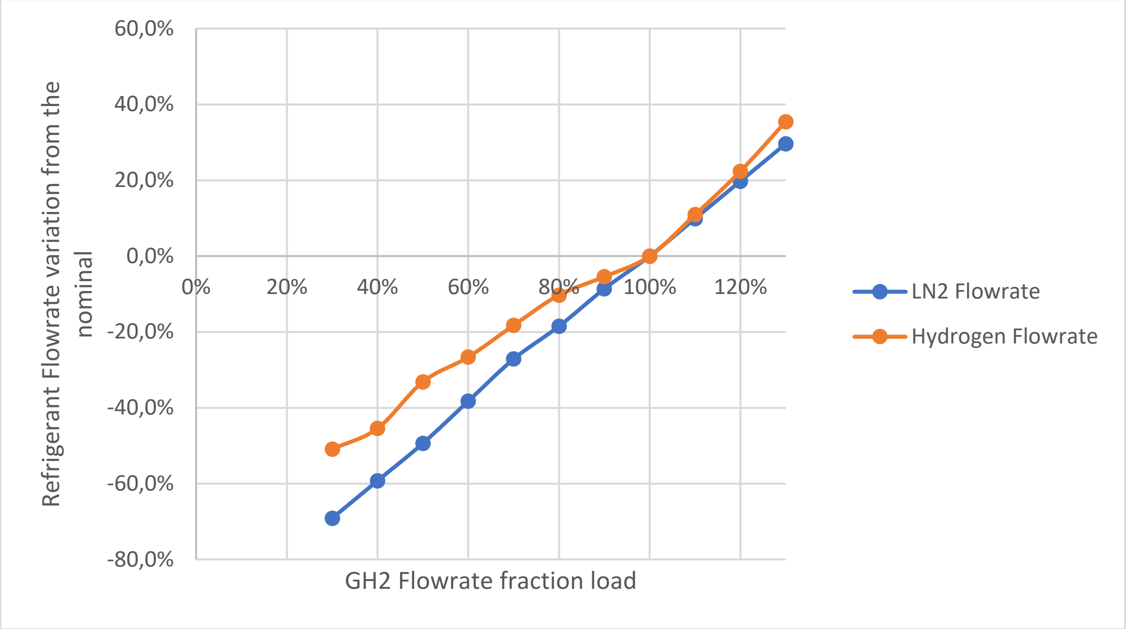

Figura S8. Variazione delle portate di refrigerante in relazione alla variazione dell'idrogeno di alimentazione

È possibile notare come la variazione dei due stream non abbia la stessa evoluzione. In particolare, la diminuzione della portata a condizioni di carico parziale è più importante per l'azoto che per l'idrogeno nel ciclo. La stessa cosa però non è vera nel caso di condizioni sovra-nominali, dove l'incremento relativo dei due refrigeranti è abbastanza similare. La diversa evoluzione ha un impatto sui consumi energetici, ovvero la SEC del processo (Specific Energy Consumption), in particolare a causa del maggiore consumo relativo del compressore.

Il valore della temperatura minima di approccio è stato valutato a diverse condizioni di carico, sia nel caso in cui siano state utilizzate le relazioni di cui sopra, sia nel caso in cui le portate dei due stream di refrigerante siano state mantenute costanti. I risultati possono essere osservati nelle figure S9 e S10.

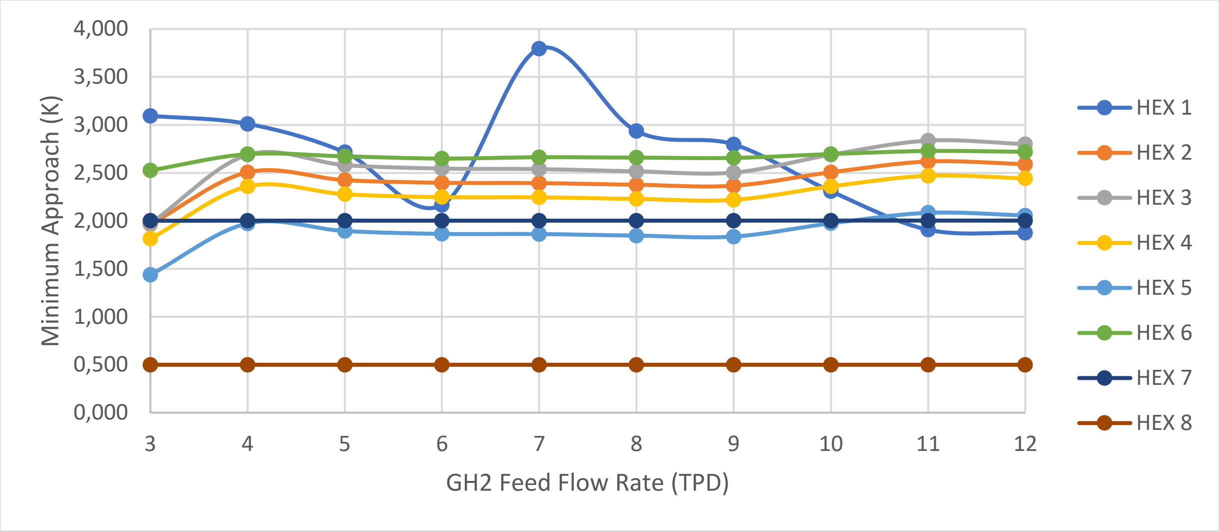

Figura S9. Evoluzione della minima temperatura di approccio considerando la variazione delle portate di refrigerante

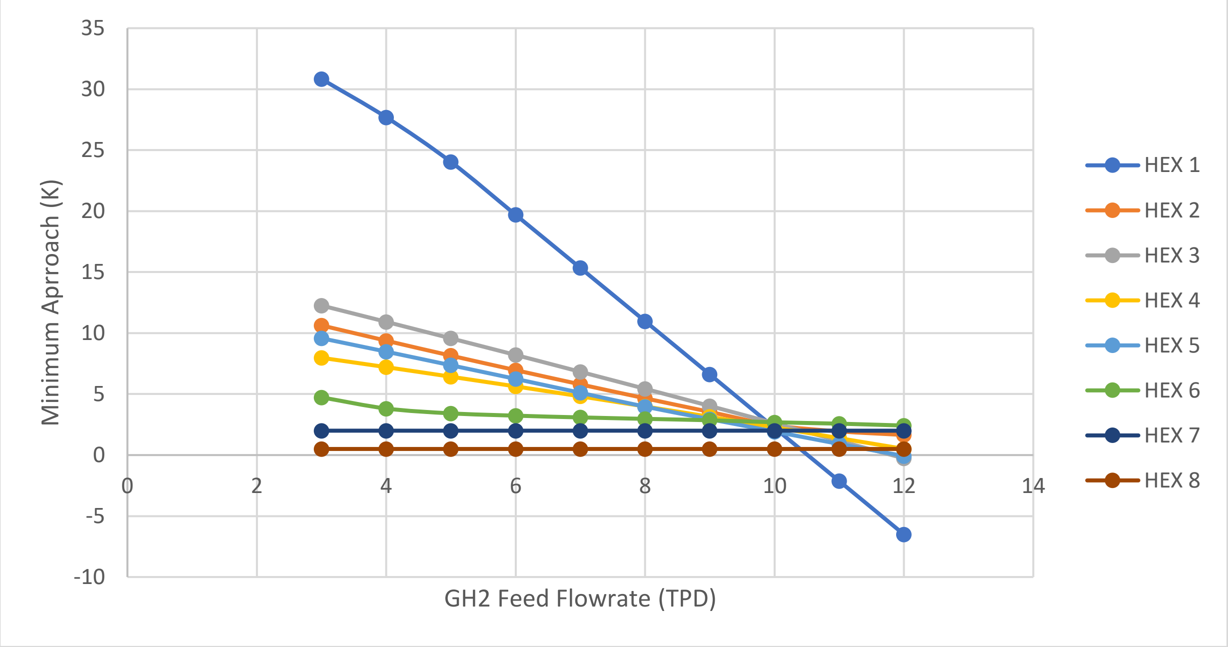

Figura S10. Evoluzione della minima temperatura di approccio senza considerare la variazione delle portate di refrigerante

È possibile notare come l'applicazione delle relazioni, e quindi la variazione delle portate degli stream refrigeranti permetta di mantenere la temperatura di approccio nel range considerato accettabile. Se essi non vengono variati e invece mantenuti costanti, i valori del parametro escono da questi range, rendendo inefficienti gli scambiatori di calore installati.

S.4. Principali risultati

I diversi scenari simulati sono stati comparati tra di loro tenendo conto di due parametri principali, la SEC (Specific Energy Consumption, misurata in kWh/kg_{H2}) e la SLC (Specific Liquefaction Cost, misurata in €/kg_{H2}), rispettivamente il parametro caratterizzante l'efficienza energetica del sistema e il parametro rappresentante l'impatto economico. I risultati sono presentati come ΔSEC e ΔSLC rispetto al caso base, rappresentato dal ciclo Linde Leuna con una capacità di produzione pari a 10 TPD (tonnellate al giorno) di idrogeno liquido.

Due principali casi sono stati analizzati e simulati: il primo è caratterizzato da un profilo di produzione costante nel tempo, con l'obiettivo di determinare l'impatto energetico del processo operante alle condizioni di off-design; il secondo invece vede l'applicazione dei risultati ottenuti ad un profilo annuale variabile di produzione di idrogeno fornito da Engie, la cui produzione media e di circa 10 TPD.

S4.1. Profilo costante

In questo caso si è considerato che l'impianto lavori a condizioni non nominali per lunghi periodi. L'obiettivo di questa parte è quello di determinare l'impatto sui consumi energetico del processo di questo tipo di condizioni. In particolare, le due condizioni di sottoproduzione e sovraproduzione rispetto al nominale sono state analizzate separatamente.

Per quanto riguarda la situazione di sottoproduzione, in questo caso si è deciso di considerare l'utilizzo di una linea di compressione avente una tecnologia a velocità variabile. In questo caso l'efficienza adiabatica dei compressori al variare della portata è stata definita attraverso la correlazione mostrata nella sezione precedente. Sulla base della letteratura e di studi interni, un limite inferiore di portata è stato definito, pari a 50% della portata nominale del compressore. La variazione della SEC è stata analizzata come può essere osservato in figura S11.

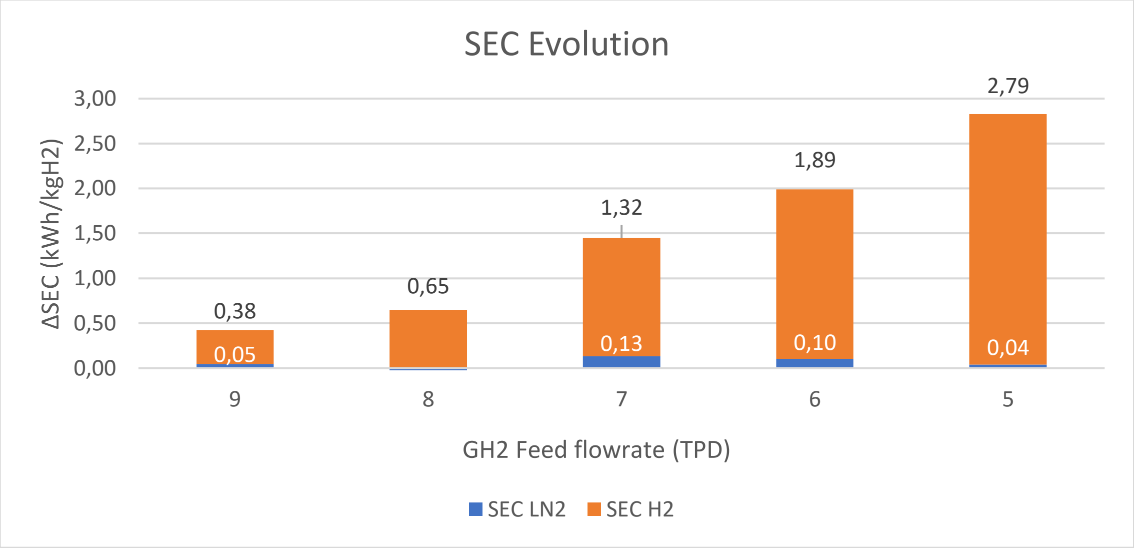

Figura S11. Evoluzione della SEC in condizioni di sottoproduzione

Il suo incremento è dovuto quasi esclusivamente alla variazione del consumo energetico dovuto all'idrogeno refrigerante. Questo è dovuto principalmente a due ragioni: il primo è che l'azoto è fornito al sistema attraverso un ciclo aperto, per cui la variazione della sua portata non influenza direttamente le performance dei compressori; la seconda ragione è dovuta al fatto che la portata di azoto necessaria al sistema decresce in maniera più importante rispetto alla portata di idrogeno, la quale quindi risulta avere un impatto ancora più importante nella fase di compressione.

Per quando riguarda la situazione di sovraproduzione, in questo caso due sono le possibilità che si possono adottare per gestire le variazioni. La prima possibilità è quella di utilizzare un sistema con compressori a velocità variabile, come nella situazione di sottoproduzione. In questo caso, però, il sistema risulta essere limitato ad un aumento del 20% della portata rispetto al nominale. La seconda soluzione risulta essere l'installazione di linee parallele di compressione che siano capaci di gestire la sovraproduzione. L'impatto delle due soluzioni, energeticamente ed economicamente, è stato analizzato e può essere osservato nella tabella S1.

Produzione (TPD)	**ΔSEC (kWh/kg_{H2})**	**ΔCAPEX (k€)**	**SLC (€/kg_{H2})**
11 (Un compressore)	0.98	0	-0.10
12 (Un compressore)	1.42	0	-0.21
11 (Due compressori)	0.05	5955	0.34
12 (Due compressori)	0.13	8668	0.35

Tabella S1. Evoluzione della SEC e della SLC in condizioni di sovraproduzione

È possibile osservare come l'utilizzo di un singolo compressore risulti in un incremento maggiore dal punto di vista energetico rispetto all'utilizzo di due compressori. Questo però va in contrasto con l'aumento della SLC dovuta all'installazione della seconda linea di compressione, la quale ha un impatto a livello di CAPEX molto importante.

S4.2. Re-liquefazione dell'idrogeno liquido

Una soluzione di miglioramento della flessibilità di processo è stata analizzata e simulata. Questa soluzione consiste nel re-liquefare parte dell'idrogeno liquido già prodotto e inviarlo nuovamente al processo di liquefazione nei periodi di sottoproduzioni di idrogeno gassoso. Questo permetterebbe al processo di operare sempre al suo valore nominale senza, di conseguenza, incorrere in inefficienze del sistema. Ovviamente questo processo ha un costo dal punto di vista energetico, in quanto una parte dell'idrogeno viene re-liquefatto. Parte di questa spesa energetica può essere attutita dall'utilizzo delle frigorie dovute all'evaporazione dell'idrogeno per produrre, ad esempio, azoto liquido, il quale può essere riutilizzato in seguito nel processo di liquefazione. È stato stimato che l'evaporazione di una tonnellata di azoto liquido può produrre fino a circa 6.8 tonnellate di azoto liquido. Questo permette di diminuire l'aumento della SEC dell'intero processo quando questa soluzione viene implementata.

I risultati riguardanti l'implementazione di questa tecnologia sono di seguito riportati nella figura S12 e S13.

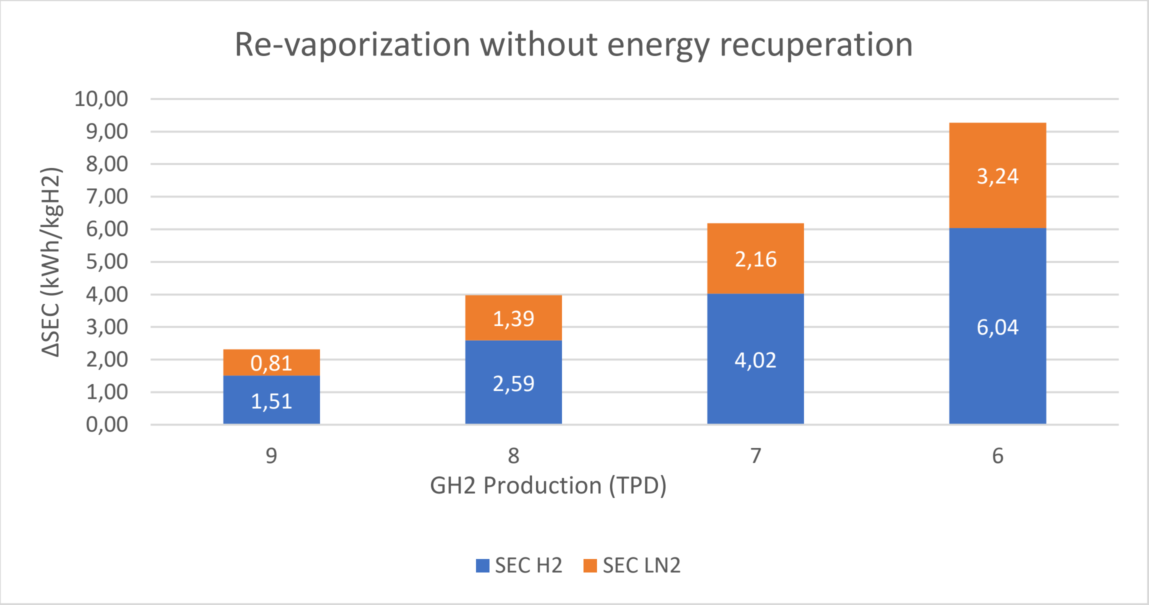

Figura S12. Evoluzione della SEC in condizioni di re-vaporizzazione senza recupero di energia

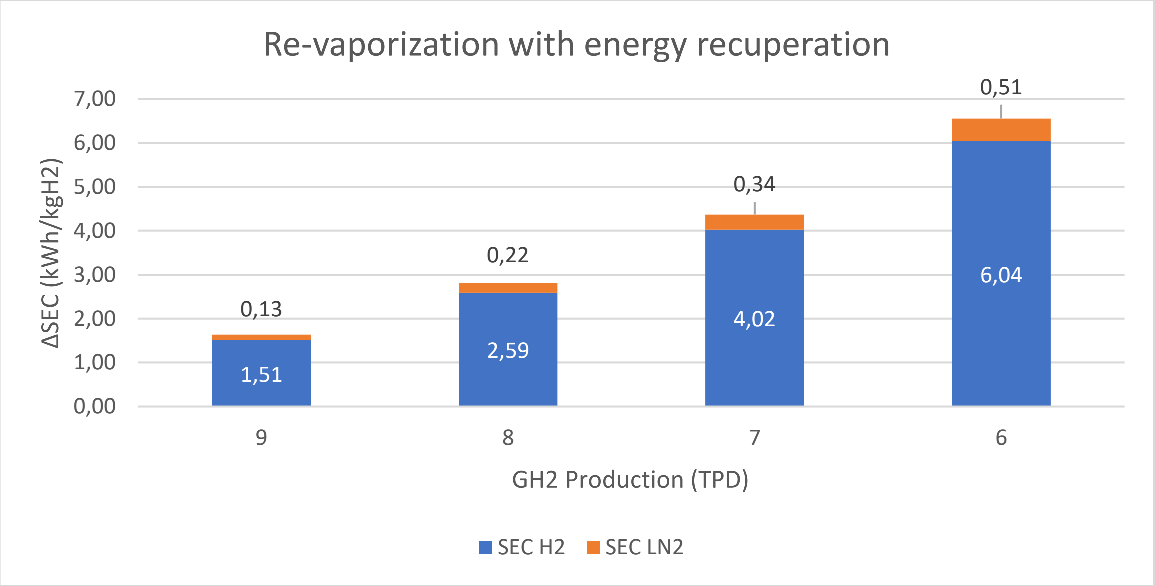

Figura S13. Evoluzione della SEC in condizioni di re-vaporizzazione con recupero di energia

Si può notare come il recupero dell'energia attraverso la produzione di azoto permetta di mantenere costante la SEC relativa a quest'ultimo, limitando quindi l'aumento generale della consumazione energetica del processo. Attraverso la comparazione con processi esistenti di liquefazione dell'idrogeno, è stato possibile affermare che una re-liquefazione che comprende 20% della produzione nominale ha un aumento di SEC risulta essere accettabile, mentre se il processo dovesse richiedere quantità più elevate questo si tradurrebbe in un incremento energetico troppo importante e di conseguenza inaccettabile economicamente.

S4.3. Stoccaggio esterno di idrogeno

Sebbene l'installazione di un sistema di stoccaggio esterno di idrogeno sia già stato studiato internamente da Engie, risultando troppo costoso, si è comunque deciso di analizzare l'installazione di un sistema più limitato, con l'obiettivo non di assorbire tutte le possibili variazioni di idrogeno durante l'anno, ma bensì delle variazioni su dei periodi limitati. L'impatto sul profilo di liquefazione può essere osservato nella sezione 8.1 dell'elaborato.

Nonostante esso abbia un interessante impatto sul profilo di liquefazione, permettendo di limitare i periodi di sovra o sottoproduzione elevata, il suo costo rimane comunque importante. In particolare, uno stoccaggio di 1.5 tonnellate e 3 tonnellate è stato considerato. I risultati sono di seguito riportati nelle tabelle S2 e S3.

Caso	ΔSEC (kWh/kg$_{H2}$)	ΔSLC (€/kg$_{LH2}$)	ΔCAPEX (k€)
Con stoccaggio	0.77	0.33	3137
Senza stoccaggio (doppia linea di compressione)	0.73	0.70	7526
Senza stoccaggio (singola linea di compressione)	1.08	0.08	0

Tabella S2. 1.5 tonnellate stoccaggio

Caso	SEC (kWh/kg$_{H2}$)	SLC (€/kg$_{LH2}$)	ΔCAPEX (k€)
Con stoccaggio	0.93	0.43	4174
Senza stoccaggio	1.01	1.04	11500

Tabella S3. 3 tonnellate stoccaggio

Anche in questo caso si è considerata la possibilità di usare due linee di compressione e le diverse possibilità sono state comparate. Il sistema di stoccaggio risulta essere favorevole economicamente rispetto all'installazione di una linea di compressione addizionale, ma comunque più costoso dell'utilizzo di un singolo compressore.

S4.4. Profilo variabile

Le analisi presentate finora sono state applicate ad un caso specifico in cui la produzione di idrogeno risulta variabile durante l'anno. Il profilo è stato fornito da Engie ed è presentato nella seguente figura S14.

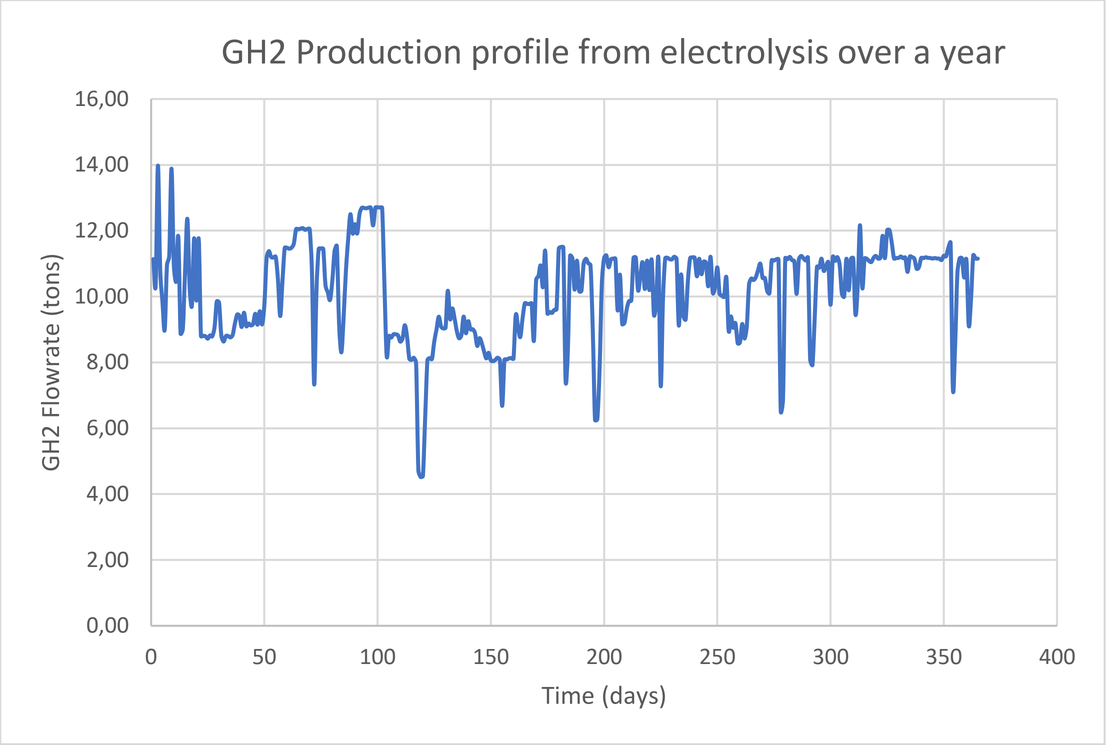

Figura S14. Profilo di produzione di idrogeno da elettrolisi durante un anno

La distribuzione dei range di produzione rispetto al nominale e le caratteristiche del profilo sono presentate nella figura S15 e nella tabella S4.

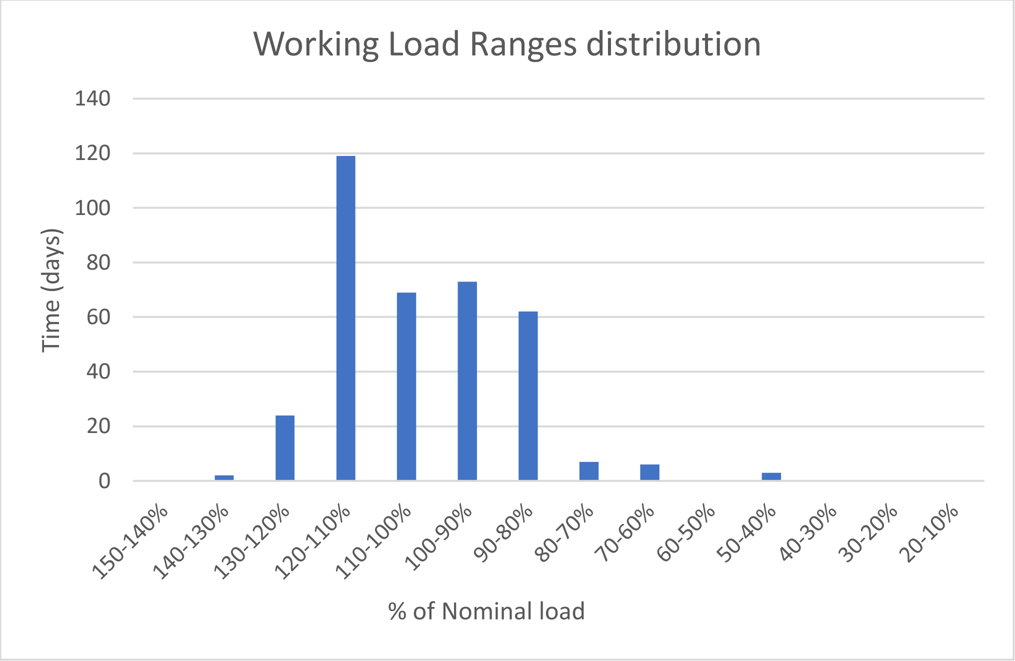

Figura S15. Distribuzione dei range di produzione di idrogeno

Media (TPD)	10.16
Deviazione standard	1.43
Valore massimo (TPD)	13.98
Valore minimo (TPD)	4.52

Tabella S4. Caratteristiche statistiche del profilo di produzione

È possibile osservare che la produzione varia tra 140% e 40% del nominale (10 TPD), ma che la maggior parte dei giorni si concentrano su dei valori compresi tra 120% e 80%. L'obiettivo di questa sezione è quella di determinare un processo che possa assorbire queste variazioni senza che i costi diventino troppo elevati.

Per far ciò si è deciso di implementare i vari scenari simulati ed analizzati precedentemente (utilizzo di compressore a velocità variabile, stoccaggio esterno, re-liquefazione), applicandoli al caso in esame.

Una limitazione nella carica di liquefazione (e quindi nella flessibilità accettata) è stata decisa. In particolare, basandosi sui risultati ottenuti nelle precedenti simulazioni e nella letteratura scientifica riguardante l'argomento, i valori di +-30% e +-20% rispetto al nominale sono stati simulati. Per determinare il profilo di liquefazione in entrata al processo, due algoritmi sono stati utilizzati. In entrambi gli algoritmi, lo stoccaggio esterno viene utilizzato solo per gestire le portate di idrogeno gassoso che sono al di fuori dei limiti superiore e inferiori di liquefazione scelti. Nel primo algoritmo, la re-liquefazione viene utilizzata per raggiungere il valore nominale di liquefazione, mentre nel secondo algoritmo essa viene attivata solo fino al raggiungimento del limite inferiore di liquefazione. Entrambi gli algoritmi possono essere osservati nella sezione 8.2.1 e 8.2.2 dell'elaborato. Il secondo algoritmo permette di avere risultati generalmente migliori e di limitare le perdite di idrogeno nel sistema, per questo motivo si è deciso di effettuare i calcoli energetici ed economici solamente su quest'ultimo. Come può essere osservato dal profilo di stoccaggio dell'idrogeno liquido, con l'utilizzo del secondo algoritmo esso spesso risulta pieno. Si rende quindi necessaria la possibilità di vendere saltuariamente una quantità di idrogeno liquido più elevata rispetto alla produzione nominale, in quanto l'impossibilità di stoccarlo in quel dato momento risulterebbe in una perdita di prodotto importante.

I risultati dell'impatto energetico e dell'impatto economico sono riportati nella seguente tabella. Essi sono calcolati in relazione al caso base, ovvero un processo che liquefi l'integrità del profilo di produzione dell'idrogeno. Esso necessita dell'implementazione di una linea addizionale di compressione, poiché la sovraproduzione può superare in alcuni casi il limite di operabilità previsto dal singolo compressore pari a +20% rispetto alla carica nominale.

Caso	ΔSEC media (kWh/kg$_{H2}$)	ΔSEC media con vendita idrogeno flessibile (kWh/kg$_{H2}$)	ΔSLC media (€/kg$_{H2}$)	ΔSLC media con vendita idrogeno flessibile (€/kg$_{H2}$)
20% Flessibilità consentita (2 compressori)	0.42	0.2	-0.10	-0.26
30% Flessibilità consentita (2 compressori)	0.41	0.03	0.10	-0.06
20% Flessibilità consentita (1 compressore)	0.5	0.11	-0.90	-1.03
20% Flessibilità consentita + 1.5 ton stoccaggio	0.54	0.36	0.21	0.11
20% Flessibilità consentita + 3 ton stoccaggio	0.77	0.57	0.32	0.22

Tabella S5. Parametri energetici ed economici dei diversi scenari simulati

Si può notare che, sebbene l'impatto energetico delle diverse soluzioni risulti essere abbastanza similare, il valore della SLC risulta essere molto differente tra i diversi casi simulati. In particolare, l'utilizzo di un solo compressore permette di abbattere i costi rispetto al caso base. L'utilizzo di due compressori, invece, comporta comunque un aumento dei costi di produzioni, così come l'implementazione di un sistema di stoccaggio temporaneo di idrogeno gassoso.

Se comparato al caso base di produzione costante, la liquefazione del profilo di produzione variabile, senza l'implementazione di nessun sistema di miglioramento della flessibilità, comporterebbe un aumento dei costi pari a circa 41%, mentre l'implementazione di un sistema di re-liquefazione con una liquefazione limitata solamente a +-20% della produzione nominale permette di ridurre questo aumento a 6.5%, che rappresenta un incremento ragionevole.

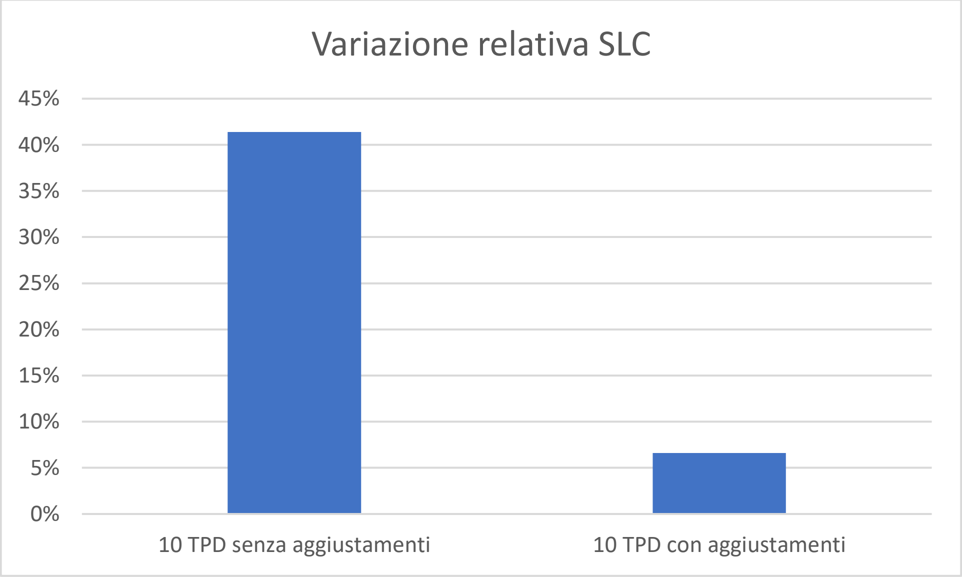

Figura S16. Valori della SLC per i diversi scenari

Questo permette di asserire che risulta possibile, sia tecnicamente che economicamente, effettuare la liquefazione di un profilo di produzione dell’idrogeno derivante da energie rinnovabili e quindi variabile nel tempo, attraverso l’implementazione di tecnologie quali compressione attraverso compressori a velocità variabile e re-liquefazione dell’idrogeno.

S5. Conclusione

Per concludere l’analisi presentata, è possibile quindi affermare, dalla letteratura scientifica riguardante l’argomento e dalle simulazioni effettuate, la possibilità tecnica ed economica di sviluppare un processo di liquefazione dell’idrogeno almeno parzialmente flessibile. L’utilizzo di una tecnologia di compressione a velocità variabile e la corretta gestione delle portate dei diversi refrigeranti che partecipano al processo permette di assicurare un’operabilità dell’impianto accettabile anche quando sono presenti variazioni di carico. Da un punto di vista energetico ed economico, le simulazioni effettuate hanno evidenziato come una variabilità maggiore di +-20% del valore nominale di liquefazione abbia un impatto significativo. Per quanto riguarda i periodi di sottoproduzione, quando questa si trova al di sotto dell’80% del nominale, il deterioramento delle performance delle unità, in particolare dei compressori, diventa importante, risultando in un maggiore aumento dei costi energetici dell’impianto; nei periodi di sovraproduzione, quando questa supera il 120% del valore nominale, si rende necessaria l’installazione di una linea addizionale di compressione, in quanto questo valore eccede il carico massimo consentito per il singolo compressore.

La soluzione più efficiente risulta quindi essere quella di effettuare la liquefazione in un range che varia tra 80-120% del valore nominale, utilizzando possibilmente l’idrogeno sovraprodotto in altre applicazioni e performando una re-vaporizzazione dell’idrogeno liquido in periodi di sottoproduzione per permettere il raggiungimento del limite inferiore consentito di liquefazione.

Table of contents

1. **Introduction** 1
2. **Hydrogen** 2
   - 2.1. Hydrogen properties 2
     - 2.1.1. Hydrogen ortho-para conversion 2
     - 2.1.2. Hydrogen thermal conductivity 3
     - 2.1.3. Hydrogen heat capacity 4
   - 2.2. Hydrogen production 6
3. **Hydrogen liquefaction** 8
   - 3.1. Interest on the hydrogen liquefaction 8
   - 3.2. Liquid hydrogen market 9
   - 3.3. Joule-Thomson effect and its inversion temperature 10
   - 3.4. Liquefaction process principles 11
     - 3.4.1. Linde-Hampson 12
     - 3.4.2. Claude 13
     - 3.4.3. Brayton 14
     - 3.4.4. Kleemenko 14
   - 3.5. Hydrogen liquefaction process main units 15
     - 3.5.1. Catalytic Plate-Fin Heat Exchangers (CPFHX) 15
     - 3.5.2. Mechanical compressors 16
       - 3.5.2.1. High pressure ratio compressors 16
       - 3.5.2.2. Cryogenic compressors 16
       - 3.5.2.3. Turbo compressors 16
     - 3.5.3. Alternative compression: metal hydride compression 16
   - 3.6. Existing plants 18
     - 3.6.1. Linde process description 18
     - 3.6.2. Praxair process description 19
     - 3.6.3. Air Products process description 20
     - 3.6.4. Kawasaki process description 21
     - 3.6.5. Conceptual plants 22
4. **The issue of process flexibility** 24
   - 4.1. State of art of flexibility in gas liquefaction processes 24
   - 4.2. Overall remarks on the literature 25

5. Purpose of the study 27
6. Methodology and problem modelling 28
6.1. Considered liquefaction cycle 28
6.2. Simulation hypothesis and procedure 30
6.2.1. Choice of the thermodynamic model 30
6.2.2. Ortho-to-para conversion modeling 31
6.3. Economic calculations 32
6.3.1. Economic model 32
6.3.2. Energetic and economic parameters 33
6.4. Additional simulation software 34
6.5. Evaluation of off-design efficiencies for compressors 34
6.6. Evaluation of heat exchangers' off-design conditions 36
6.6.1. Evaluation of streams' outlet temperatures and heat exchanger behavior 36
6.6.1.1. Two streams HEX: outlet temperatures variation and used HEX length 36
6.6.1.2. Five streams HEX 39
6.6.1.3. Connected heat exchangers 42
6.6.2. Risks related to inattentive temperature variation 44
6.6.3. Evaluation of refrigerants' flowrates variations at off-design conditions 45
7. Case studies of simulation: Results and discussion 47
7.1. Results presentation 47
7.2. Constant off-design conditions 47
7.2.1. Part-load conditions results 48
7.2.2. Overload conditions 49
7.3. Nominal liquefaction conditions with LH_2 re-vaporization 51
7.4. Off-design and re-vaporization coupling 54
7.5. External Compressed H_2 storage 56
7.5.1. 1.5 Tons storage 57
7.5.2. 3 Tons storage 57
8. Application case: GH_2 variable production profile 58
8.1. CGH_2 storage impact 59
8.2. Allowed Flexibility and re-vaporization impact 62
8.2.1. Re-vaporization to nominal value (Algorithm V_1) 63
8.2.2. Re-vaporization to lower bound (Algorithm V_2) 64
8.2.3. Simulation results 65
8.2.3.1. Profiles evolution 65

8.2.3.1.1. 20% Allowed Flexibility and re-vaporization 65
8.2.3.1.2. 30% Allowed Flexibility and re-vaporization 66
8.2.3.1.3. 20% Allowed Flexibility, re-vaporization and CGH2 Storage 68
8.2.3.2. Energetic and economic results 70
9. Conclusion and future works 73
10. Bibliographic references 74

List of Figures

Figure 1. The allotropes of hydrogen: Ortho-hydrogen (a) and para-hydrogen (b); p – proton, e – electron, the arrows correspond to spin direction of the nucleus. [2] 2
Figure 2. Evolution of ortho-para concentration at different temperatures[4] 3
Figure 3. Thermal capacity with temperature at different para-ortho hydrogen compositions at 21 bar (Hysys® simulation) 4
Figure 4. Thermal capacity with temperature of n-H2 at different pressures (Hysys simulation) 4
Figure 5. Molar heat capacity of hydrogen with temperature at different compositions at 21 bar (Hysys simulation) 5
Figure 6. Molar heat capacity of normal hydrogen with temperature at different pressures (Hysys simulation) 6
Figure 7. Repartition of Hydrogen production[5] 6
Figure 8. Comparison of different hydrogen storage technologies; LOHC – Liquid Organic Hydrogen Carriers; MOF – Metal Organic Frameworks; GH2 – Gaseous Hydrogen; LH2 – Liquid Hydrogen.[11] 8
Figure 9. Share diagram of LH$_2$ supplier's production capacity (2015) 9
Figure 10. Regional LH$_2$ production and main suppliers (internal data) 9
Figure 11. J-T inversion curves for various cryogenic fluids; a) Methane; b) Air; c) Neon; d) Hydrogen; e) Helium [13] 11
Figure 12. Hydrogen liquefaction process simplified scheme 11
Figure 13. PFD of the Linde-Hampson cycle with precooling, here presented with the typical temperature level for hydrogen liquefaction 13
Figure 14. Schematic diagram of open Claude Cycle [14] 13
Figure 15. Schematic diagram of closed Claude Cycle 14
Figure 16. Reversed Brayton cycle, here integrated with H2 feed stream; and general representation on a Temperature-Entropy diagram [15] 14
Figure 17. The dual pressure Kleemenko cycle 15
Figure 18. Catalytic plate-fine heat exchangers structure 15
Figure 19. Hydrogen chemical compression with metal hydrid system principle 17
Figure 20. Ratio pressure for different intermetallic compounds[18] 18
Figure 21. PFD of hydrogen liquefaction plant in Leuna [20] 19
Figure 22. Praxair hydrogen liquefaction process[20] 20
Figure 23. Air Product liquefaction process PFD, US Patent n°US4765813, 1988. 21
Figure 24. Kawasaki liquefier process (USA Brevet n° US95988536, 2017) 22
Figure 25. SEC comparison of the different LH$_2$ technology[14] 23
Figure 26. Linde Leuna PFD 29
Figure 27. Schematic of the ortho-para conversion using a conversion reactor 32
Figure 28. Repartition of the CAPEX of the Linde Leuna process 35
Figure 29. Efficiency of the compressor with frequency conversion adjustment method from [43] 36
Figure 30. Scheme of a two stream HEX 37
Figure 31. Outlet streams temperature evolution vs GH2 feed variation 38
Figure 32. Outlet streams temperature variation vs LN$_2$ flowrate variation 38
Figure 33. Evolution of the GH$_2$ temperature along the length of the HEX at different load conditions 39
Figure 34. Five streams HEX scheme 39
Figure 35. Evolution of the hot streams' outlet temperatures bs GH$_2$ flowrate variation 40
Figure 36. Evolution of the cold streams outlet temperatures bs GH$_2$ flowrate variation 41
Figure 37. Evolution of the GH$_2$ temperature along the length of the five streams HEX at different load conditions 41
Figure 38. Evolution of the GH$_2$ and GN$_2$ temperatures vs GH$_2$ flowrate variation 42
Figure 39. Simplified Linde Leuna PFD simulated in dynamic mode 43
Figure 40. Evolution of GH$_2$ temperature at the exit of the three HEXs 43

Figure 41. Relative decrease from nominal conditions of the outlet GH_2 temperature............44
Figure 42. Evolution of HEXs minimum temperature approaches considering refrigerants' flowrate variations.........45
Figure 43. Evolution of HEXs minimum temperature approaches considering refrigerants' flowrate variations.........46
Figure 44. Refrigerants' flowrate variation related to GH2 feed flowrate variation.........46
Figure 45. Part load conditions SEC evolution.........48
Figure 46. Part load conditions SLC evolution.........49
Figure 47. Overload conditions SEC evolution.........50
Figure 48. Overload conditions SLC evolution.........50
Figure 49. LH_2 re-vaporization system scheme Japan patent n° JP2020024064A, 2020.........52
Figure 50. Re-vaporization without energy recuperation SEC evolution.........53
Figure 51. Re-vaporization with energy recuperation SEC evolution.........53
Figure 52. SLC variation from nominal with re-vaporization system.........54
Figure 53. Off-design and re-vaporization SEC comparison.........54
Figure 54. 8 TPD solutions mix impact.........55
Figure 55. 7 TPD solutions mix impact.........55
Figure 56. 6 TPD solutions mix impact.........56
Figure 57. GH_2 production profile.........58
Figure 58. Working load ranges distribution.........59
Figure 59. CGH2 storage implementation algorithm.........60
Figure 60. Profiles comparison.........60
Figure 61. Working load ranges impact.........61
Figure 62. CGH_2 storage profile.........61
Figure 63. Algorithm V_1.........63
Figure 64. Algorithm V_2.........64
Figure 65. Algorithm V1 20% Flexibility profiles comparison.........65
Figure 66. Algorithm V2 20% Flexibility profiles comparison.........65
Figure 67. Algorithm V1 30% Flexibility profiles comparison.........66
Figure 68. Algorithm V2 30% Flexibility profiles comparison.........67
Figure 69.Algorithm V1 20% Flexibility and CGH_2 profiles comparison.........68
Figure 70. Algorithm V2 20% Flexibility and CGH_2 profiles comparison.........68
Figure 71. 20% Flexibility and CGH_2 storage LH_2 storage profile comparison.........69
Figure 72. CGH_2 Storage profile.........69
Figure 73. Relative SEC variation for different solutions.........71
Figure 74. Relative SLC variation for different solutions.........71
Figure 75. SLC values for the different scenarii simulated.........72

List of Tables

Table 1. Hydrogen physical and thermal properties[1] 2
Table 2. Sum-up of the different cooling principles and their application in hydrogen liquefaction 12
Table 3. Main units' flexibility ranges and summary of off-design mitigation solutions. 26
Table 4. Properties of hydrogen allotropes, from HYSYS® databank 31
Table 5. Simulation parameters for the two streams HEX 37
Table 6. Simulation parameters for five streams HEX 40
Table 7. Part load conditions simulation results 48
Table 8. Overload conditions simulation results 50
Table 9. CGH_2 tank characteristics 56
Table 10. 1.5 tons CGH_2 storage results 57
Table 11. 3 tons CGH_2 storage results 57
Table 12. GH_2 production profile characteristics 59
Table 13. Energetic and economic parameters for the simulated cases 70

List of Abbreviations

CAPEX	Capital Expenditures
$CCGH_2$	Cryo-Compressed Gaseous Hydrogen
CGH_2	Compressed Gaseous Hydrogen
J-T	Joule-Thompson
GH_2	Gaseous hydrogen
GN_2	Gaseous nitrogen
HEX	Heat Exchangers
LH_2	Liquid hydrogen
LNG	Liquefied Natural Gas
LN_2	Liquid nitrogen
NPV	Net Present Value
$n\text{-}H_2$	Normal hydrogen
$o\text{-}H_2$	Ortho-hydrogen
OPEX	Open expenditures
PFD	Process Flow Diagram
$p\text{-}H_2$	Para-hydrogen
SEC	Specific Energy Cost
SLC	Specific Liquefaction Cost
TPD	Tons per day

1. Introduction

The interest in hydrogen as an actor of the energetic transition is rising in the last years, thanks to the possibilities that it could offer as energy carrier in applications related to the exploitation of renewable energies. The 2050 carbon-neutral objective fixed for Europe fixed by the European Green Deal is a challenge to which hydrogen could represent one of the major solutions and tools to reach this scope.

Liquid hydrogen has risen importance as energy carrier for energy storage and transportation, offering higher energetic densities than gaseous hydrogen, which result in easier transportation and lower need of storage volumes. Nevertheless, its application is still limited, in particular to the aerospace industry, due to the high energetic costs of the liquefaction process.

Gaseous hydrogen is produced mostly via steam methane reforming, using therefore fossil fuels as raw material. However, the increasing maturity in renewable energy production, which resulted in a higher overall electricity production, has increased the need in energy storage. Hydrogen will then become more and more produced via water electrolysis with the objective to store renewable energy. However, historically the hydrogen liquefaction process has been developed at steady nominal charge, thanks to the gaseous hydrogen provided by the steam reforming process. The intermittent nature of renewable energies such as solar and wind energy would result in the variation of the hydrogen produced throughout the year, and therefore the variation of the charge entering the liquefaction process. This could lead to inoperability to the process due to malfunctions of units which are not able to work at these conditions.

In order to improve the impact of the liquid hydrogen as an actor in the energetic transition, it is therefore critical to investigate the flexibility of the known hydrogen liquefaction process, in order to determine the allowed operability ranges of the units used in the process and to evaluate methods and improvement to allow a better functioning of the process far from the nominal conditions. Energetic and economic analysis can be performed to evaluate whether the process can sustain such variations with an acceptable impact on these parameters or the management of the variability of the renewable energies would need to be treated in another point of the hydrogen production chain.

2. Hydrogen

2.1. Hydrogen properties

Hydrogen is the lightest element with a standard atomic weight of 1.008. It is formed by a single proton and an electron and nowadays it is used mostly for the ammonia production process and refinery processes. The use of hydrogen as energy carrier and for mobility is still under development, with an industrial activity in this domain mostly limited to aerospace applications.

The physical and thermal property of hydrogen are resumed in Table 1.

Table 1. Hydrogen physical and thermal properties [1]

Density	0.08988 g/L (0 °C, 1 atm)
Specific heat	14.304 J/kg-K (1 atm)
Heat of vaporisation	0.904 kJ/mol (1 atm)
Boiling point	20.28 K, -252.87 °C (1 atm)
Melting point	14.01 K, -259.14 °C (1atm)
Triple point	13.80 K, -259 °C, 7.042 kPa
Critical point	32.97 K, 1.293 MPa
Conductivity	187/m-K

2.1.1. Hydrogen ortho-para conversion

Hydrogen exists in nature under two isomers: ortho hydrogen (o-H_2) and para hydrogen (p-H_2). The former presents an electronic configuration with parallel nuclear spins, while the latter presents an electronic configuration with antiparallel spins. Figure 1 shows the two aforementioned configuration.

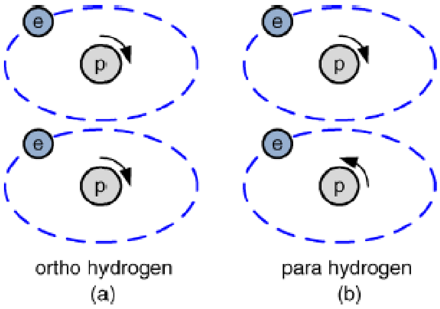

Figure 1. The allotropes of hydrogen: Ortho-hydrogen (a) and para-hydrogen (b); p – proton, e – electron, the arrows correspond to spin direction of the nucleus. [2]

The composition of a o-p hydrogen mixture in equilibrium is temperature dependant, as can be seen in Figure 2. At 0K, only p-H_2 exists, while at higher temperatures, such as room temperatures, the composition is limited with a ratio of 3:1 between o-H_2 and p-H_2. This composition is generally called "normal" hydrogen (n-H_2) while the equilibrium composition at a certain temperature is generally indicated with e-H_2. The conversion from the ortho form to the para form is exothermic, but is it generally slow, especially at low temperatures if not properly catalysed. There are not many differences in the physical-chemical characteristics between the two forms. There are only slightly differences between the melting and boiling points, which differ of around 0.1-0.2K at every pressure. The main differences between the two forms can be detected in its heat capacity and its related properties, for example thermal conductivity[1], as showed in the next Section 2.3.

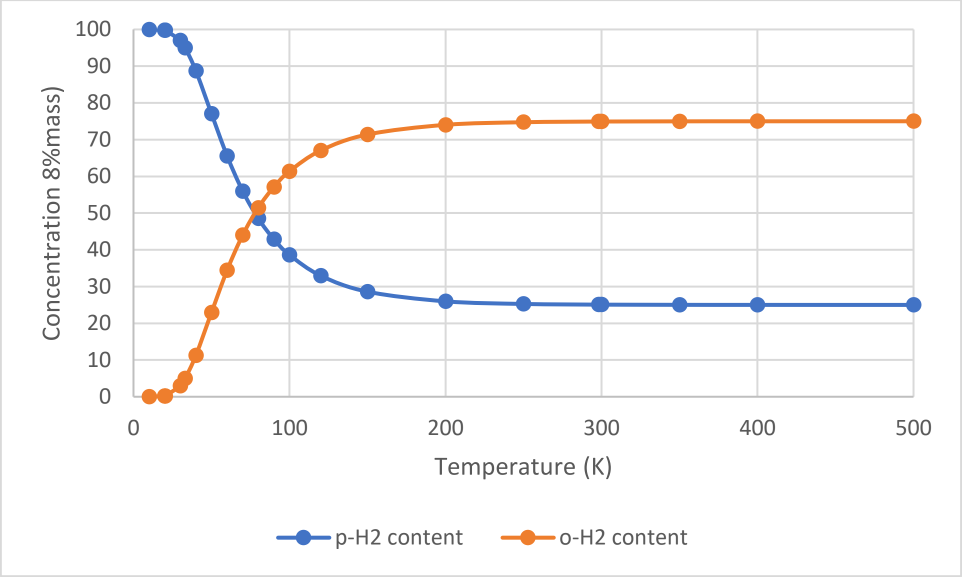

Figure 2. Evolution of ortho-para concentration at different temperatures[4]

One of the main problems related to this conversion is due to the fact that the conversion enthalpy of the ortho-to-para reaction is higher than the vaporisation enthalpy. For example, at 20K (usual temperature at which the liquid hydrogen is stored), the conversion enthalpy is equal to 520 kJ/kg, while the vaporisation enthalpy is equal to 454 kJ/kg[2]. For this reason, if liquid hydrogen is stored over a long period without having attained its equilibrium concentration, the o-H_2 will slowly transform into p-H_2. This conversion produces a non-negligible amount of heat leading to vaporization and of loss of the liquid hydrogen, even if the storage is perfectly insulated. It has been estimated that from a normal composition stored at 20K, the ortho-to-para conversion causes a loss up to 18% of the liquid hydrogen within 24h after liquefaction (based on an internal study).

To avoid this problematic, hydrogen is generally converted with the use of catalysers during the liquefaction process into para-hydrogen[3]. Commercial plants generally work with a concentration of p-H_2 in the product of at least 95%[4]. This reaction is usually performed in catalytically filled plate-fin heat exchanger. Hydrous ferric oxide $Fe(OH)_3$ and ferroxyde (Fe_2O_3) are the most commonly used catalyst since they are cheap and non-reactive with the air and a wide range of chemicals. Other catalyst materials are used such as activated coal for adsorption vessels. This results in an increase of the specific energy consumption of the liquefaction process, due to the increase of temperature generated from the o-p conversion in the different heat exchangers. It has been estimated that the conversion increases the minimum liquefaction work of around 0.59 kWh/kg_{H2} which represents around 15% of the total reversible work.

2.1.2. Hydrogen thermal conductivity

The thermal conductivity of the hydrogen is one of the key parameters for process optimization, since it measures its ability to conduct heat. The higher it is, the better will heat exchanges be led. Thermal conductivity (W/m-K) increases with temperature and pressure as long as the refrigerant remains in a same physical state. Figure 3 shows thermal capacity with temperature at different para-ortho hydrogen compositions at 21 bar (Hysys®, MBWR) presents for different para-ortho composition the behavior of thermal conductivity (Hysys®, MBWR, 21 bar), while Figure 3 shows the evolution of n-H_2 thermal conductivity with temperature for different values of pressure (Hysys®, MBWR, 25% p-H_2 / 75% o-H2).

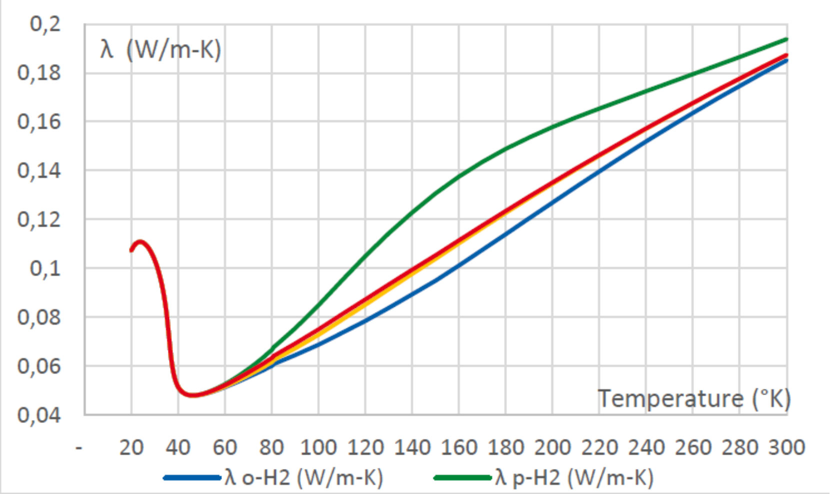

Figure 3. Thermal capacity with temperature at different para-ortho hydrogen compositions at 21 bar (Hysys® simulation)

It has been observed that composition has no influence under a certain temperature related to the pressure – here at 21 bar, under 60 k – whereas for higher values of temperature than this limit, thermal conductivity increases with para-hydrogen fraction. While the difference is quite important between n-H_2 and p-H_2 ($\lambda_{p\text{-}H2} > \lambda_{n\text{-}H2}$; up to 28%; 14% on average), it appears to be insignificant between e-H_2 and n-H_2 (<3%).

Finally, as mentioned before, the interest to operate at the highest possible pressure in the range [20 – 80] K is highlighted in Figure 4 by a significative difference of 20% between 20 and 30 bars. However, the increase of the pressure has to be correctly balanced with the increase of the exchanger costs and the addition of an inlet compressor. These observations lead to consider the use of converted para-hydrogen for the refrigeration cycle and precooling while it remains reasonable to operate the cooling with normal-hydrogen. Increasing the system pressure might as well be a source of optimization for the process.

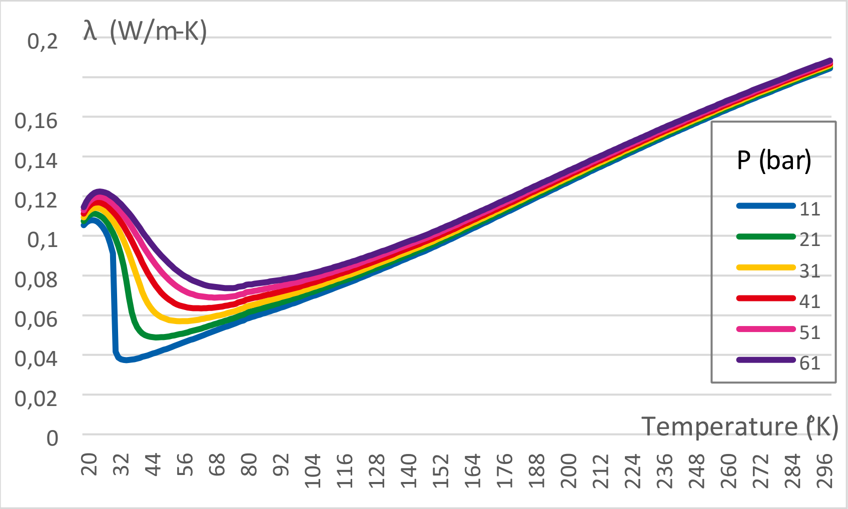

Figure 4. Thermal capacity with temperature of n-H2 at different pressures (Hysys simulation)

2.1.3. Hydrogen heat capacity

The heat capacity of the hydrogen is another key parameter for process optimization since it measures its ability to stock heat. While it has to be as small as possible for hydrogen liquefaction, since it directly drives the quantity of heat that has to be supplied, a high Cp value seems interesting for a refrigerant since it can extract more heat.

Hydrogen molar heat capacity fluctuates depending on ortho-para hydrogen fraction from 0 to 30% with on average 16% (between 0 and 9.8 kJ/kmol with an average of 4.8 kJ/kmol). The more hydrogen is converted to para, the higher its molar heat capacity is. Molar heat capacity of equilibrium hydrogen is always higher than normal hydrogen between 60 K and 300 K. Both increase with temperature by around 15% (4 kJ/kmol) in this range. No difference is observed under 60 K at 21 bar.

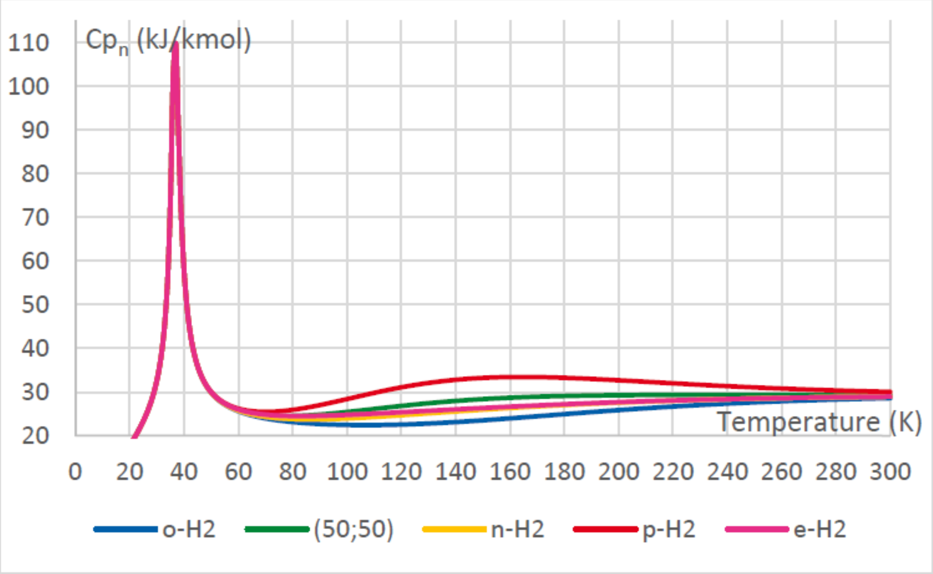

Figure 5. Molar heat capacity of hydrogen with temperature at different compositions at 21 bar (Hysys simulation)

On Figure 5 it is possible to observe molar heat capacity of hydrogen with temperature at different compositions at 21 bars (Hysys, MBWR). A peak for the molar heat capacity value is observed at liquefaction temperature (depending on the pressure). A maximum increase of pressure seems necessary to mitigate the heat capacity peak in order to facilitate the heat transferred from the “to liquefied” hydrogen to the cooling refrigerant.

As refrigerant, hydrogen should be converted to para-hydrogen and its pressure should be increased to an optimum for its refrigeration power and heat extraction capacity. For hydrogen liquefaction, ortho-hydrogen seems to be more efficient over 80 K. Hydrogen conversion while pre-cooling is then not profitable for the heat capacity.

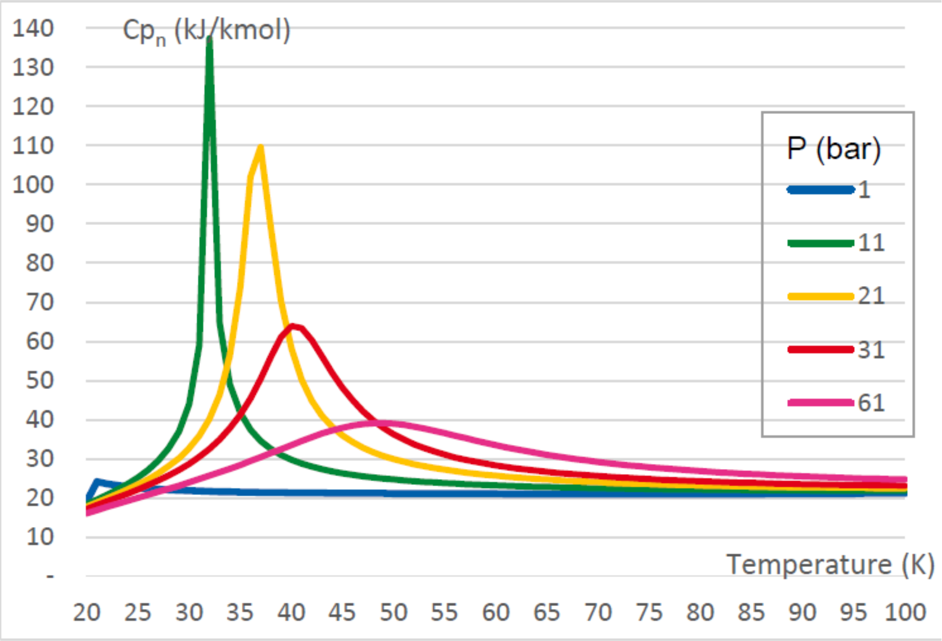

Figure 6. Molar heat capacity of normal hydrogen with temperature at different pressures (Hysys simulation)

2.2. Hydrogen production

Nowadays hydrogen can be produced with different processes. Currently the main production of hydrogen (around 96%) is based on the exploitation of fossil fuels thanks to processes known as steam reforming. These processes allow to transform natural gas (and heavier components such as naphtha and coil) into hydrogen[5][6]. The remaining hydrogen production is accounted from water electrolysis, as showed in Figure 7. Although this technology occupies only a low share of the total H_2 production, its attraction has been growing in the last years due to its possible environmental impact coupled with an increasing maturity and decrease of technology cost[7].

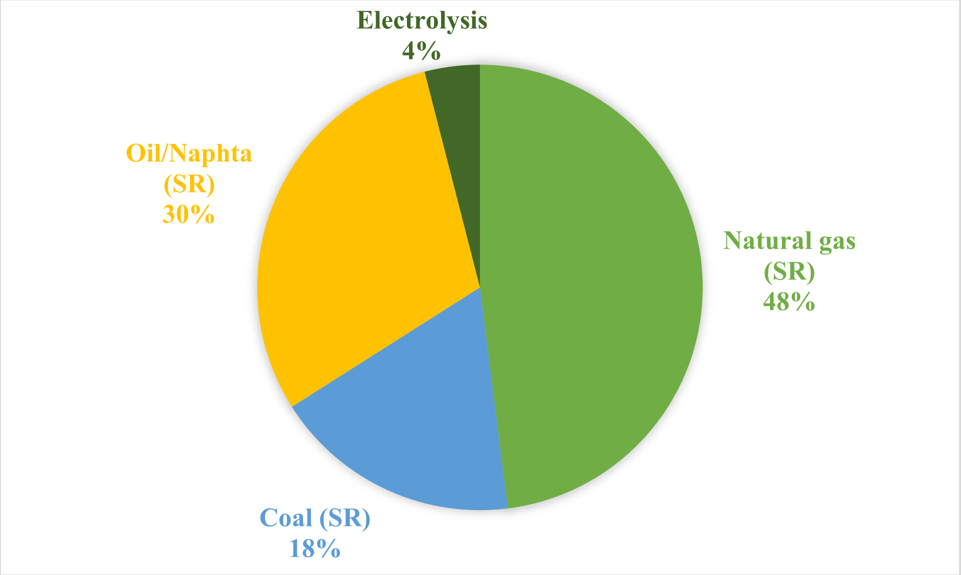

Figure 7. Repartition of Hydrogen production[5]

The interest in this technology is supported by numerous publications that have enlightened the interest in energy storage by hydrogen for variable renewable energy sources, such as solar or wind energies in Power-to-Gas application development[8]. These energies will likely have an increasing impact in the energetic mixes of different countries, hence having their overall demand growing in terms of supplied electricity. Hydrogen will have an advantageous impact in this domain thanks to different usage possibilities, such as electricity conversion with fuel cell and an easier fuel transportation [9]. Moreover, the use of hydrogen as energy carrier would allow a higher volumetric energy density than the currently energy storage systems, mainly represented by pumped-hydro energy storage.

3. Hydrogen liquefaction

3.1. Interest on the hydrogen liquefaction

The increasing interest and development of renewable energies has risen the challenge of energy storage. Indeed, certain renewable energies, such as wind or solar energies, have an intermittent nature which results in a non-constant electricity production over a certain period. The amount of energy produced depends on various factors, such as geographical location and seasonality. The use of hydrogen could represent a solution to the energy storage challenge, due to the possibility to produce it via water electrolysis using renewable electricity[10]. One of the problem related to hydrogen storage is its low density (0.09 kg/m^3), that results in a very low energy density (0.003 kWh/l), even with a high specific energy (33 kWh/kg)[11]. If compared with conventional fuels, for example gasoline, which has an energy density of around 10 kWh/l, it is clear the necessity to found ways to improve this parameter, since for transportation technologies it would lead to lower specific costs thanks to lower volumes and weight.

Hydrogen can be stocked with various methods, as showed in Figure 8, with the most common one to be the compressed hydrogen. Even at high storage pressure, however, the energy density remains low (1.3 kWh/l at 700 bar), with the downside of a high investment cost in the storage technology and in the compression. The LH_2 technology allows to increase the density at around 2.4 kWh/l, with an energetic requirement in industrial plants between 8-15 kWh/kg of electricity. This amounts to around 24-45% of the overall energy contents. As a result, H_2 can be stored in low pressure tanks and allows the use of large storage systems with high energy densities. Increasing development of LH_2 could allow to reduce the energetic demand for the liquefaction process, making this solution more competitive above other storage technologies.

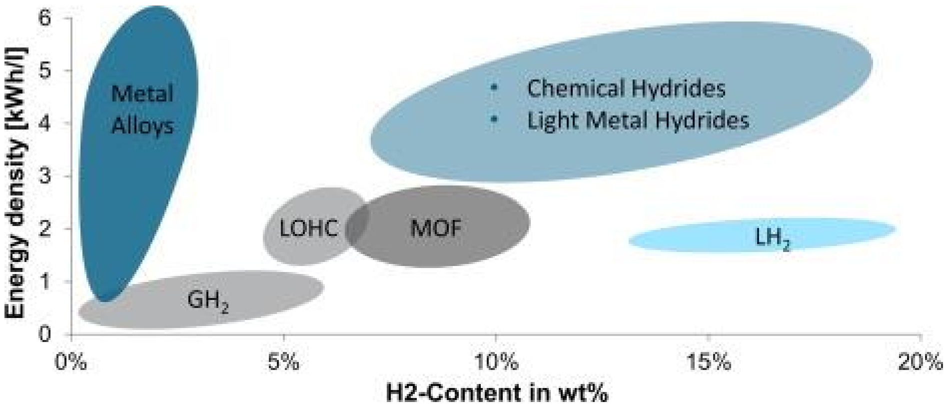

Figure 8. Comparison of different hydrogen storage technologies; LOHC – Liquid Organic Hydrogen Carriers; MOF – Metal Organic Frameworks; GH2 – Gaseous Hydrogen; LH2 – Liquid Hydrogen.[11]

3.2. Liquid hydrogen market

The global LH_2 production is equal to around 300 TPD. Four enterprises are the main LH_2 suppliers, and they provide about 94% of the total market capacity (Figure 9 and Figure 10): Air Products (38.7%), Praxair (30.5%), Linde (13.5%) and Air Liquide (11.7%). Praxair is only implanted in the USA, while Air Liquide has the main position in Europe and enters on the Asian market.

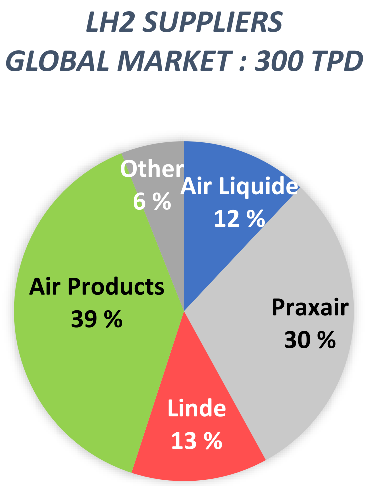

Figure 9. Share diagram of LH_2 supplier's production capacity (2015)

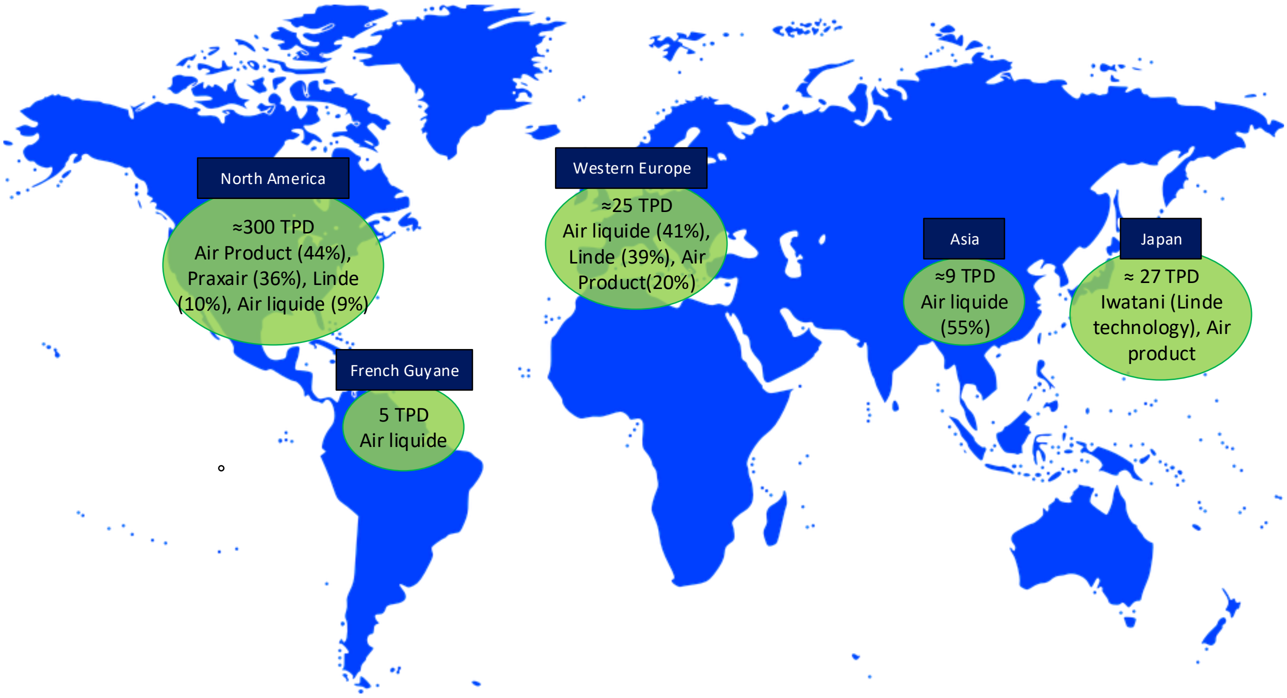

Figure 10. Regional LH_2 production and main suppliers (internal data)

3.3. Joule-Thomson effect and its inversion temperature

Most of the existing gases liquefaction processes uses throttling valve to perform the liquefaction of non-ideal fluids[12]. These types of fluids can be cooled down thanks to an isenthalpic expansion based the Joule-Thomson effect. The Joule-Thomson effect refers to the variation in temperature in a gas that occurs because of a sudden pressure change over a valve. To measure this effect, the Joule-Thomson coefficient has been defined. It allows to evaluate the temperature variation related to the pressure variation that occurs in the isenthalpic expansion.

$$\mu_{JT} = \left(\frac{\partial T}{\partial P}\right)_h = \mu_{JT}(P, T) \tag{1}$$

$$H = U + PV \tag{2}$$

This effect can be exploited only working with non-ideal gases, because for an ideal gas enthalpy is function only of temperature and it is independent from the pressure, hence a pressure variation cannot result in a change in temperature. In the case of study, hydrogen is not an ideal gas and therefore this effect can be exploited in the liquefaction process. One of the issues is that the cooling effect of the enthalpic expansion does not occur at every temperature. The value of the J-T coefficient can be either be negative or positive depending on the temperature and on the gas, and its value represents respectively a heating or a cooling effect on the gas that is being expanded. The temperature at which occurs the transition from a positive to a negative value of the J-T coefficient is called inversion temperature. Below inversion temperatures, the coefficient is positive, and an expansion produces a decrease in temperature. The value of the inversion temperature is different for every gas. In the case of hydrogen, this temperature is equal to 202K (-71 °C), and for this reason it can be cooled down or liquefied with a J-T expansion only under this temperature. The inversion temperatures of different gases can be observed in Figure 11.

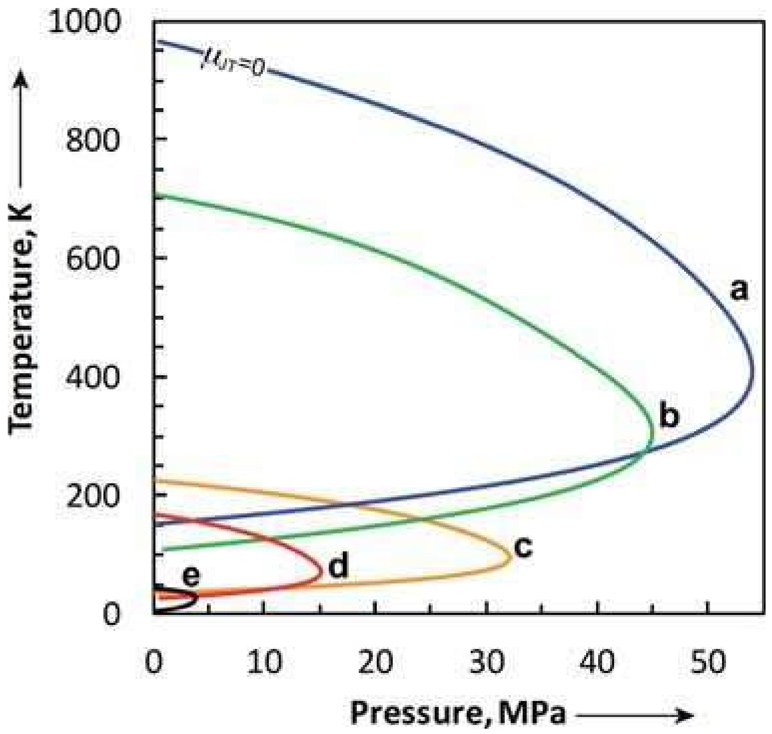

Figure 11. J-T inversion curves for various cryogenic fluids; a) Methane; b) Air; c) Neon; d) Hydrogen; e) Helium [13]

3.4. Liquefaction process principles

The hydrogen liquefaction processes can be resumed and schematized as Figure 12. They generally include three main parts: the compression stage, where the refrigerants' pressure is increased before reaching the two other parts; the pre-cooling stage, where a refrigerant fluid is used to cool down the feed H_2 to around 80K; and the cooling part, where the hydrogen is cooled down to around 21K before being expanded in a J-T valve and liquefied. H_2 is generally supplied at around 290K and 20 bar, while LH_2 is obtained at around 21K and 2 bar.

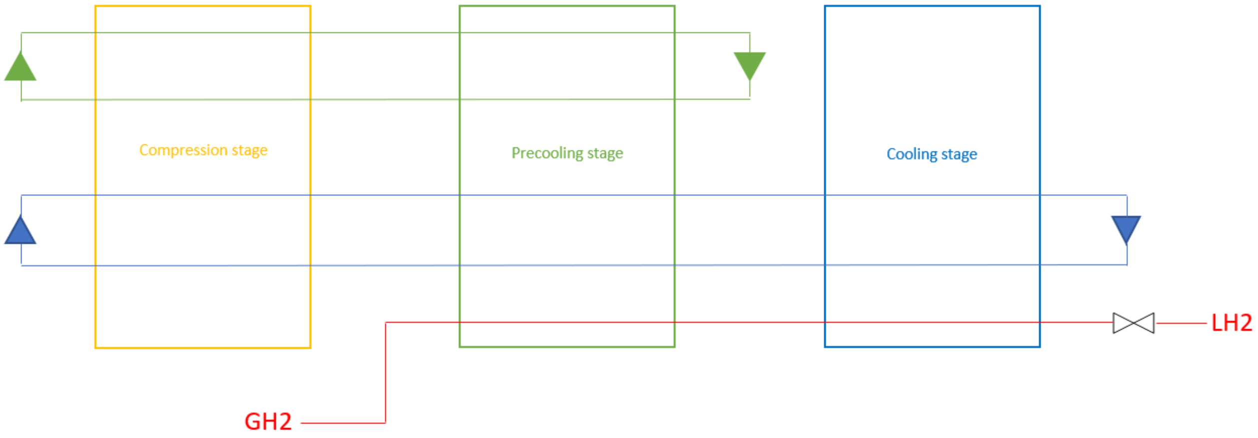

Figure 12. Hydrogen liquefaction process simplified scheme

The different liquefaction processes are generally differentiated by their cooling cycles. The two main cooling cycles used in the LH_2 industry are Brayton and Claude. The former works with cooling power provided by an isentropic expansion while the latter is a mixed cycle based on cooling energy provided by isenthalpic expansion and partial isentropic expansion.

Basic recuperative systems principles that can be used to mass liquefy hydrogen are listed in the following table:

Table 2. Sum-up of the different cooling principles and their application in hydrogen liquefaction

Cycle	**Principle**	**Type**	**Fluid used**	**Application**	
Precooled Linde-Hampson	Working fluid cooled by an external fluid and the vapor generated by throttling (isenthalpic expansion)	Open	LN_2 precooling, H_2	-	Theoretical
Claude	Working fluid cooled by the vapor generated by throttling, isentropic expansion and if needed an external fluid (N2, He, MR, LNG)	Open/Closed	N_2, He, H_2, C_3	Precooling/Cooling cycle (for closed cooling cycles) or main cycle (for open cooling cycles)	Conceptual and in application (for Hydrogen only)
Brayton	Working fluid compressed and cooled by the isentropically expended return	Closed	N_2, He, Ne, H_2	Precooling/cooling	In application (He) / Conceptual
Kleemenko	"Claude cycle" in cascade with a biphasic mixed refrigerant at room temperature	Closed	MR	Precooling cycles	Conceptual

3.4.1. Linde-Hampson

The Linde-Hampson cycle is based on the Joule Thomson cycle. It is based on the enthalpy difference at different pressure levels at a given temperature. In the precooled Linde-Hampson process (Figure 13) the feed gas, at ambient temperature, is compressed and cooled to room temperature using water or air. After further precooling by an external fluid, typically liquid nitrogen (LN_2), the working fluid is cooled through heat exchangers with the returning gas from the last stage. Passing through a Joule-Thomson valve, the gas expands and reaches the biphasic state, with a significantly colder temperature. The liquid part is collected while the cold gas is used as cooler and recycled to be compressed with the feed stream.

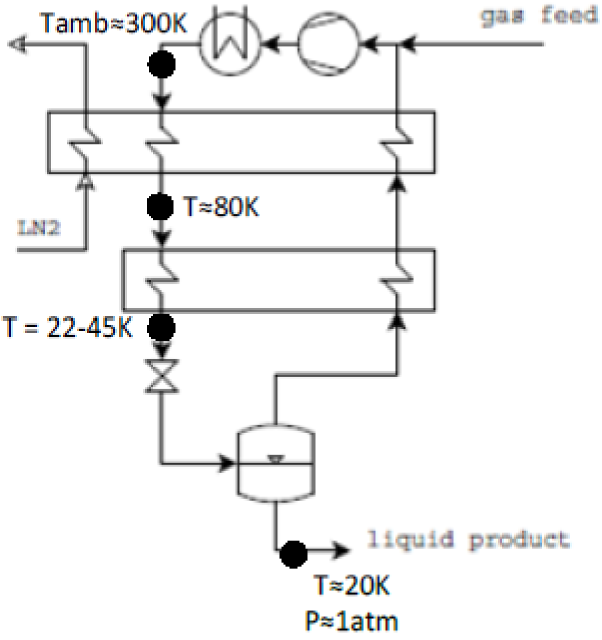

Figure 13. PFD of the Linde-Hampson cycle with precooling, here presented with the typical temperature level for hydrogen liquefaction

3.4.2. Claude

The Claude cycle (Figure 14) basis is the Linde-Hampson process (Joule-Thomson cycle), but it combines the Joule-Thomson effect with the expansion in a machine. Indeed, a portion of cooled gas is expanded in an isentropic expander to provide extra cooling compared to the previous process, and thus a bigger fraction of liquid can be recovered after the throttling area. If the cold generated is not sufficient, a precooling system can be added, using LN_2, helium or a Mixed refrigerant (MR) for example, as additional cold given to the first heat exchangers. This cycle can be open, with the liquid fraction collected as final product, or closed, with the liquid used as refrigerant, as presented on Figure 15.

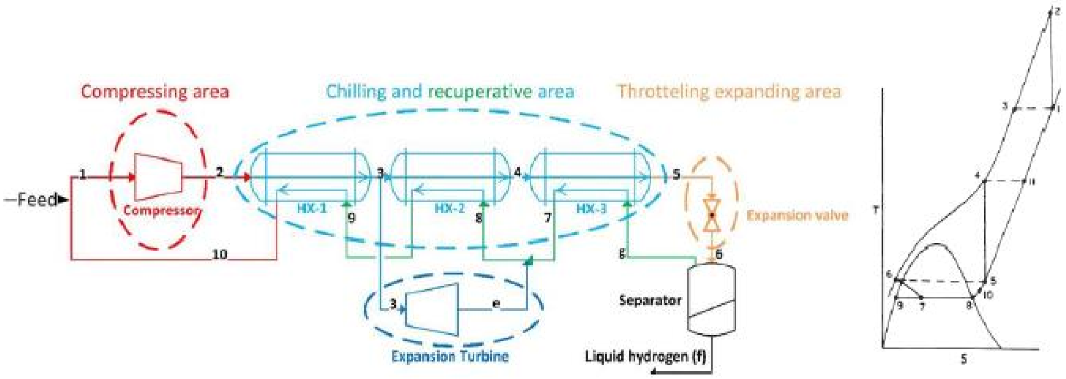

Figure 14. Schematic diagram of open Claude Cycle [14]

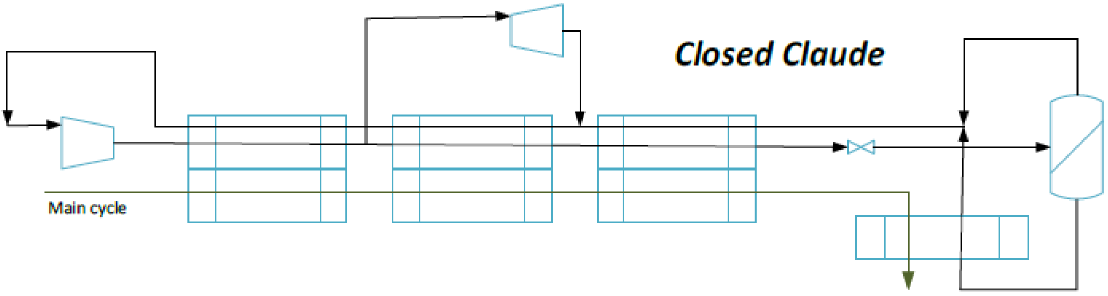

Figure 15. Schematic diagram of closed Claude Cycle

3.4.3. Brayton

The system operates on a thermodynamic reference cycle known variously as the Joule cycle (in England) and the Brayton cycle (in North America), or Joule-Brayton process in order to avoid any misunderstanding.

The Brayton cycle does not use the Joule-Thomson effect and can therefore be used on an ideal gas.

The system in Figure 16 presents a closed "reversed" Brayton (which produces cold and not heat) system that can be used for H_2 cooling and precooling, depending on the refrigerant used, and so the temperature levels achievable. Nitrogen or MR (precooling only), and Hydrogen, Helium or Neon can be used for precooling/cooling in the liquefaction of hydrogen application.

The principle is to use the cold generated by the gas expansion in a machine (turbine). The heat is extracted from the system under the form of mechanical work. The frigories cool down the working fluid as well as the refrigerant itself before its expansion stage. The refrigerant is then compressed, cooled to room temperature by water or air chiller, and possibly precooled by another system (as seen on Figure 16). In this process, unlike the Claude, the refrigerant remains gaseous, and is not throttled.

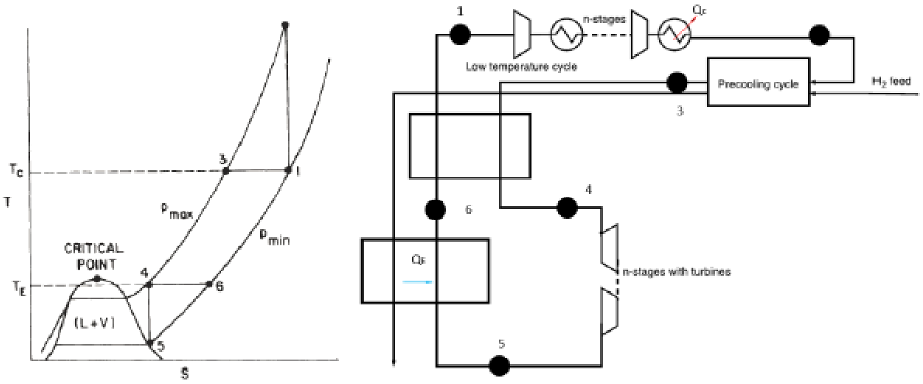

Figure 16. Reversed Brayton cycle, here integrated with H2 feed stream; and general representation on a Temperature-Entropy diagram [15]

3.4.4. Kleemenko

The term Kleemenko cycle (Figure 17) is used if a biphasic mixed refrigerant (MR) stream is used to cool down the working fluid. The phase separation enables to use the latent heat of the liquid MR, which is further throttled to reach colder temperature. The MR cycle is closed, and the mixture should be biphasic at ambient temperature. The Kleemenko cycle is only used for precooling up to 130K and cannot be used to liquefy hydrogen, as the hydrocarbon mixtures freeze under 160-130K.

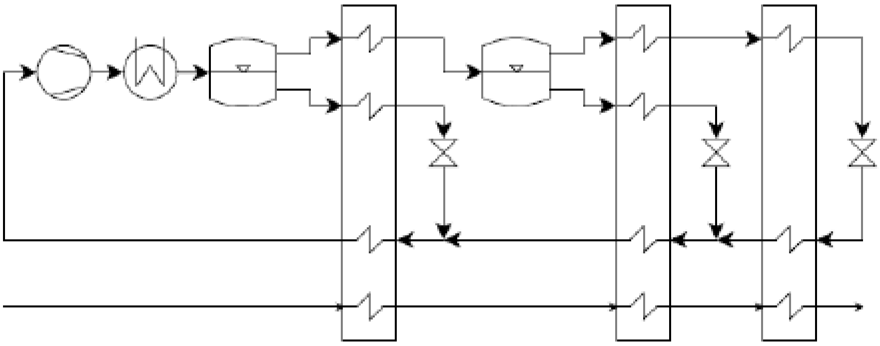

Figure 17. The dual pressure Kleemenko cycle

3.5. Hydrogen liquefaction process main units

3.5.1. Catalytic Plate-Fin Heat Exchangers (CPFHX)

Industrial hydrogen liquefiers are multi-stream aluminum brazed plate-fin heat exchangers. They work in countercurrent flow. Their main advantages are the compatibility with the cryogenic process conditions and fluids in hydrogen liquefiers[16]. Furthermore, a high-specific surface (500 – 1800 m^2/m^3), lower pressure drops and small temperature differences between warm and cold streams make this technology highly efficient. Finally, due to the cooling and continuous catalytic conversion of the hydrogen in the PFHX, a thermodynamically more efficient conversion close to the equilibrium is achieved using catalyst material.

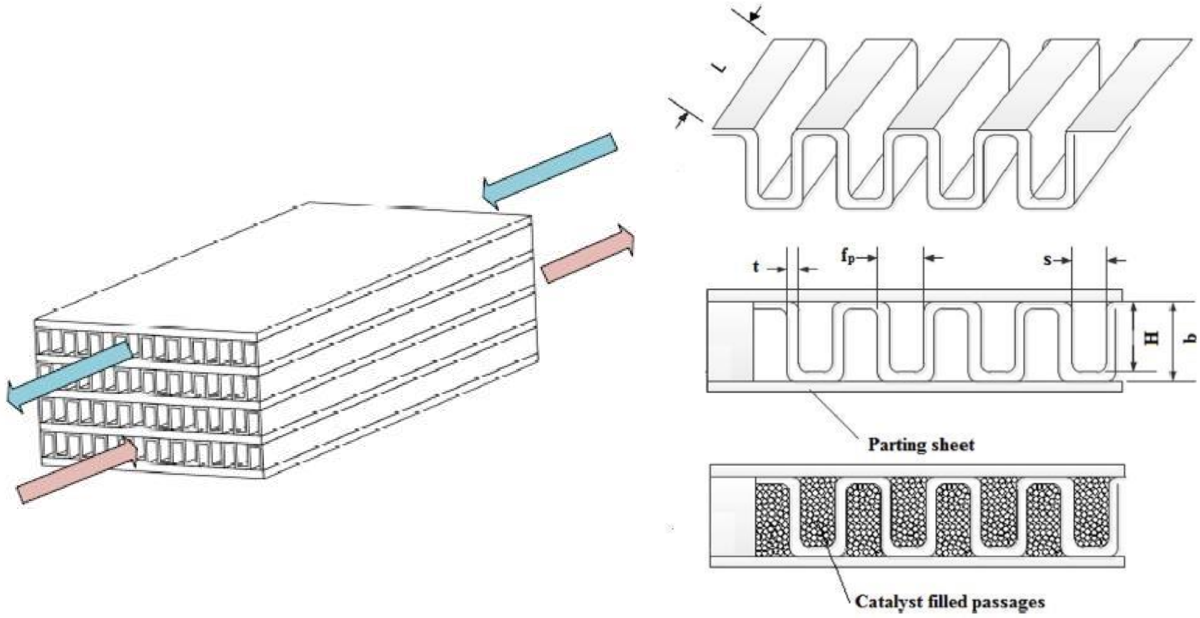

Figure 18. Catalytic plate-fine heat exchangers structure

It has been demonstrated in Fundamentals of Heat Exchanger Design (R.K. Shah, 2003) that a 1% increase in the effectiveness of a cryogenic heat exchanger, used in an air separation plant, decreases the compressor power consumption by 5%. If such a result can be extrapolated directly to hydrogen liquefaction heat exchangers, innovation to increase their performance might represent a lever for reducing cost of liquefaction.

3.5.2. Mechanical compressors

The work input required to provide refrigeration to the hydrogen liquefaction process is partly carried out by the compression of the refrigerant fluid with compressors. Common and current type of compressors used in hydrogen liquefiers are reciprocating piston compressors and rotary screw compressors [17]. Those compressors are restricted in the maximum feasible capacity. If it has been seen that refrigerant fluid can have a strong impact for the optimization of compressors electrical cost, the further development of compressors themselves adapted to hydrogen liquefaction seems unavoidable for a real amelioration of the process competitivity.

3.5.2.1. High pressure ratio compressors

The compression pressure ratio is mainly limited by the maximum allowed outlet temperature after each compressor stage, which is typically limited to values between 410 and 430K. For hydrogen compression, pressure ratios between 2 and 3 can be implemented. Multi-stage reciprocating piston compressors with up to 4 compressor stages with inter-cooling are typically installed. This restriction mainly comes from elastomer used in mechanical part of the compressor (internal study). Implementation of high temperature handling elastomers might be a way to improve compressors efficiency. To the knowledge of the author at the time of writing, no research seems available on this thematic.

3.5.2.2. Cryogenic compressors

As another possibility, the development of sub-atmospheric temperature handling elastomer would allow to create a new type of compressors: cryogenic compressors. Reducing inlet temperature of the fluid increases its volumetric flow allowing a more efficient work of the compressor. Furthermore, intercooler working at sub-atmospheric temperature would be boosted. To dive compressors in such an environment, the necessity of a cheap cold power is however inevitable. Some ongoing studies on the coupling between the LNG regasification and the H_2 liquefaction could allow the use of this technology.

3.5.2.3. Turbo compressors

The axial-flow turbo compressors are one of the two type of turbo compressors, the radial-flow turbo compressors being inadequate in the volumetric flow involved for large scale hydrogen liquefaction plant. It is employed for low operating pressures (limited to 20 bar) and works in a range of volumetric flow between 1000 m^3/h and 200 000 m^3/h. It can then be implemented for larger production of liquid hydrogen (from 5 up to 450 tons per day). It can achieve an isentropic efficiency of 0.88. It presents then both high efficiencies and low capital investment while being particularly appropriate for the next decades scalability.

3.5.3. Alternative compression: metal hydride compression

Metal Hydride (MH) hydrogen compression is based on a heat-driven reversible reaction of a hydride-forming metal, alloy, or intermetallic compound with hydrogen gas to form MH. This technology, which initially arose in early 1970s, still offers a good alternative to both conventional (mechanical) and newly developed (electrochemical, ionic liquid pistons) methods of hydrogen compression. MH compression benefits are its simplicity in design and operation, its safety and reliability and there are no mechanical parts[18]. Moreover, the process consumes heat that could be provided by industrial waste heat instead of electricity.

Applications of metal hydrides, including hydrogen compression, utilize a reversible heat-driven interaction of a hydride-forming metal/alloy, or intermetallic compound (IMC) with hydrogen gas, to form a metal hydride:

$$M(s) + x/2\,H_2(g) \underset{\text{desorption}}{\overset{\text{absorption}}{\rightleftarrows}} MH_x(s) + Q;$$

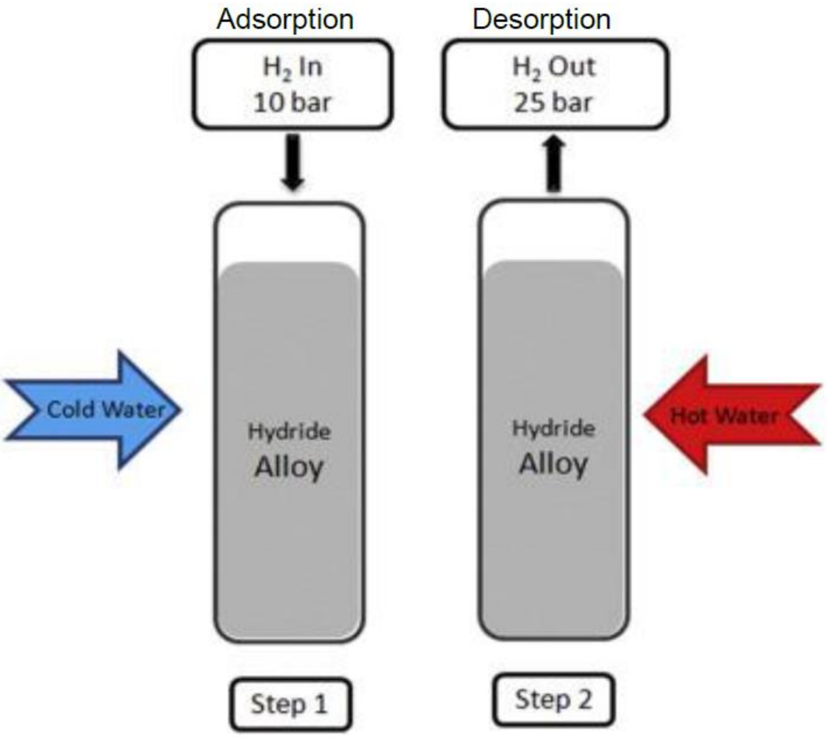

Figure 19. Hydrogen chemical compression with metal hybrid system principle

Main parameters of this operation are the type of metal hydride, the heat provided for the desorption and the inlet pressure which will define the pressure ratio. In the case of the Linde process, an intermetallic compound belonging to AB5-type has to be selected such $LaNi_5$ or $MmNi_{4,8}Al_{0,2}$ since this category generates pressures in the range of 2 to 200 bar.

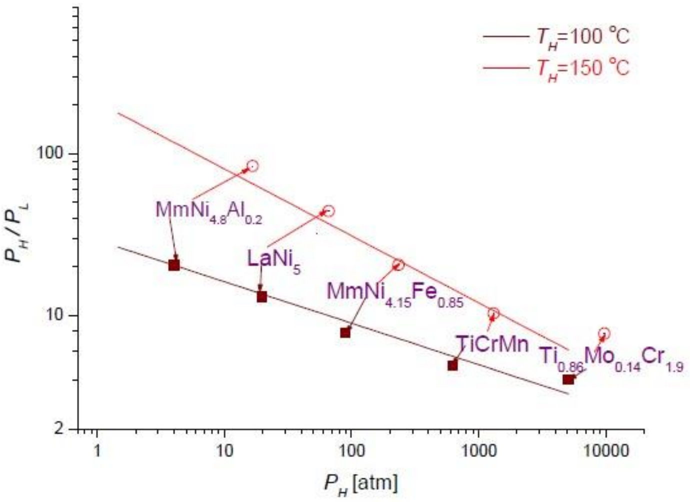

Figure 20. Ratio pressure for different intermetallic compounds[18]

As seen in Figure 20, a pre-stage would be needed to increase the pressure which could be completed with another type of metal hydride or a mechanical compression. The principal drawback is the current low capacity of proofed system since the maximum scale tested is 15 m^3/h but the development brings continuous amelioration for scale increase.

3.6. Existing plants

Hydrogen liquefaction is energy-intensive and low efficiency of equipment and processes represents nowadays the main obstacle to the realization of a hydrogen economy. Besides pressure, temperature and ambient conditions, the liquid-product exergy content is also dependent on the composition of hydrogen (o-H_2 and p-H_2 content).

Given a feed stream of n-H_2 at ambient conditions of 1.0 bar and 300 K, the thermodynamically ideal minimum specific power required to obtain saturated liquid at 1.0 bar (20.23K) and equilibrious ortho-para composition, equals 3.94 kWh/kgLH_2. The contribution from conversion of ortho-to para-H_2 corresponds to 0.59 kWh/kgLH_2 or about 15% of the total reversible work. Commercial LH_2 production normally operates with a product para-fraction of at least 95% (the equilibrium hydrogen composition at 33K) to have an acceptable boil-off rate during storage. In the higher end, Quack proposes in his conceptual plant an equilibrium composition for saturated liquid at 1.0 bar, corresponding to a para content of 99.8% [19].

In the following subsections the major existing plant will be presented and described.

3.6.1. Linde process description

Linde owns two LH_2 plants in Germany: one in Ingolstadt, built in the '90s and one in Leuna built in 2008. The Linde Leuna liquefaction system consists of a Claude-Brayton cycle. It consists of eight heat exchangers: the two first heat exchangers are responsible for the precooling stage, where the GH_2 is cooled from the feed temperature (around 298K, 21 bar) to 80K with the use of an open-cycle LN_2 refrigerant stream and the refrigerant H_2 of the cycle. The feed GH_2 stream is then cooled down in the following HEXs until around 20K and then liquefied with the help of a JT expansion to 1.3 bar. The ortho-to-para conversion is performed in the HEXs which are filled with catalytical materials and allow to reach the desired p-H_2 content in the final product. The scheme of the aforementioned process is showed in the following Figure 21. Total specific consumption of the plant is around 12 kWh/kg$_{LH2}$.

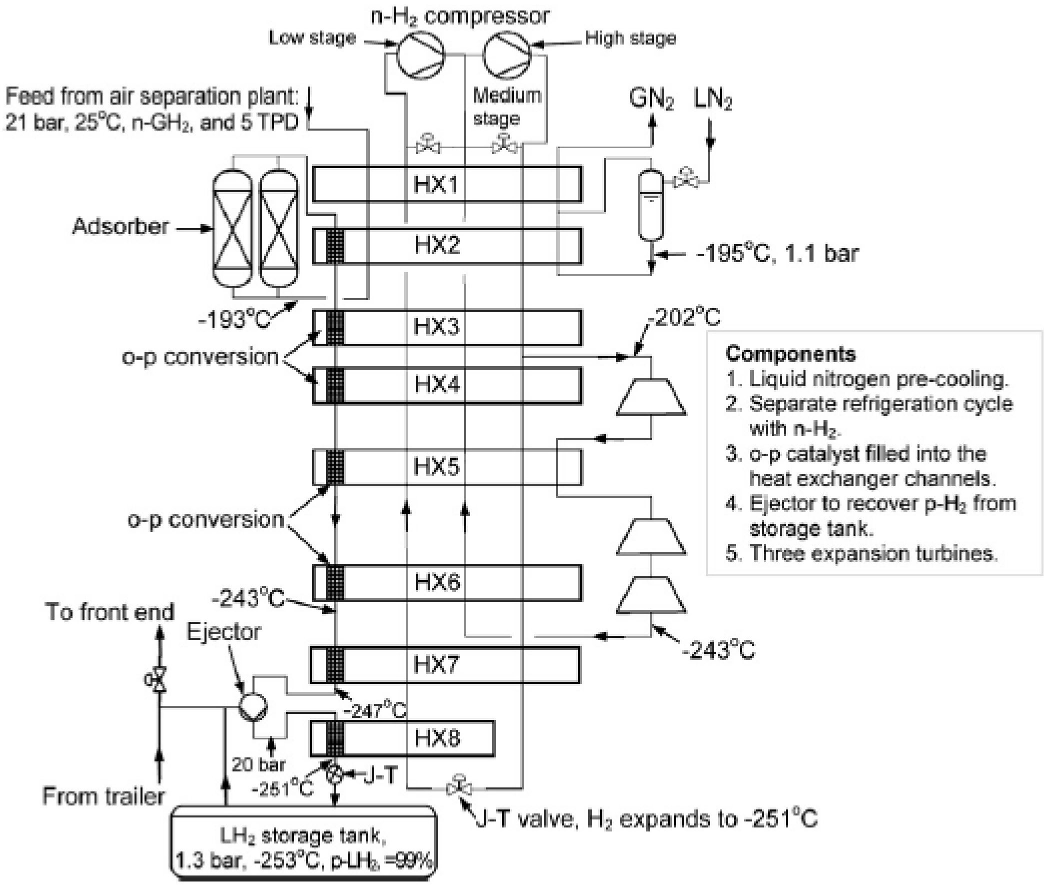

Figure 21. PFD of hydrogen liquefaction plant in Leuna [20]

3.6.2. Praxair process description

Praxair has five hydrogen liquefaction plants in the US today with production rates between 6 and 35 TPD LH_2. Typical specific power consumptions are between 12.5 and 15 kWh/kgLH2. Figure 22 shows a Praxair LH_2 process flow sheet. It consists of three heat exchangers. The first heat exchanger is cooled by nitrogen gas (GN_2) and an external refrigeration system. The second heat exchanger is cooled by liquid nitrogen (LN_2) and some of the H_2 feed. The third is only cooled by a hydrogen refrigeration system that uses some of the feed to expand through turbines and the Joule–Thomson (J–T) valve[20].

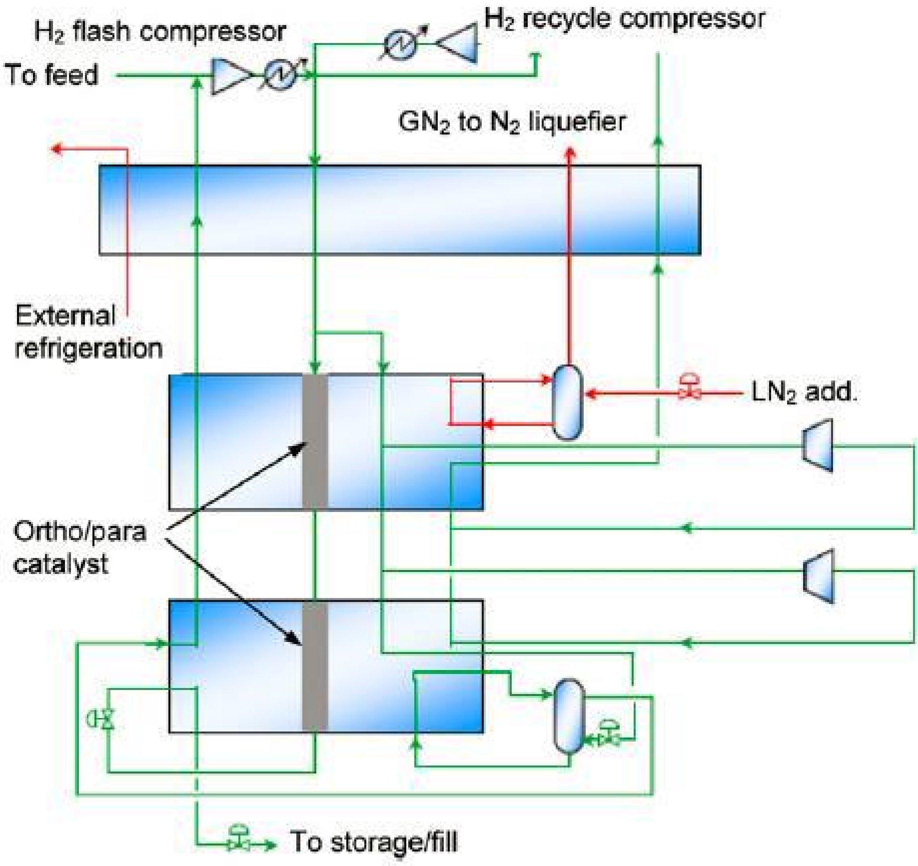

Figure 22. Praxair hydrogen liquefaction process[20]

3.6.3. Air Products process description

Air Products plants are designed for a production of around 20-30 TPD, with a specific energy consumption of 12-15 kWh/kg_{LH2}. The GH_2 is fed at 305K and 18 bar. It passes four heat exchangers, two of which are filled with catalyst material to perform o-p H_2 conversion to over 95% para content. The precooling stage is performed with the use of an open LN_2 cycle combined with a compressed Neon loop, which is afterward expanded to provide cooling power. The scheme of the process is shown in the following figure 23.

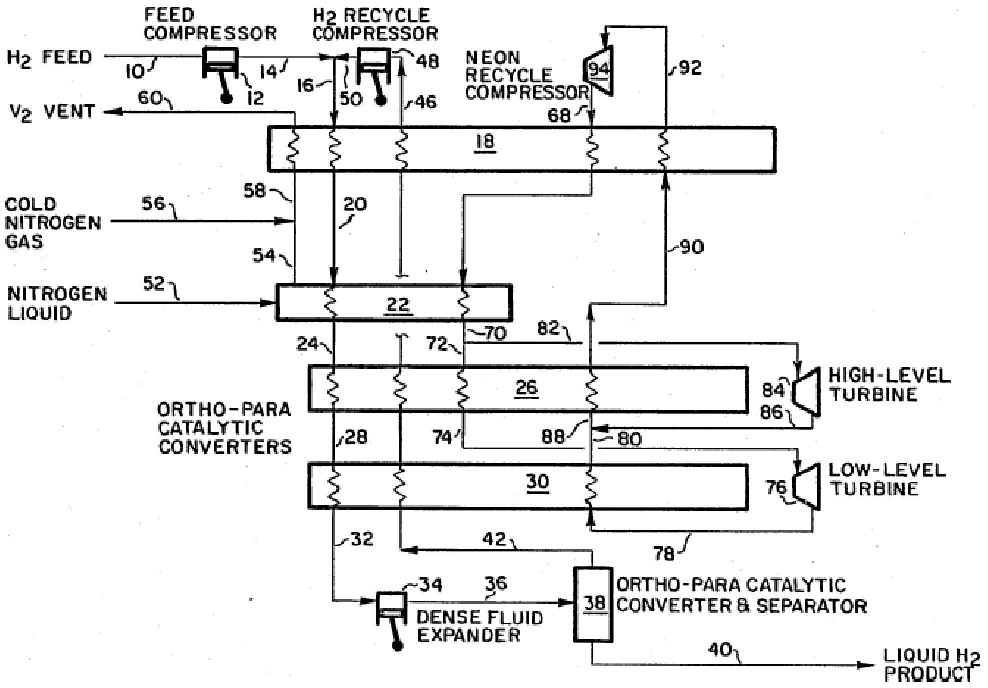

Figure 23. Air Product liquefaction process PFD, US Patent n° US4765813, 1988.

3.6.4. Kawasaki process description

Kawasaki Industries has developed a liquefier system that can be used to produce 5TPD of hydrogen, helium, or neon (Figure 24). The liquefier system includes: a raw material tank, a liquefied hydrogen tank, a feed line, a plurality of heat exchangers, a liquid reservoir, and a cooling medium circulation line. The raw material tank 1 is a source of supply of the raw material gas and stores the hydrogen gas at a normal temperature and pressure. The liquefied hydrogen tank stores liquefied hydrogen which is obtained by liquefying the hydrogen gas. A feeding compressor and a Joule-Thomson valve are provided on the feed line. Between the feeding compressor and the Joule-Thomson valve, the feed line extends sequentially through the five heat exchangers to and the liquid reservoir.

The cooling medium for cooling down the raw material gas circulates through the cooling medium circulation line 5. The cooling medium circulation line forms a closed loop, and the hydrogen gas that serves as the cooling medium circulates through the cooling medium circulation line.

The patent does not specify how the ortho-para conversion is realized. Some of the heat exchangers are probably catalytic ones. No figures are given on energy consumption, para content, temperature, flowrate, or pressure. Thus, the process could not be simulated.

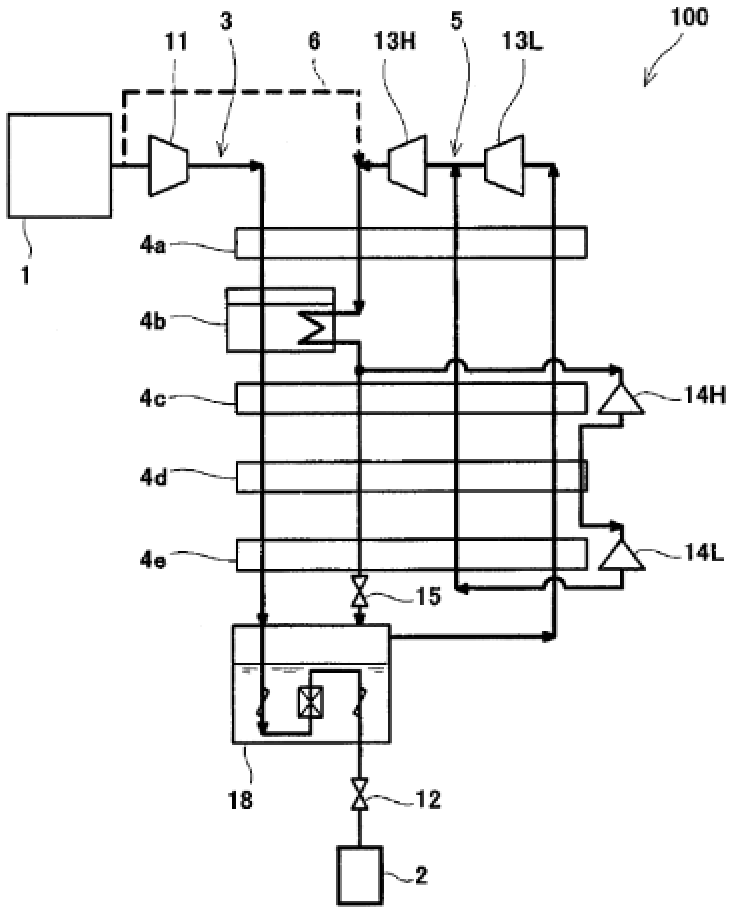

Figure 24. Kawasaki liquefier process (USA Brevet n° US95988536, 2017)

3.6.5. Conceptual plants

Ongoing study and development of LH$_2$ have led to propositions of different types of cycles and use of various refrigerants with the purpose of reducing the Specific Energy Consumption of the process. Conceptual plants are more efficient than the one in application. SEC are lower, usually about 7 instead of 12-15 kWh/kg$_{H2}$. The conversion to p-H$_2$ is usually higher than 95%, which means that the conversion also takes place in liquid phase. Unlike in the actual plants, many research are focusing on the use of Mixed-Refrigerants or Ne/He as precooling system. Conversion often takes place in a continuous way, or continuously after a first adiabatic stage at 130-80K. Some examples are represented by the conceptual plants proposed by Quack (2002, SEC equal to 7.39 kWh/kg$_{LH2}$)[21], Berstad et al. (2013, SEC equal to 6.3 kWh/kg$_{LH2}$)[19] and Krasae-in (2014, SEC equal to 5.91 kWh/kg$_{LH2}$)[22].

A comparison between the usual values of the SEC for the different existing and conceptual plants is showed in the next Figure 25.

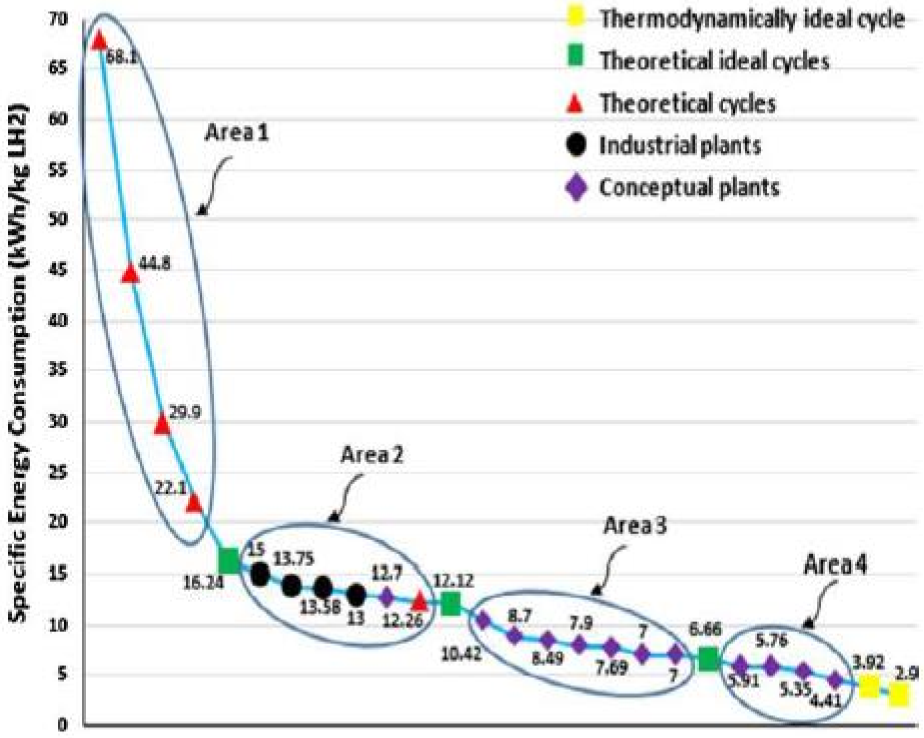

Figure 25. SEC comparison of the different LH_2 technologies[14]

4. The issue of process flexibility

The increasing development and use of renewable energies could drive away the necessity of the industry to be dependent on fossil fuels-based energy and reduce their usage. The penetration of renewable energies is however still difficult, since generally chemical processes operate continuously at steady state with a constant energy demand, operation that could be incompatible with the intermittent nature of some renewable energies, such as wind and solar energy[23]. Moreover, the storage costs for energy and raw materials, in particular gases, that could mitigate the impact of these variations on the process operability, are relatively high [24]. For these reasons, in recent years, an increasing interest in development of flexible processes has risen. The purpose of these studies is to design a process that can be able to “adapt” to certain parameters variation remaining in an acceptable range of operability and without undergoing a dramatical increase of operative costs. Two types of studies are possible and presented in the scientific literature: the flexibility analysis, i.e., an investigation of the flexibility ranges and allowed parameters’ variations of an existing plant and process; the flexible process design, i.e., the conception of a new process considering a certain number of uncertainties in chosen parameters. For the latter conception, one of the approach that has been conducted is a theoretic and mathematical one: this type of problem can represented as a multi-objective non-linear problem which can be presented with complex a model and resolved by using algorithms such as the Genetic algorithm methods[25], [26], [27]. Even if this approach can help to propose a flexible design of a given process, it will not be used in this work due to its difficulty of applicability to the concerned liquefaction process.

For what concerns the green hydrogen liquefaction, as already mentioned, the process is dependent on the intermittent nature of the renewable energies when they are employed in water electrolysis processes to produce GH_2. Obviously, the processes that uses hydrogen produced via steam reforming or other technologies based on the exploit of fossil fuels are not impacted by this problematic, since the flowrate and the conditions of the feed gas entering the liquefaction train are constant during time. The feed flowrate variation can cause problems to the operative units, that couldn’t be ready to work at off-design conditions or work with an efficiency such that the energetic costs or the final product are not acceptable. A solution generally implemented to reduce the variability of the feed gas is the implementation of an external storage of CGH_2 which can be used to stock the surplus of hydrogen produced during the periods of overproduction, which is afterward supplied during under-production periods. This is a common solution adopted by many processes that uses hydrogen as raw materials, such as methanol[23], [28] and ammonia production[24], [29]. The downsides of this technology, costs, and volume of storage, have already been presented in section 3.1. and the implementation of this technology in the LH_2 chain have already been investigated with an internal study [30] which resulted in unacceptable increase of costs which make this solution inoperable in this type of process.

It is therefore necessary to study the various methods and solutions that allow to improve the process flexibility or allow to mitigate the impact of the aforementioned variation on the operability of the plant.

4.1. State of art of flexibility in gas liquefaction processes

The literature studies regarding the various mentioned problematics related to process flexibility it is not wide enough when the application field is the gas liquefaction. Indeed, most of the publications are related primarily on the flexibility analysis and comparison between already existent processes, which have been designed without considering parameters variation. Moreover, hydrogen liquefaction process flexibility has almost not be treated in the scientific literature, where the studies are restricted mostly to the LNG production. The results obtained by these works should then be applied to the LH_2 processes to evaluate if their impact on the operability of the process can be considered significant or if they are merely restricted to the LNG technologies.

As examples of these works, it can be cited studies where different LNG technologies have been compared, as in the cases of the studies of He et al.[31] and in the study of Eini et al.[32]. In these cases, two LNG cycles have been compared, each of them using a different refrigerant technology. The two cycles compared were the Parallel Nitrogen expander cycle (PNEC), using nitrogen as refrigerant, and the Single Mixed Refrigerant cycle (SMR), which uses a refrigerant composed of a mixture of hydrocarbons. Overall results showed that the latter solution allowed a wider range of operability, thanks to the possibility to modify the refrigerant composition thus adapt it to the variation of some process parameters. The application of this solution to the LH_2 process will be limited to the precooling stage, where the solution is already been implemented in some of the aforementioned conceptual plant but without the publication of results of the impact of the process flexibility parameter.

In the study of Sun and Ding[33], it is stated that the operability ranges of a LNG process are mainly based and limited by the operability ranges of the compressors. Indeed, compared to other units presents in the process, like heat exchangers, the operability ranges of these units are limited and therefore they are responsible for the overall operability ranges of the liquefaction process. This assertion has found confirmation in other scientific publications, which presented the value of 60% of the nominal condition as a working limit for the classical fixed speed compressors used in these plant [34], and with internal discussions with suppliers of these technology. The implementation of compressors technologies which allow to have a larger operability range, such as variable speed technology compressors, seems to have a positive impact of the energetic consumption of the plant working at off-design conditions. For example, such types of compressors allow to obtain energy savings that can go up to around 40% at part-load conditions compared to the situation where no load adjustment methods are included in the compression stage. This solution will be explored in a more detailed way in Section 6.5.

Another work related to the LNG process designed proposed by Lee et al.[35] highlights the possibility to approach the design of a process considering possible load variation from the nominal production value over a fixed period of time. This type of approach considered in the paper allowed to reduce the total costs of the process when the load is kept for long periods under 80% of its nominal. This shows the impact of such approach when the profile production is not constant over time, as for the GH_2 production from intermittent resources.

Even though the literature about this subject is not wide, some of the solutions that have been proposed in the LNG processes and some of the major problematic related to operability ranges can nevertheless be applied and evaluated in the $LH_{2,}$ to estimate their impact on the energetic consumption and costs of the considered process.

4.2. Overall remarks on the literature

As an overall summary of the literature of the subject, it is possible to state that the improvement of the process flexibility represents a difficult challenge to face due to numerous factors that can decrease the process efficiency and therefore increase dramatically the costs. One of the main problems related to the off design working conditions is represented by the decrease in efficiency of some units, since they are not designed to work at such conditions. This is the case for example of the compressors, where the efficiency decrease is important if no adjustment methods are implemented, making the specific energy consumption of the unit too huge and thus incompatible with the needs of the process. Solutions such as the implementation of variable speed compressors allow to reduce this decrease in efficiency and thus have better specific energy consumption in the process.

Other equipment that are generally involved in the liquefaction processes, and in particular the LH_2 process, are the heat exchangers, turbines and the J-T valve used for the expansion of the compressed hydrogen to perform the liquefaction in the final stage of the process. For what concerns the J-T valve, the part load conditions don't represent a problematic in the management of the process, since the possibility to modify the %rate of opening allows to adjust the pressure drop to the flowrate variation. The valve must be sized properly in this case and controlled in order to avoid possible clogging problems and unwanted pressure drop values. The turbines can be as a first hypothesis considered with a similar behavior at off-design conditions of that that of the compressors, so the decrease of efficiency can be calculated in the same way as a first hypothesis. Obviously further studies are necessary to determine the real behavior of such machines, in order to evaluate better results.

Lastly, heat exchangers have a wider range of operability if compared to compressors, based on internal discussions with HEXs suppliers, and therefore they can be considered flexible for the following studies. The main regulation will therefore perform on the management and variation of the various streams flowrate to maintain acceptable conditions in the overall process and to avoid the problematics that will be presented in Section 6.6. The methods, obtained by the presented literature that can therefore be used to improve the process flexibility and allow a better functioning at off design conditions are summarized in the next 3.

Table 3. Main units' flexibility ranges and summary of off-design mitigation solutions.

	Compressor	HEX	Valve	Internal	External
Flexibility range	60 – 120 %	0 – 200%	0 – 100%		
Mitigation Solutions	Throttle Valve Frequency variation Increasing the number of parallel units MR composition variation	Flowrates and temperatures management Increasing the number of parallel units MR composition variation	Increasing the number of parallel units	Intermediate storage of products and management of the refrigerants' flowrate	External GH_2 buffer

5. Purpose of the study

The presented state of art showed how liquid hydrogen could represent a promising energy carrier and storage solution. Even though gaseous hydrogen is mainly produced from fossil fuels via steam reforming, the increasing interest and development of renewable energies has risen new necessities in terms of energy storage. This energy could be used to produce GH_2, and its liquefaction has been indicated as one of the possible solutions to solve the energy storage problematic. Even though the use of liquid hydrogen could represent an important actor of the Power to Gas from renewable sources technologies development, no studies have been conducted on the H_2 liquefaction from an intermittent source and its feasibility has not been clearly assured. The issue of the flexibility has not yet been considered for what concerns the LH_2 process and therefore it is not clear the possibility (technical and economical) to perform such processes.

The objective of this study is therefore to study in the first place the impact of the use of a varying source in the liquefaction process. In particular, the interest is to evaluate the technical and economic impact caused by possible off-design working conditions of an existing plant due to the penetration of intermittent sources. Moreover, this study aims to explore some of the solutions proposed in other processes, such as processes that use H_2 as a raw material or gas liquefaction processes, such as LNG (Liquefied Natural Gas) processes, and to adapt them to the LH_2 process to evaluate their impact.

The objective of the work is thereby to investigate the behavior in these conditions of the various units that are commonly used in the liquefaction process. Finally, thanks to the possibility to perform simulations of the considered processes on a process simulation software (Aspen Hysys®), economic and energetic parameters will be evaluated for the different scenario.

The study will be conducted considering simplified assumptions and processes, in particular related to the considered off-design conditions of rotary machine, that would need a more detailed study and confrontation with suppliers of these technologies to define not only the efficiency variations, but also the impact of other parameters such lifespan and fatigue.

6. Methodology and problem modelling

To evaluate the energetic and economic impact of the off-design conditions and the different solutions to improve the process flexibility, simulations of the aforementioned processes and studies of the behavior of the various operative units, in particular compressors and heat exchangers, have been conducted.

For instance, the behavior of the compressors under part-load conditions and its efficiency variation at different load conditions have been investigated.

The details of these studies are presented in the next sections.

6.1. Considered liquefaction cycle

In the following simulations and relative analysis, the liquefaction cycle used as base case is the Linde Leuna liquefaction cycle presented in section 3.6.1. A more detailed explication of the abovementioned cycle is given in this section. The PFD of the process is shown in the following Figure 26.

The GH_2 feed enters the process at 290K and 21 bar. It passes through eight heat exchangers where it is cooled down to 21K. Afterwards, a Joule-Thomson valve allows to perform an expansion which provide LH_2 at 1.5 bar. Starting from the second, the heat exchangers are filled with catalytical material which assure the ortho-para conversion that is performed along the liquefaction process. The p-H_2 content at the exit of the process is around 98.4%. The two first heat exchangers are used for the precooling part. The GH_2 feed is cooled down to 80K in this stage and this cooling is performed using liquid nitrogen (LN_2). Nitrogen is provided to the process with an open cycle. The hydrogen used as a refrigerant in the cycle has a composition equal to n-H_2. It is compressed in the compression stage at around 30 bars using two intercooled (at 290K) stages of compression and it is cooled down alongside the GH_2 feed until the seventh exchanger. The stream undergoes an expansion in three turbines which power is hypothesized to be recovered and used as an energy source for the compressors. It is then expanded and liquefied using a J-T valve and used as a refrigerant in the cycle. The detailed calculation concerning energetic consumption and costs of the process are presented in section 7.

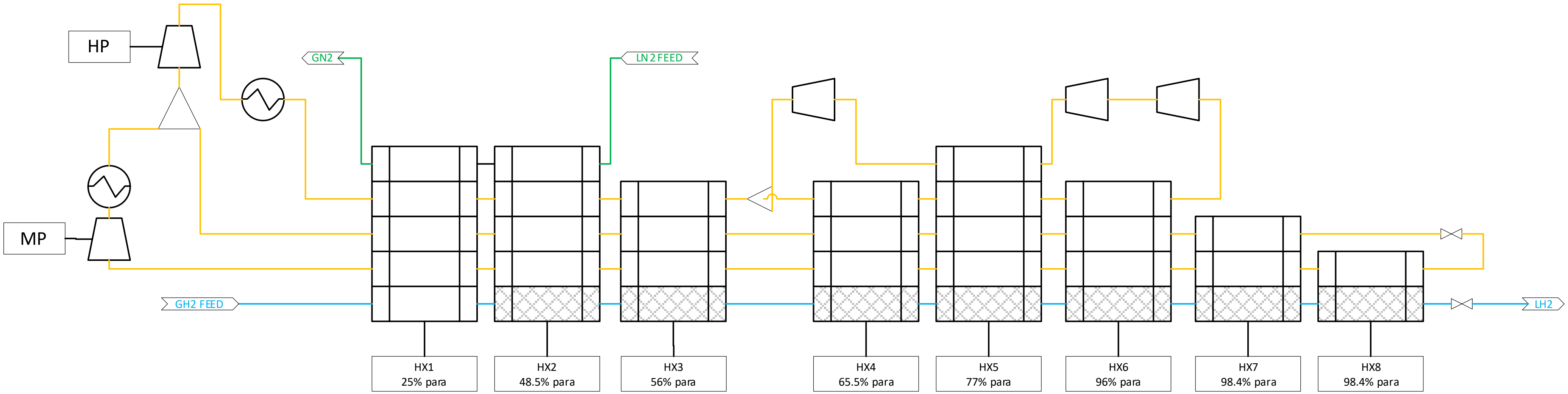

Figure 26. Linde Leuna PFD

6.2. Simulation hypothesis and procedure

Gaseous feed hydrogen (GH_2) is fed to the liquefaction unit at 21 bar and 290K with a composition equal to the normal hydrogen ($n-H_2$) composition: 25% $p-H_2$ and 75% $o-H_2$. The feed is converted inside the cooling part of the process along with cooling and liquefaction to around 20K and 1.5 bar. The $p-H_2$ content is higher than 95% at the outlet.

All the simulations are performed using Aspen Hysys® software with the following assumptions.

- H_2 is fed at 21 bar and 290K. LH_2 is supplied at 21K and 1.5 bar.
- Stream properties are constant.
- Compressors' isentropic efficiency is fixed at 80% when the process is simulated at its nominal conditions. Electrical-to-mechanical efficiency of the compressors is set at 95%
- Expanders isentropic efficiency is set at 85% and it is assumed a complete recovery of the produced energy that can be supplied to compressors.
- Pressure drops in pipes are neglected
- The temperature of streams exiting from the same side of the heat exchangers are considered to be equal.
- Isomer composition of refrigerant hydrogen is assumed to be equal to $n-H_2$ composition along the process
- The lowest value of the minimum approach of heat exchangers is established at 2K, except for the last heat exchanger due to easier heat exchange.
- A pressure drop value of 0.1 bar for every stream in the HEX has been considered (based on literature [36] and internal analysis).

6.2.1. Choice of the thermodynamic model

In the considered liquefaction cycles, three different main streams are considered: GH_2 feed that is cooled down and liquefied which undergoes ortho-para catalytic reaction, H_2 refrigerant and N_2 refrigerant present in the pre-cooling part of the process. For what concerns the two hydrogen streams, the former has its composition changing along the process with the conversion that takes place in the heat exchangers of the cooling part, the latter has a fixed composition that is considered equal to the $n-H_2$ composition. The thermodynamic model chosen for the H_2 streams was MBWR (Modified Benedict-Webb-Rubin) advised by Aspen Hysys® support. To simulate the N_2 stream, Peng-Robinson model has been chosen. It is the most enhanced thermodynamic model available in Aspen Hysys® with a large applicability range in terms of temperature and pressure ($T> 2K$, $P< 1000$ bar), but it does not include the ortho and para specifications and the behavior of the ortho-para mixture it is not aligned to the one described in publications, and therefore it cannot be used to simulate the conversion of the H_2 along the liquefaction process.

In the following Table 4 are resumed the properties of the hydrogen allotropes obtained from Aspen software databank.

Table 4. Properties of hydrogen allotropes, from HYSYS® databank

Properties	p-H2	o-H2	n-H2
Molecular weight (g/mol)	2.016	2.016	2.016
Normal boiling point (K)	20.27	20.43	20.39
Ideal Liq density (kg/m^3)	70.84	70.55	70.57
Heat of formation @25°C (kJ/kmol)	58	-	-
Heat of combustion @25°C (kJ/kmol)	-2.419e5	-2.418e5	-2.419e5
Enthalpy basis offset (kJ/kmol)	-9325	0	-8288
Mass vapor enthalpy (ideal gas at 0K) = $a+bT+cT^2+dT^3+eT^4+fT^5$ (kJ/kg) (heat of vaporization)	0/1.67668e1/ -5.35667e-3 /5.74841e-6/ -2.76062e-9 /5.49333e-13	0/1.0796e1/ 1.98671e-2/ 3.82053e-5/ 3.13544e-8/ -8.86155e-12	-49.68312/ 13.83761/ 2.999806e-4/ 3.45893e-7/ -9.712927e-11/ 7.731201e-15
T^C (K)	32.98	33.26	33.19
P^C (bar)	12.93	13.20	13.13
V^C (m^3/kmol)	0.06414	0.0641	00641
Acentricty	-0.2208	-0.2144	-0.2160
Viscosity coefficient a/b	-0.00296/0.2833	0.00701/0.2926	-0.36739/0.13233

As a side note, when H_2 is in supercritical conditions (over 13 bar and 33K), Aspen Hysys® identifies H_2 as a vapor phase, but with no repercussion during the calculation of fluid properties.

6.2.2. Ortho-to-para conversion modeling

In Aspen Hysys it is not possible to perform the simulation of a chemical reaction inside of a heat exchanger, therefore it is not possible to properly recreate the conversion occurring in a real plant. For this reason, based on internal work, it has been decided to couple the heat exchangers with adiabatic reactors where the ortho-to-para conversion of H_2 occurs. The conversion considered by Hysys has a polynomial form:

$$Conversion\ (\%) = C_0 + C_1T + C_2T^2 \tag{3}$$

At a given temperature the H_2 equilibrium composition can be calculated using the following correlations.

For 10K < T < 50K

$$\%pH_2 = -0.0169T^2 + 0.4747T + 97.209 \tag{4}$$

For T > 50K

$$\%pH_2 = \frac{25 * 9.7016 * 10^{-7} T^{3.331496} + 100}{9.7016 * 10^{-7} T^{3.331496} + 1} \tag{5}$$

Thanks to these correlations it is possible to calculate the p-H_2 content at the outlet temperature of each heat exchanger. It is assumed that equilibrium is reached in every HEX and therefore it is possible with a conversion reactor to simulate this reaction. Since the outlet temperatures of the HEXs are fixed, the equilibrium composition can be calculated using the presented correlations that allow to obtain the % of o-H_2 that is converted into p-H_2.

Since the reaction is exothermic, the generated heat should be considered in the heat transfer process. To perform the simulation, the outlet HEX stream is sent to the adiabatic reactor where the conversion is performed. Hysys calculate the corresponding heat transfer and the corresponding increased temperature of the stream at the outlet of the reactor. This stream passes again through the previous HEX to be cooled down at the same temperature of the stream entering the reactor. As a result, the exothermic nature of the reaction is correctly considered through the process.

A scheme of the presented HEX and reactor coupling is showed in the following Figure 27.

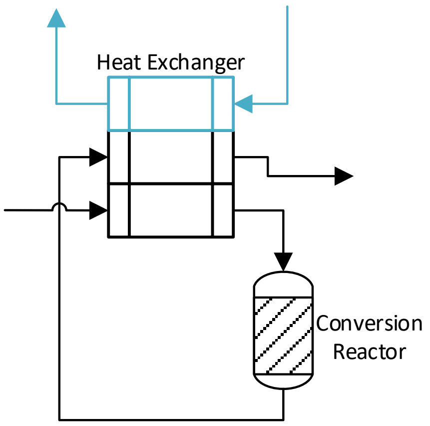

Figure 27. Schematic of the ortho-para conversion using a conversion reactor

6.3. Economic calculations

6.3.1. Economic model

The objective of the study is to estimate the LH_2 production cost in the various scenario considered. This study has been validated in the restricted context of empirical relationships based on internal data related to previous studies conducted on LNG at CRIGEN and on an economic analysis of hydrogen liquefaction systems published by the International Association for Hydrogen Energy (SYED, SHERIF, VEZIROGLUS, & SHEFFIELD, 1998). To evaluate liquid hydrogen price, it will first be necessary to evaluate the equipment costs, that will determine the plant's CAPEX and OPEX. Finally, liquid hydrogen price will be estimated by an NPV calculation (Net Present Value).

For what concerns the CAPEX parameter, it is possible to define the final CAPEX, which resumes the installed liquefaction costs of different parts of the plant. In particular it is possible to divide the costs into:

- **Major equipment**. Equipment costs that will be determined through this study are the most expensive ones: compressor, turbine and cryogenic exchanges lines.

- **Collateral equipment**, which are chillers, valves, pumps and piping.
- **Equipment installation**. The installation includes engineering costs, construction, insurances and unexpected events.
- **Complete plant installation**. The plant includes the liquefaction process, the pretreatment, liquid hydrogen storage and utilities (feeding, electricity, buildings,).

The CAPEX formula can therefore be defined as

$$CAPEX = ME_{costs} * f_{coll} * f_{inst} * f_{comp} \tag{6}$$

The different factors of the presented formula refer to the aforementioned considered costs and their value is based on internal economic models and therefore confidential.

For what concerns the OPEX parameter, this is divided into:

- Fixed OPEX, representing maintenance and labor costs.
- Variable OPEX, representing utilities, especially

The liquid hydrogen price will be the one for which the NPV is equal to 0. NPV is the addition of the plant cash-flows along its life, containing all the investments cost, depreciation, and aging. Thus, NPV is related to the plant CAPEX and OPEX and to the following financial assumptions:

- Plant lifetime: 20 years
- Use/availability rate: 85%/year
- Actualization rate: 10%
- Imposition rate: 35%
- Inflation rate: 1%

6.3.2. Energetic and economic parameters

The key parameters that will be considered and presented on this study are the Specific Energy Consumption (SEC) and Specific Liquefaction Cost (SLC). The former allows to calculate the energetic performances of a given process. It is defined as the energy necessary to perform the production of a kilogram of liquefied hydrogen. Since hydrogen liquefaction is a great energy-consuming process, this parameter results to be critical to define the level of optimization of a process. For instance, the theoretical minimum specific power amounts to 3.94kWh/kgH2 for the transformation of normal hydrogen at 300K into saturated liquid hydrogen (≈20K, -253°C) with an ortho-para composition in equilibrium and feed and product stream at a pressure of 1 bar. The SEC, measured in kWh/kgLH2, is defined as follow:

$$SEC = \frac{Liquefaction\ required\ power}{LH_2 mass\ flow} \tag{7}$$

The required power represents the sum of the compressors and the expanders correspondent powers.

For what concerns an open precooling cycle, which does not include energetic costs related to the compression of the precooling refrigerant fluid, this one is considered into in the SEC calculation as follow:

$$SEC_{Precooling} = \frac{Precooling\ refrigerant\ cost}{Electricity\ cost} * \frac{Precooling\ refrigerant\ FLow}{LH_2\ mass\ flow} \tag{8}$$

The total SEC will therefore be the sum of the SEC of the precooling and the cooling part of the process.

The SLC is defined as the minimum price liquid hydrogen should reach to obtain a neutral net profit value. It is expressed in €/kg$_{LH2}$. It is therefore the price of hydrogen correspondent of a value of NPV equal to 0. It is thereby function of the economic parameters already presented, CAPEX and OPEX, the capacity of the plant and the electricity cost.

6.4. Additional simulation software

As an addition to the already mentioned Aspen Hysys®, other softwares have been used to properly simulate the off-design conditions of the process. The main issue with Aspen Hysys® is that the steady state simulation does not allow to fix any design or geometry in the operative units. This is extremely important especially for the correct heat exchange simulation. The steady state mode calculates heat exchanges based on heat balance without considering the geometry of the HEX [37]. The design of the HEX can be implemented in the simulation using the Dynamic module of Aspen Hysys® or the software Aspen Exchanger Design & Rating® (EDR) [38]. The two software have been used to better simulate the off-design conditions of the process by fixing the design of the various units allowing a more rigorous and detailed simulation of the process.

6.5. Evaluation of off-design efficiencies for compressors

Compressors represent one of the more important unit of the hydrogen liquefaction process and their functioning is critical for the operability of the plant. Moreover, they represent the most expensive unit both in terms of CAPEX and in term of OPEX. The repartition of the costs can be resumed on the next Figure 28. The compressors train represents 75% of the total investment necessary for a liquefaction process. The study of these units become therefore crucial to avoid a dramatic increase of the costs.

In the purpose of the study, the compressors have been considered to work at off-design conditions. Unlike other units, it is confirmed by the literature that these machines suffer more from these types of conditions and their range of operability is tighter. Their efficiency decreases rapidly and consequently the energetic costs increase drastically. Moreover, off-design conditions have also a negative effect on the mechanical parts of the machine causing an increasing effect of the fatigue with a consequently shortening of the lifespan of the unit. In particular, overload conditions seems to have the worst impact on the functioning of the machine[39].

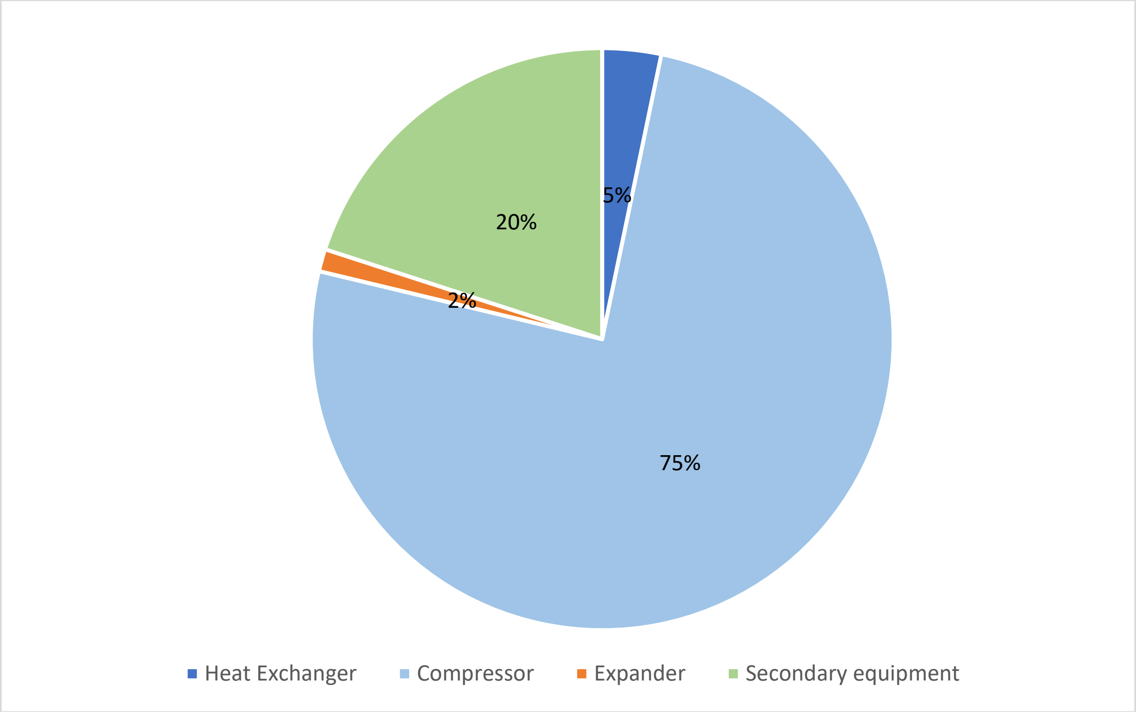

Figure 28. Repartition of the CAPEX of the Linde Leuna process

Some solutions have been proposed in the literature to face the problem of compressors working at non-constant conditions. One example and also the most interesting one, which has also been proposed as a possible solution to increase the flexibility of a LNG process, is the use of variable speed compressors rather than the classical fixed speed compressors[40], [41]. This type of technology has been proposed both for dynamic compressors, such as centrifugal compressors, and for positive displacement compressors, such as the screw types. These types of compressors revealed to have a huge impact on the energetic consumption of a process which have a variable flowrate over a certain period. They allow to work at lower part-load conditions than the fixed speed compressor limiting the decrease in efficiency.

Some studies investigated the performance at off-design conditions of aforementioned variable speed compressors, in order to evaluate parameters such as the efficiency at different load conditions. For example, on the works of Brasz [42] and of Wang et al.[43], the performances of compressors working at different load conditions have been evaluated. A comparison has been made between the use of different load adjustment methods, in particular the use of a valve to regulate the flow entering in the compressor or the use of a variable speed compressor. Since the latter showed better overall performances, it has been decided to extrapolate a correlation between the load condition and the correspondent efficiency which has been used to simulate on Hysys® the part-load conditions. In particular, the variation of the efficiency with the feed gas flowrate has been evaluated considering the efficiency of a screw compressor with the frequency conversion adjustment method, which uses the variable speed compressor technology This correlation is showed in the following Figure 29.

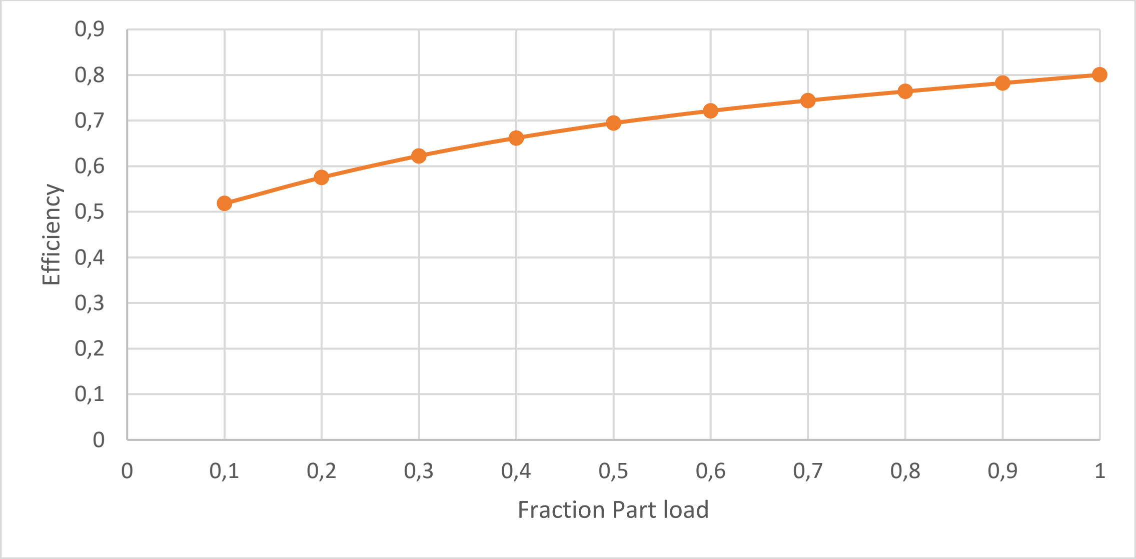

Figure 29. Efficiency of the compressor with frequency conversion adjustment method from [43]

6.6. Evaluation of heat exchangers' off-design conditions

The heat exchangers are the second unit whose off-design behavior needs to be investigated. The literature concerning multi stream HEX is poor and is limited to the study of a single HEX and not a series of HEX, which is the case of the liquefaction process. For this reason, simulations have been necessary to evaluate the off-design impact on the functioning of these units at these working conditions.

6.6.1. Evaluation of streams' outlet temperatures and heat exchanger behavior

A first analysis has been performed considering the effect of the variation of the various stream flowrates on the functioning of an isolated HEX, i.e., a heat exchanger which is not connected to other heat exchangers, and therefore the cascade effect of the variation is not considered. The analysis has been conducted by fixing the geometry of the heat exchanger using Aspen EDR. The evolution of certain parameters, such as outlet temperatures and the used length of the HEX to perform the heat exchange has been investigated.

Analysis have been conducted on different exchangers considering various number of streams. In the following sections, two HEX are presented: a simplified two stream HEX and a five stream HEX which simulate the heat exchanger used in the precooling section of the Linde Leuna liquefaction process.

6.6.1.1. Two streams HEX: outlet temperatures variation and used HEX length

First simulation has been conducted considering a simple heat exchanger whit only a cold and a hot stream as showed in Figure 30.

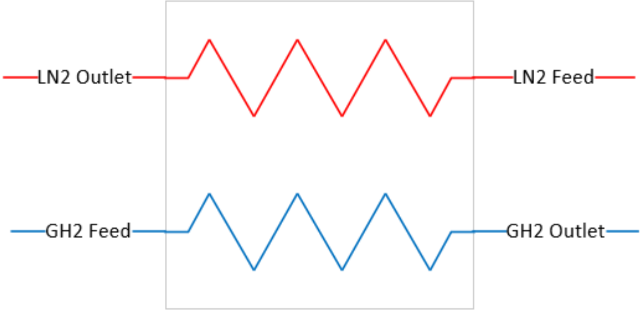

Figure 30. Scheme of a two stream HEX

The considered streams are a hydrogen stream to be cooled down from 290K to 80K and a cold LN_2 stream. The simulation parameters are resumed in the Table 5.

Table 5. Simulation parameters for the two streams HEX

GH_2 Flowrate (TPD)	10
GH_2 Inlet Temperature (K)	290
GH_2 Inlet Pressure (bar)	21
LN_2 Flowrate (TPD)	80
LN_2 Inlet Temperature (K)	78
LN_2 Inlet Pressure (bar)	1.2

The outlet temperature of the two streams when one of the two flowrates is varied has been investigated. The results of respectively the variation of the GH_2 flowrate and the LN_2 flowrate are showed in the Figure 31 and Figure 32.

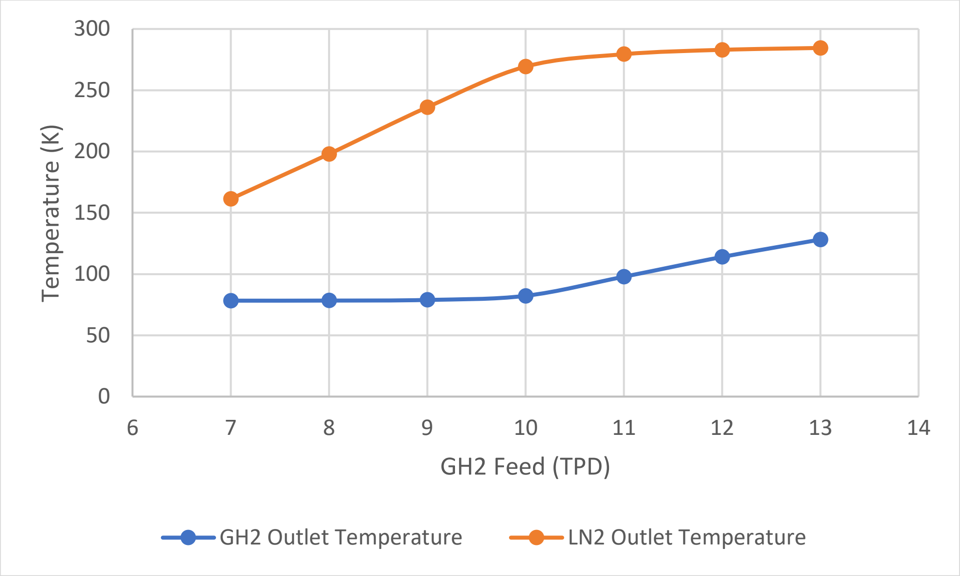

Figure 31. Outlet streams temperature evolution vs GH2 feed variation

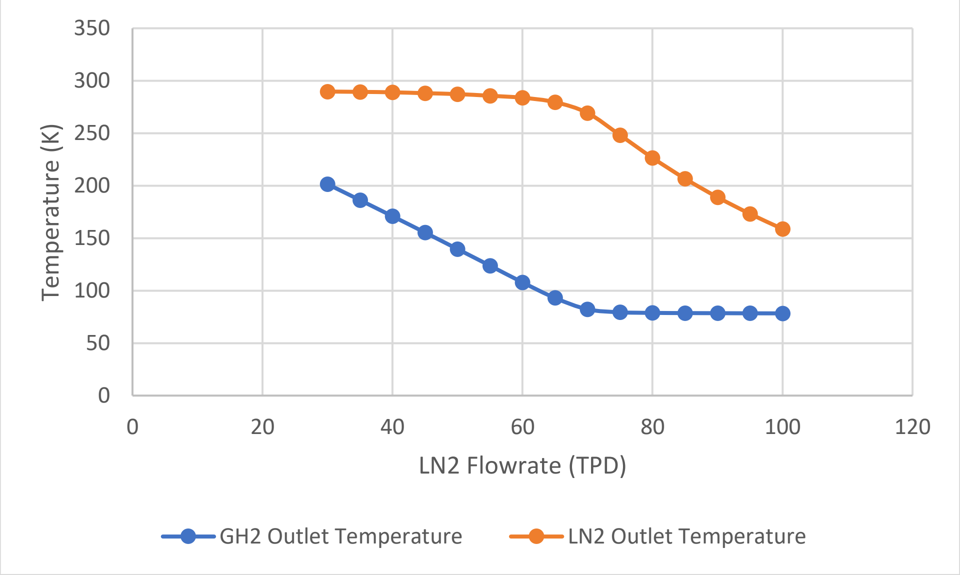

Figure 32. Outlet streams temperature variation vs LN_2 flowrate variation

The obtained results show how the variations of one of the two flowrates causes a modification on the outlet temperature of the streams. In particular, a decrease of the GH_2 flowrate does not have a significant impact on its outlet temperature, since it has already reached the inlet temperature of the LN_2, and therefore it cannot be cooled down further. On the other hand, its increase results also in an increase of the temperature: the LN_2 flowrate is insufficient to perform the cooling at the desired conditions. For what concerns the LN_2 stream, as for the GH_2 stream, its temperature cannot increase more than the inlet GH_2 when the latter flowrate is increased, and its temperature decrease when the GH_2 flowrate is decreased due to the fact that it is necessary less refrigerant power to perform the cooling.

A similar behavior can be observed when the LN_2 flowrate is varied. In any case, the temperature variation when it does exist, has a linear evolution.

The variation of the GH_2 flowrate has an effect that can be observed over the length of the HEX, as showed in the following Figure 33.

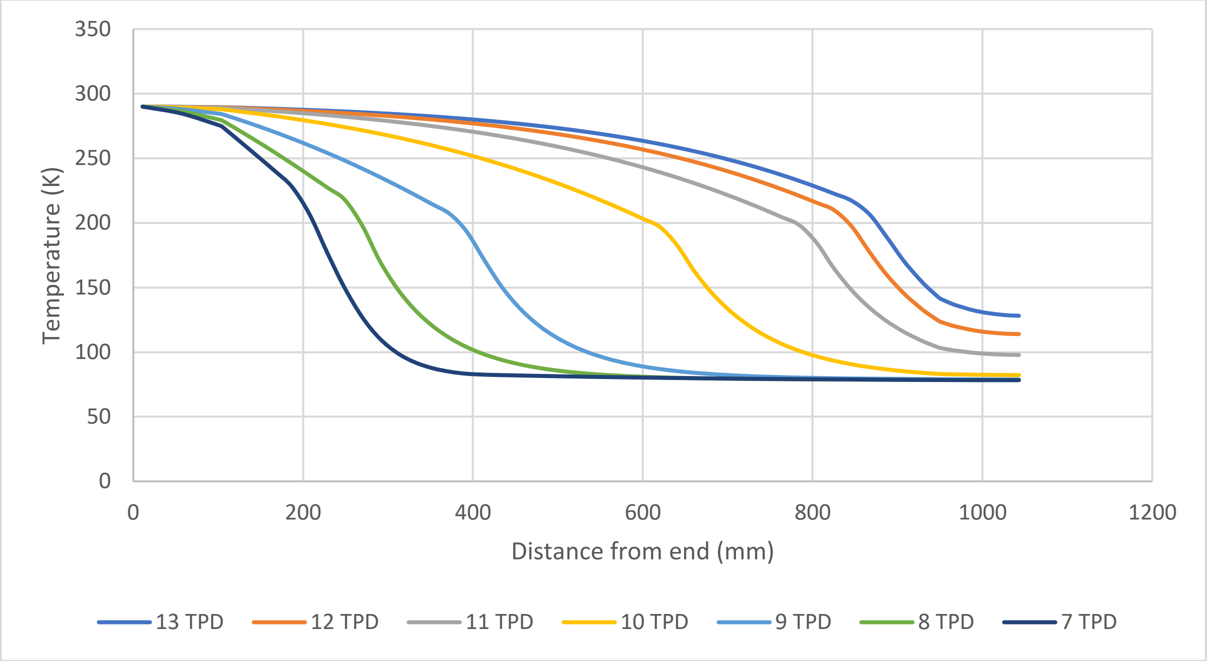

Figure 33. Evolution of the GH_2 temperature along the length of the HEX at different load conditions

As already showed in the previous section, a decrease of the GH_2 flowrate results in the attainment of the inlet LN_2 temperature. With this study it is possible to add that this temperature is reached faster, hence a part of the HEX is not used. It is possible to observe that a decrease of the feed of 30% (form 10 TPD to 7 TPD) causes a "loss" in used exchanger of around 600 mm, which represent 60% of the HEX length, hence making the HEX less effective with a higher actual/required area ratio. Therefore, with 30% less flowrate in the feed, only 40% on the total length of the heat exchanger is actually used.

6.6.1.2. Five streams HEX

The same simulation has been performed on a five streams HEX. In this case, the HEX used simulates the pre-cooling part of the Linde Leuna plant, which presents three cold streams (LN_2 et H_2 refrigerant at low and medium pressure) and two hot streams (GH_2 Feed and H2 in the refrigeration cycle).

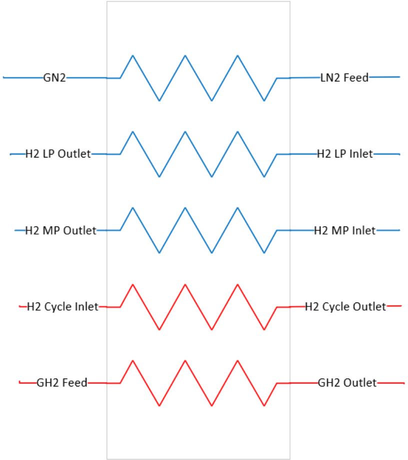

Figure 34. Five streams HEX scheme

Table 6. Simulation parameters for five streams HEX

GH2 Flowrate (TPD)	10
GH2 Inlet Temperature (K)	290
GH2 Inlet Pressure (bar)	21
LN2 Flowrate (TPD)	80
LN2 Inlet Temperature (K)	78
LN2 Inlet Pressure (bar)	1.2
LP H2 Flowrate (TPD)	5.5
LP H2 Temperature (K)	75
LP H2 Pressure (bar)	1.6
MP H2 Flowrate (TPD)	49.5
MP H2 Temperature (K)	75
MP H2 Pressure (bar)	5
HP H2 Flowrate (TPD)	55
HP H2 Temperature (K)	290
HP H2 Pressure (bar)	31

The variation of the outlet temperatures in regard to the GH_2 feed variation of the streams are presented in the following Figure 35 and Figure 36.

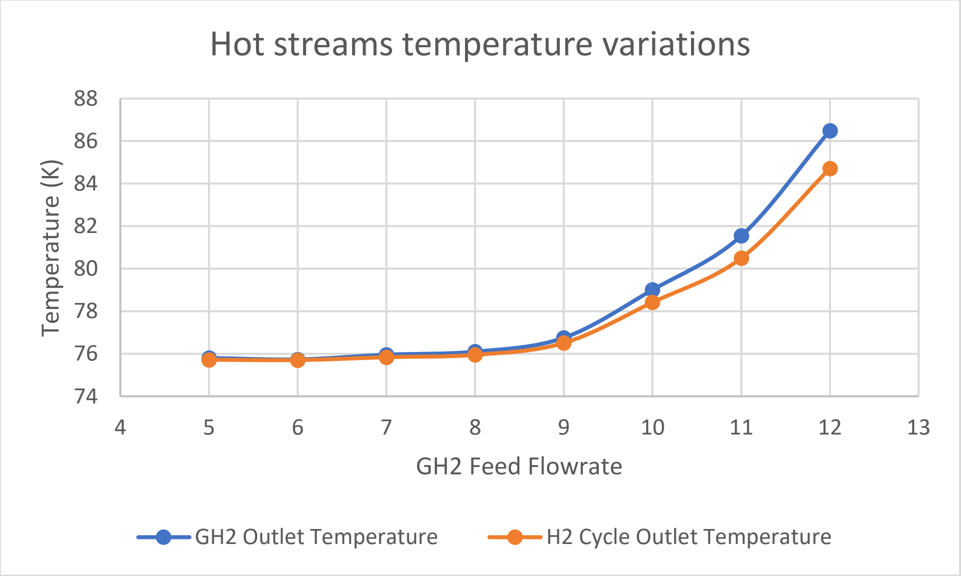

Figure 35. Evolution of the hot streams' outlet temperatures vs GH_2 flowrate variation

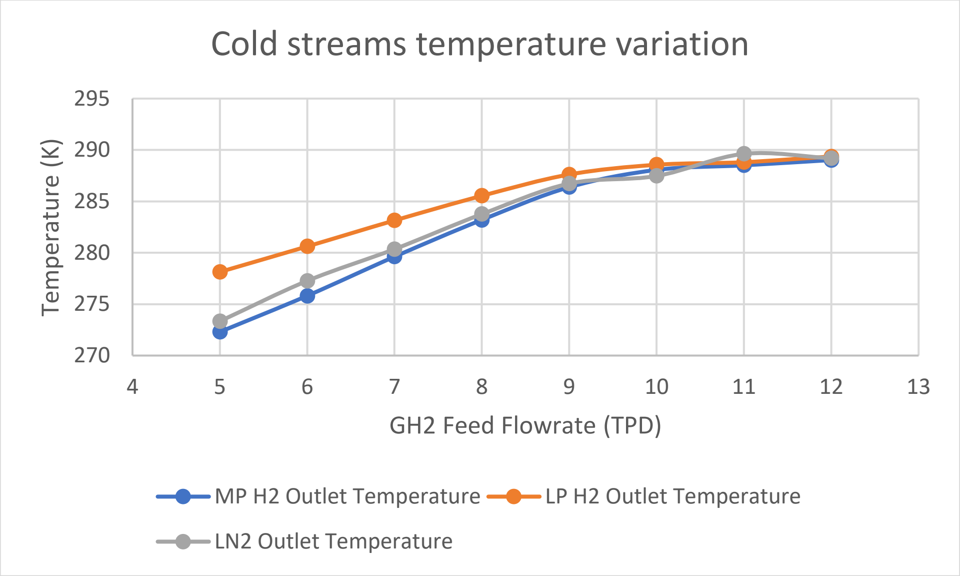

Figure 36. Evolution of the cold streams outlet temperatures vs GH_2 flowrate variation

A similar behavior as the one seen on the two-stream case can be remarked also in this case. The existent temperature variations vary with a linear evolution, and they remain constant when they approach the minimum or maximum inlet temperatures as already observed. It can be therefore inferred that the relation that exists between the GH_2 feed flowrate variation and the outlet temperatures is of a linear type.

Also, in this case the total unused length of the HEX increase with the decrease of the GH_2 feed flowrate, since it reaches the minimum attainable temperature (the minimum inlet cold stream temperature) before reaching the end of the heat exchanger. This "loss" increases to around 60% of the total length for a decrease of the feed flowrate of 50%. The evolution of this phenomenon is presented in the following Figure 37.

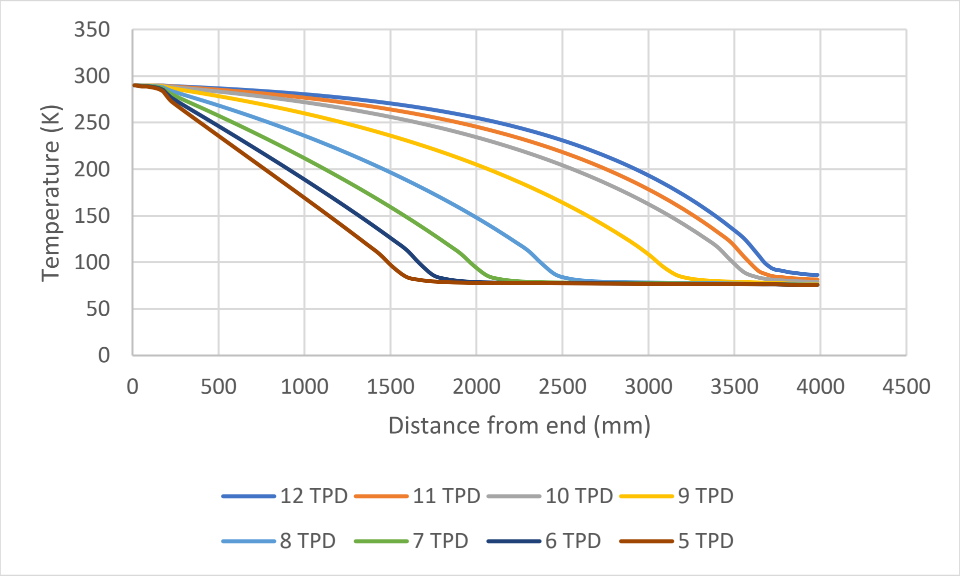

Figure 37. Evolution of the GH_2 temperature along the length of the five streams HEX at different load conditions

6.6.1.3. Connected heat exchangers

In the liquefaction processes the MHEX are likely placed in series as a part of the refrigeration cycle. In this case, one or more of the outlet streams of one of the HEXs represent the inlet streams of the other one. For this reason, the heat exchangers are interconnected with each other and a modification in one of them will cause a modification both in the following heat exchangers and in the previous ones. The problematic of the simulation of such configuration is represented by the fact that the simulation cannot be performed without providing a correct number of constraints, even if the geometry of the various considered exchangers is fixed. This is because the characteristics (such as temperature) of the intermediate streams are calculated by the two exchangers, and if they are not given, for each HEX some information are missing and therefore the calculation cannot be performed. The necessity to fix the intermediate temperatures results in the impossibility of performing the same study as in the previous cases concerning only one HEX.

This issue can be overcome by using the Dynamic mode of Aspen Hysys. Indeed, this feature allows, through the rating tab of the different units, to provide some information about the HEX geometry, even if the calculation in this case results to be less rigorous than the EDR model. The upside is the possibility to simulate series of HEXs only providing the inlet streams conditions. On the other hand, information such as composites or the evolution of the temperature along the HEX are not available in dynamic mode and thus, they cannot be evaluated. The evolution of the outlet GH_2 temperatures from the two exchangers and the LN_2 stream has been evaluated using this method. The results are presented in the following Figure 38.

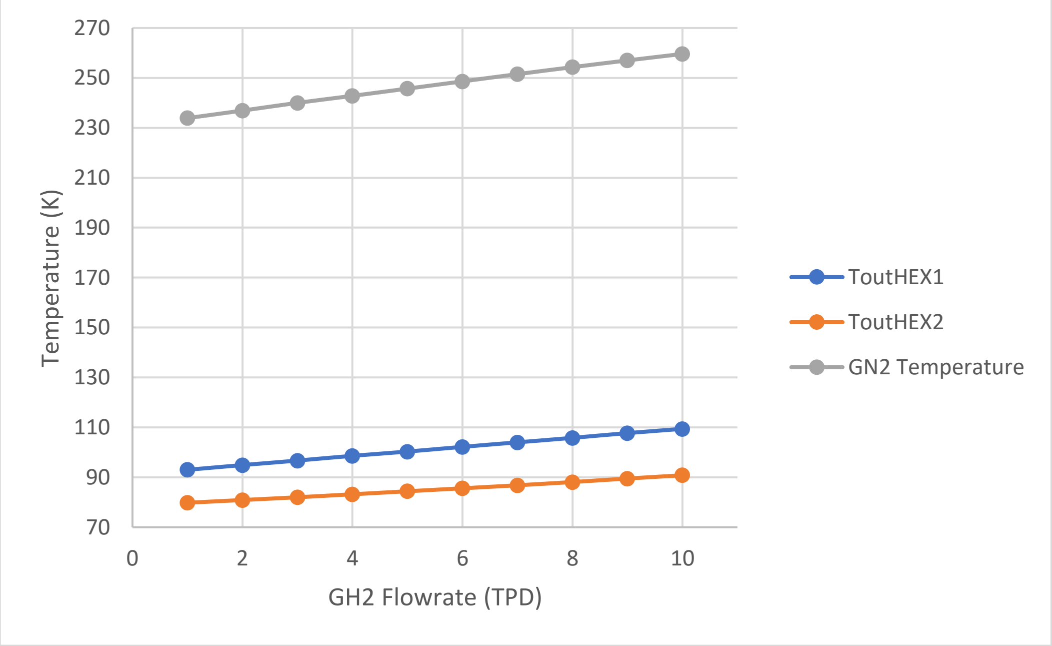

Figure 38. Evolution of the GH_2 and GN_2 temperatures vs GH_2 flowrate variation

As can be observed, the linear relation between GH_2 flowrate and outlet streams temperatures exists also in this case as observed for the HEXs simulated with the EDR model.

Another simulation has been performed, in this case with the objective to simulate a cycle as close as possible to the Linde Leuna liquefaction cycle. The cycle has therefore been simplified into three HEXs in series. Because of the difficulties of the dynamic simulation, it was not possible to simulate the part of the cycle corresponding to the last two heat exchangers. Indeed, the pressure solver of the dynamic mode failed to solve the cycle giving as results negative pressure which are obviously not acceptable. This is probably because the H2 reaches supercritical conditions in the last part of the cycle, and the dynamic mode is not capable to manage well this condition hence leading to errors in the simulation.

The simulated cycle is therefore showed in the next Figure 39.

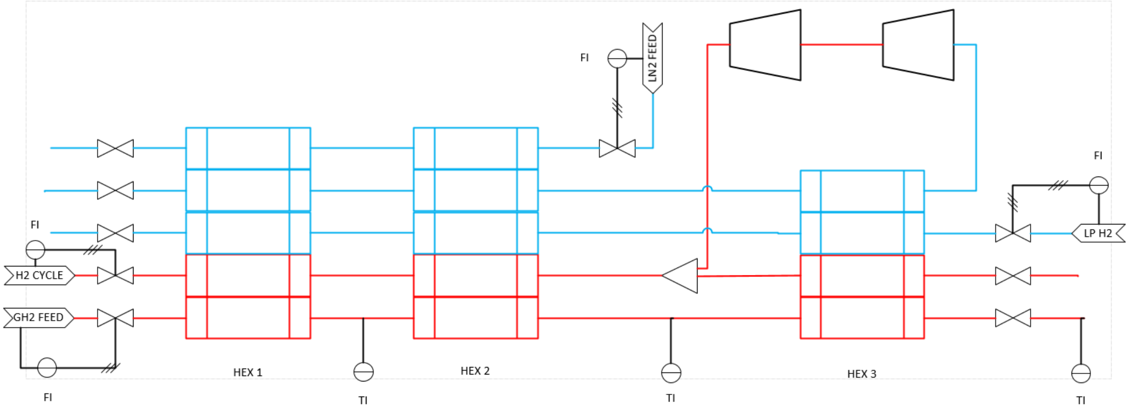

Figure 39. Simplified Linde Leuna PFD simulated in dynamic mode

The evolution of temperature of the GH_2 exiting from the three streams with the variation of its feed is showed in the next Figure 40.

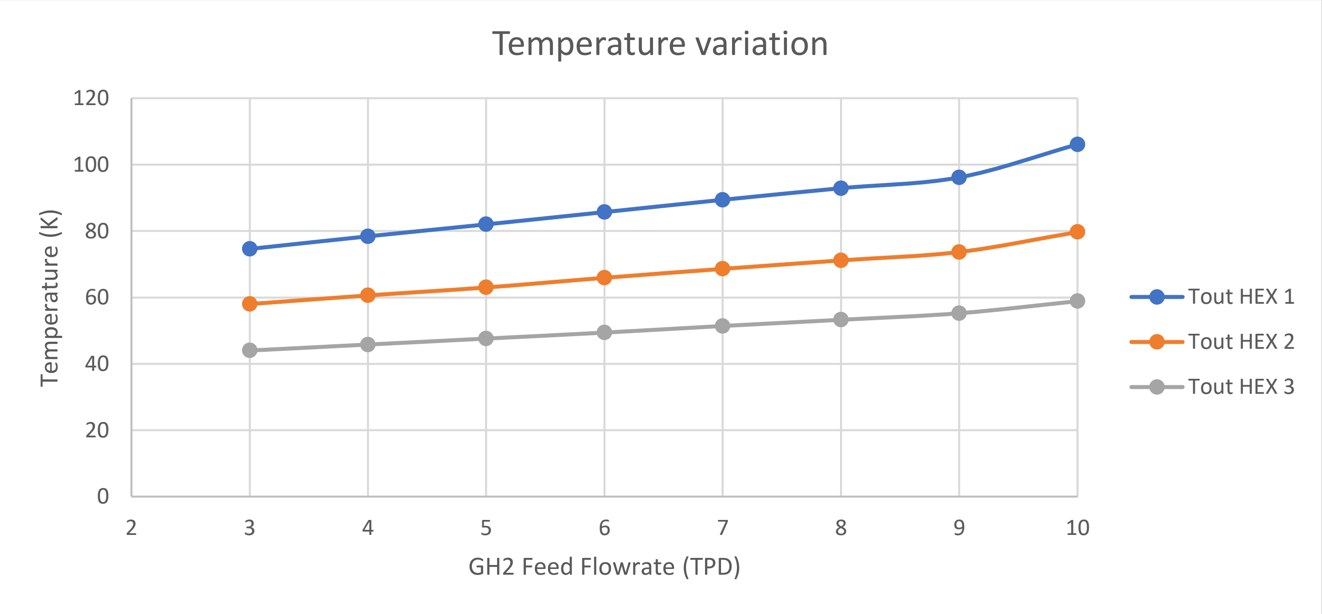

Figure 40. Evolution of GH_2 temperature at the exit of the three HEXs

Again, the linear relation can be observed. It can also be noticed that the temperature decrease is less important if compared to the outlet temperature at nominal conditions, as showed in Figure 41, and this behavior will likely continue for the next exchangers, and for the last one, where the minimum approach of the HEX is close to 0, the variation of the flowrate will probably not influence the outlet temperature.

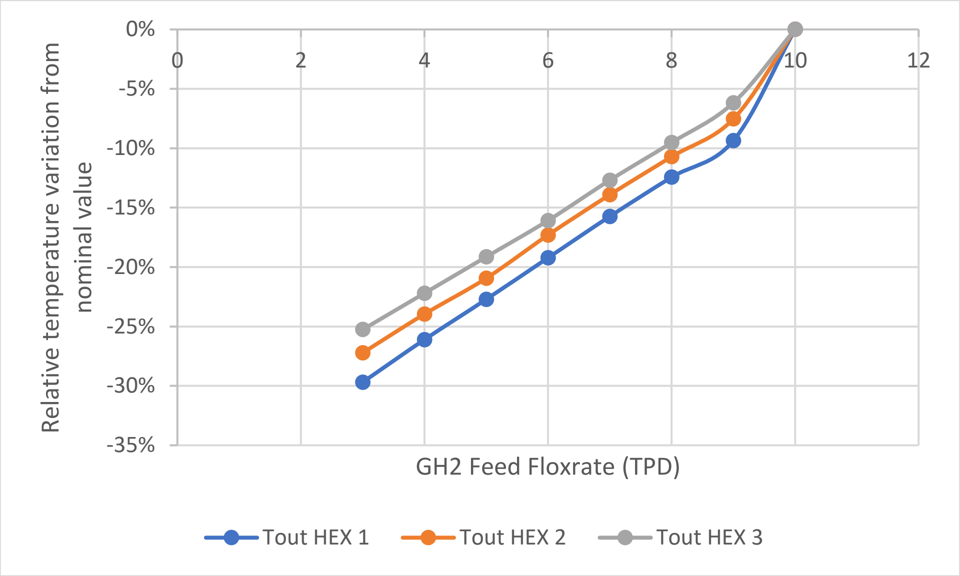

Figure 41. Relative decrease from nominal conditions of the outlet GH_2 temperature

6.6.2. Risks related to inattentive temperature variation

The interest of the study of the outlet temperature is related to the fact that the attaint of some temperatures cannot be accepted to ensure the correct operations of the plant. For this reason, if the effect of the variation of the GH_2 feed that has been presented is not met with modifications of other parameters, such as the flowrate of the refrigerants (see Section 6.6.3), the results could be represented by not only a correct functioning of the cycle but also possible damages to the different units, in particular compressors and turbines.

An increase of the GH_2 flowrate will result in an overall increase of the temperatures of the cycle: the GH_2 would need a greater refrigerant power to be cooled down to the desired temperature and if the refrigerant power that could be supplied by the refrigerant streams is not enough, those temperatures won't be reached. For the same reason, also the refrigerant streams undergo an increase in their temperature. The main risk in this case is represented by the detection of temperature crosses along the heat exchangers due to insufficient heat exchange between the stream that would result in an inefficient liquefaction process because the temperatures necessary to perform the liquefaction won't be reached. This would therefore in a diminution of the production of LH_2 or in the worst case the impossibility to perform any liquefaction.

For what concerns a decrease of the GH_2 feed flowrate, the effect is the opposite to the aforementioned one. In this case, the overall effect is a decrease in the streams' temperatures in the cycle because the refrigerant power that can be supplied by the refrigerant streams is higher than the actual power required, resulting in a greater decrease in the outlet temperatures as showed in the previous sections (with the physical limitation represented by the minimum inlet temperature). This is important for what concerns the expander stages of the cycle: it necessary to avoid that at the inlet of the expander the hydrogen is at its critical temperature (33,2 K) or at a temperature that cause the presence of liquid droplet inside the expander. Some simulations have been made, and considering only one expansion stage for simplicity from 30 bar to 5 bar, the limit temperature that can be accepted at the inlet of the expander is 50K. Under this value, droplets of liquid will be formed inside the expander causing damages to the machine. The same idea could be applied to the compressor's stages, which could not accept liquid droplets at its inlet. For what concerns the H_2 compressors, this situation is unlikely due to the value at which the stream should be to have the formation of liquid droplets, but for other types of refrigerants in the pre-cooling stage of the process, this could be an issue. On the other hand, a lower temperature stream at the inlet of the compressor which result in a lower-consuming compression and a lower need of cooling after compression.

6.6.3. Evaluation of refrigerants' flowrates variations at off-design conditions

In order to proper simulate the process at it off-design conditions, it is necessary to be able to simulate the impact of the variation of the feed on the other flowrates of the process (in particular the refrigerant flowrates, N_2 and H_2) to be able to maintain a proper functioning process without a dramatic increase of the costs. Indeed, if the refrigerant flowrates are not changed, the variation of the feed gas H_2 flowrate could lead to a greatly increase of the SEC of the process. For this reason, it has been studied the existence of a relation allowing to calculate the variation of the refrigerant flowrate along with the feed gas variation. To perform this task, a simulation on Hysys® Dynamics have been performed. The use of Dynamics allows to fix the design of certain units, in particular the heat exchangers. To obtain the aforementioned relations, the outlet temperature of the streams in the different heat exchangers has been controlled to a fixed value chosen for every heat exchanger. When the feed gas flowrate has been varied, the various streams have been also varied to meet these temperature specifications with the constraints of avoiding the detection of temperature crosses along the heat exchangers. The obtained relations of the simulated part of the plant have been later used in steady state mode in order to evaluate them. The chosen parameter of evaluation has been the minimum approach temperature of the heat exchangers, which is one of the parameters that allow to evaluate the performances of the heat exchange. The results are showed in Figure 42.

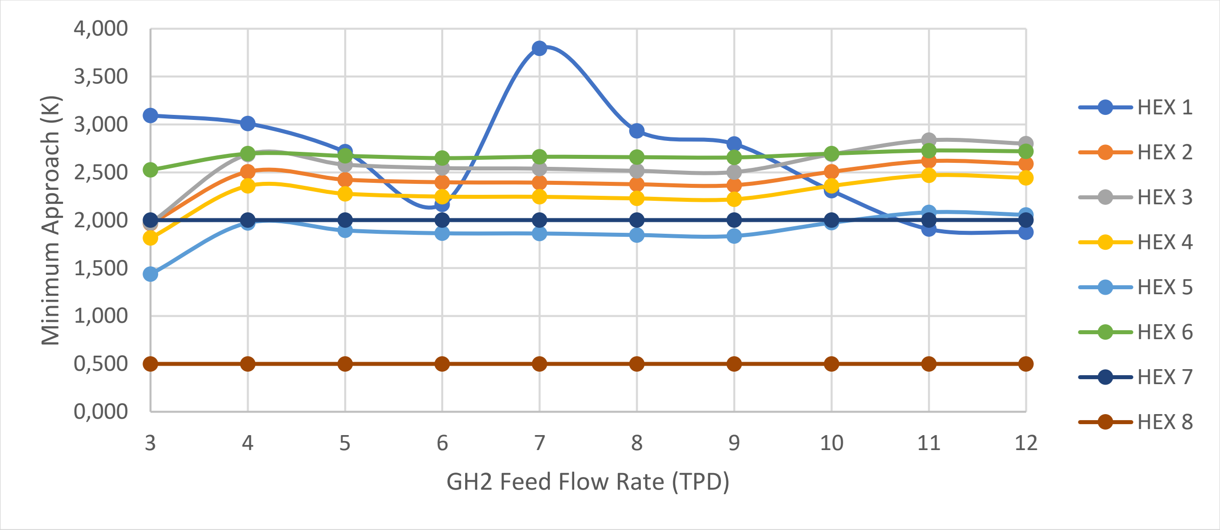

Figure 42. Evolution of HEXs minimum temperature approaches considering refrigerants' flowrate variations

As can be noted, the variation of the minimum approach remains quite constant for all the exchangers and among acceptable values (2-4K). For instance, the same process has been simulated without considering the refrigerant flowrates variation, and the results are showed in Figure 43.

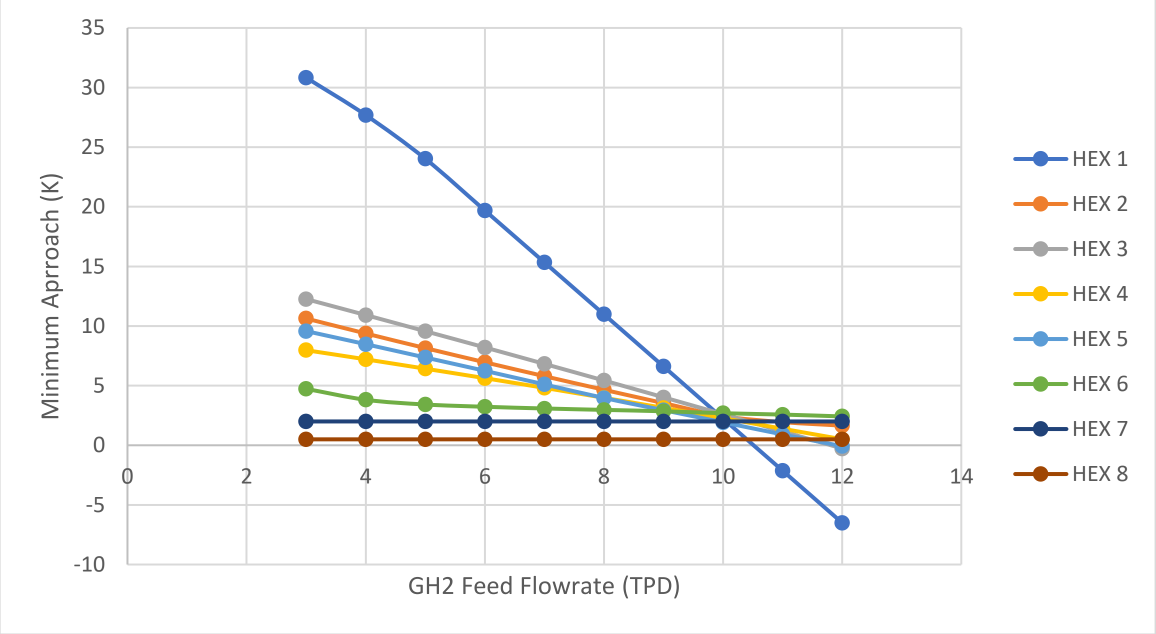

Figure 43. Evolution of HEXs minimum temperature approaches considering refrigerants' flowrate variations

If compared with the other case, it is clear that here the variation is much more important, and some temperature crosses are detected in some of the heat exchangers. This shows that the method used to evaluate the variation of the refrigerant flowrate can be considered acceptable and can therefore also be used in steady state mode.

The two refrigerants whose flowrate vary with the flowrate variation are the LN_2 flowrate and the hydrogen presents in the cycle. The obtained relations are presented in Figure 44.

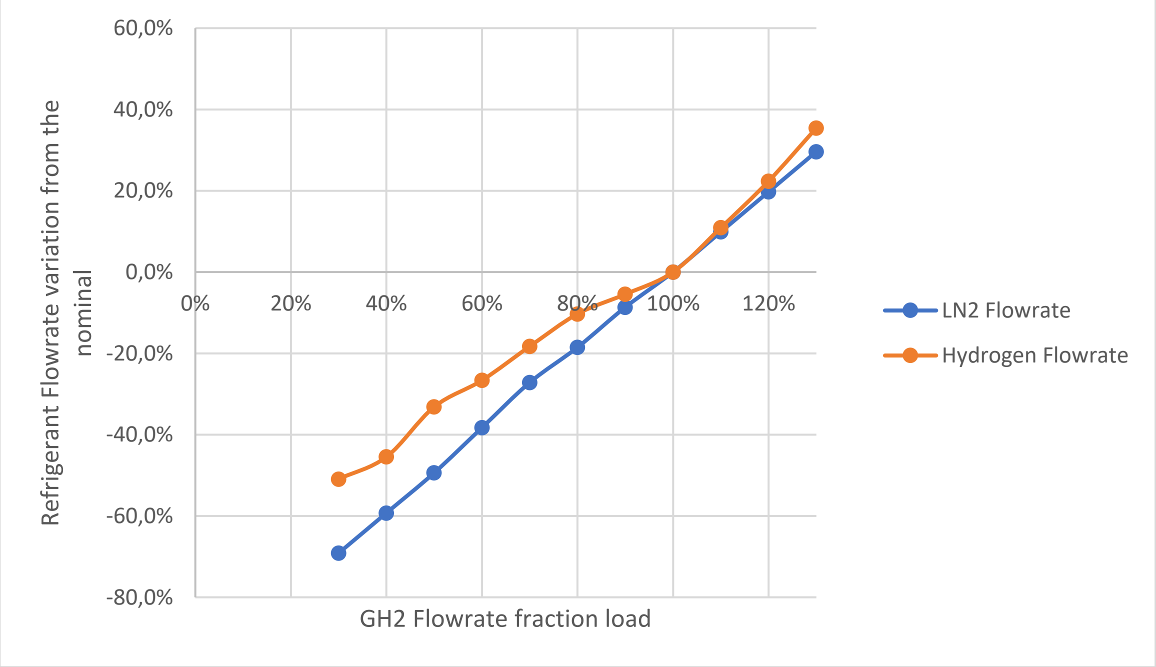

Figure 44. Refrigerants' flowrate variation related to GH2 feed flowrate variation

These relations have been later used to evaluate the variation of the refrigerant flowrates and therefore the SEC of the processes. It is possible to notice how the variation of the two streams does not have the same evolution. In particular, the decrease of flowrates at part load conditions is more important for the LN_2 than for the hydrogen in the cycle. The same is not true over nominal conditions, at least for moderate values, where the relative increase of the two refrigerants is quite similar. This different evolution will have an impact on the SEC, especially for the compressor's consumption, which will have a relative increase of the specific power required at the different flowrates considered.

7. Case studies of simulation: Results and discussion

In the next section will be presented the various case studies concerning some of the solutions of the presented problematic that have been investigated. The impact of the off-design conditions and of these solutions on the process has been evaluated energetically and economically using the parameters presented in section 5.3.2. Simulations have been performed using Aspen Hysys® V8.6.

7.1. Results presentation

All key parameters and economic results will be expressed in relation to chosen reference values. This reference case is Linde Leuna system delivering 10 TPD of LH_2, considering process hypothesis as stated in section X. Therefore SEC, SLC, and CAPEX will be given in relation to the base Linde Leuna case SEC, SLC and CAPEX values. Therefore, relative parameters are introduced as follow:

$$\Delta SEC = SEC - SEC_{BASE} \ [kWh/kg_{H_2}]$$

$$\Delta SLC = SLC - SLC_{BASE} \ \left[€/kg_{LH_2}\right]$$

$$\Delta CAPEX = CAPEX - CAPEX_{BASE} \ [k€]$$

7.2. Constant off-design conditions

First simulations have been performed with the assumption that the GH_2 production, and, consequently, the flowrate entering the liquefaction process were held constant at a certain value over the lifetime of the plant. The process is therefore working at constant conditions. Since the objective of the study is to evaluate the impact of the off-design conditions, they have been considered to remain constant. Even though this scenario is unlikely, it allows nevertheless to estimate the energetic impact, rather than the economic impact. Indeed, it is implausible that a process will be designed specifically to work at off-design conditions over the lifetime of the plant (20 years), and for this reason the variation of the SLC parameter from the nominal case will have less importance than the SEC variation.

The process has been simulated at different load conditions. In particular, based on the literature and internal studies, the range of investigation have been limited to 50%-120% of the nominal charge. For what concerns the part-load conditions, the relations presented in Section 6.5 for the compressors and in 6.6.3 for the refrigerants' flowrates have been used to evaluate the energetic consumption of the process. On the other hand, for overdesign conditions, no clear relations to evaluate the evolution of the compressor efficiency and functioning exist in the scientific literature. For this reason, two cases have been evaluated: it has been decided to consider the addition of a parallel train of compressors, as suggested in the literature as a possible solution to flexible process design [34], and it has been considered the use of a variable speed compressor with a maximal overload condition of +20% from the nominal condition. The parallel line will consist of fixed-speed compressors working at their nominal conditions, which will be represented by the considered overdesign value of the load. This process solution, if compared to the one compressor line working at overdesign conditions, will result in an increase of the CAPEX of the project but in a underestimation of the energetic consumption, since both the lines will have compressors working at their nominal conditions and therefore at their peak efficiency.

7.2.1. Part-load conditions results

In the next Table 7 are summarized the results of the simulations for the different considered working conditions.

Table 7. Part load conditions simulation results

Production (TPD)	**ΔSEC (kWh/kg$_{H2}$)**	**ΔCAPEX (k€)**	**ΔSLC (€/kg$_{H2}$)**	**Installed Power (MW)**
9	0.43	0	0.24	3.64
8	0.65	0	0.52	3.29
7	1.45	0	0.92	3.13
6	1.99	0	1.41	2.82
5	2.83	0	2.1	2.52

The detail of the evolution of the SEC and the SLC are resumed in the following Figure 45 and Figure 46.

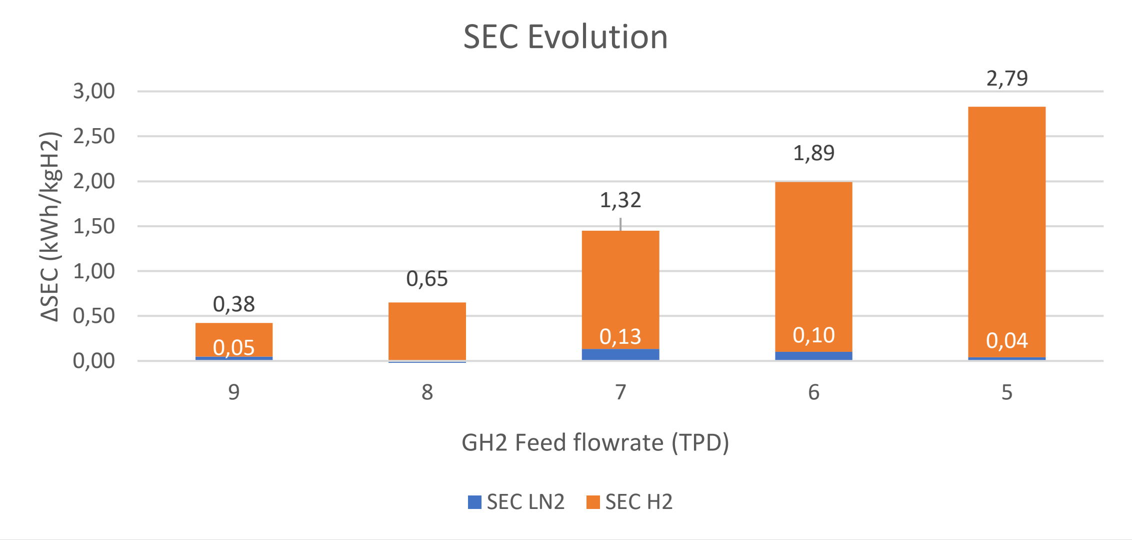

Figure 45. Part load conditions SEC evolution

For what concerns the SEC evolution, it can be observed that its increase is driven almost exclusively by the variation of the energetic consumption related to the H_2 refrigerant. This is due to two reasons: the first is that being the LN_2 an open refrigerant cycle, its flowrate variation does not have an impact on the compression system. If the cycle would have been closed, the compressors related to the compression of this stream would have suffered a decrease in their efficiency due to the off-design condition, thus increasing their energy consumption. The second reason is that the variation of the LN_2 flowrate due to the feed variation has a more linear evolution than the H_2 refrigerant variation, which has a lower relative decrease and thus a higher specific consumption in the compression stage.

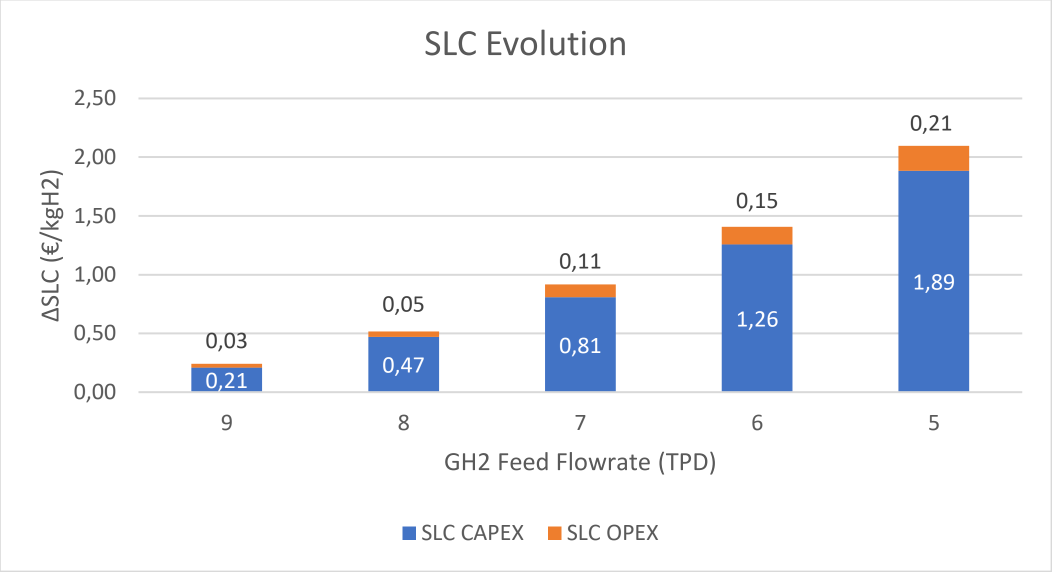

Figure 46. Part load conditions SLC evolution

As already mentioned, the observation of the SLC is not very significant. This is because the main part of its value is represented by the CAPEX, whose impact is even greater when the plant is overdesigned. The impact of the energetic cost is, on the other hand, is showing an increase of 30% of its value when the feed flowrate is decreased at 50% of its nominal value, but its variation remains quite small (+4%) when the off-design condition is limited to 80% of its nominal value.

7.2.2. Overload conditions

As already mentioned, two are the possibilities to manage the overload conditions: using two trains of parallel compressors which can process the overload condition, or the use of a compressor with variable speed able to adapt itself to the increased variation. For the latter solution, no data are available on the literature on the range of operability of such compressors in overload conditions and on the evolution of their performances. For this reason, an assumption of a maximum operability range of +20% has been made. For what concerns the efficiency variation, it has been used the relation presented for the part load conditions considering a symmetrical evolution. This assumption has been considered reasonable based on the operating limits of the compressors indicated in the literature [39].

Simulations have been performed for simplicity considering two compressors, one working with a nominal design equal to the overload value and the other one working with its nominal value equal to the optimized value for the base case of 10TPD. In this case, the two compressors are respectively a fixed compressor and a variable speed compressor. In this study this observation has no impact, but the consideration of parallel trains in the variable production profile application can help to increase the energetic savings. Indeed, considering two variable compressors whose load is optimized in part load applications allow to increase energetic savings of around 2-5%.

The comparison between the results of the two cases are presented in the next Table 8 and Figure 47 and 48.

Table 8. Overload conditions simulation results

Production (TPD)	ΔSEC (kWh/kg_{H2})	ΔCAPEX (k€)	SLC (€/kg_{H2})	Installed Power (MW)
11 (One compressor)	0.98	0	-0.10	4.7
12 (One compressor)	1.42	0	-0.21	5.31
11 (Two Compressors)	0.05	5955	0.34	4.27
12 (Two compressor)	0.13	8668	0.35	4.7

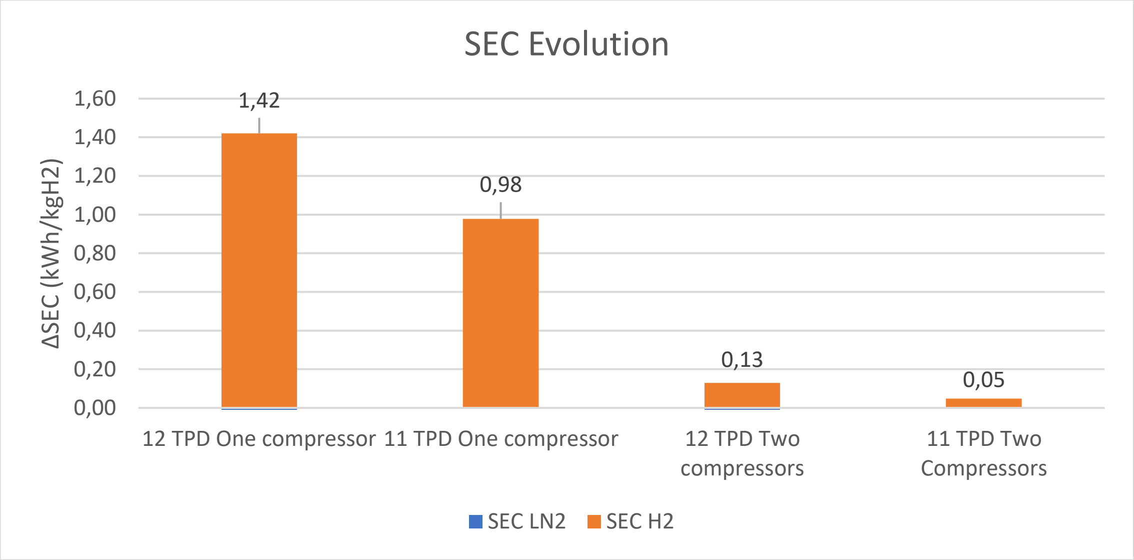

Figure 47. Overload conditions SEC evolution

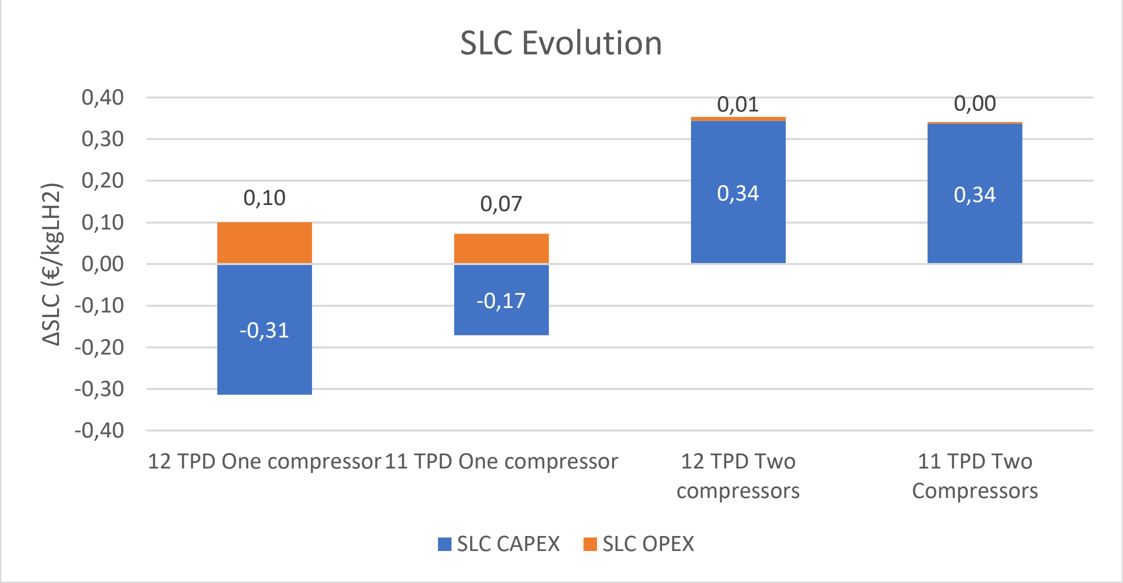

Figure 48. Overload conditions SLC evolution

As can be observed by the results, the use of a single compressor results in the increase of the energetic consumption if compared with the two compressors. On the other hand, with the available data about the compressor's costs, the comparison shows that the costs related to one compressor is much lower than the cost with two compressor, difference due to the increased CAPEX because of the addition of the second compressor.

7.3. Nominal liquefaction conditions with LH_2 re-vaporization

One solution to overcome the off-design conditions in the liquefaction process has been proposed by Kawasaki in its patent n° JP2020024064A, where the nominal liquefaction is assured by a system of re-vaporization of LH_2. This process has for objective to provide a constant feed to the liquefaction process, even when the production of GH_2 is insufficient, condition that can exist when it is produced via water electrolysis using renewable energies as energy sources. To provide this constant feed, part of the LH_2 stored in the liquid storage downstream the process is vaporized and reinjected in the process with the GH_2 to reach the nominal value of the process. The advantage of this solution is the fact that it is possible to perform the liquefaction process being always at the nominal conditions, avoiding all the decreases in efficiency and work off-design of the different units. The downside is represented by the fact that this process is energy consuming since a part of the hydrogen is being re-liquefied, thus increasing the energetic costs.

The LH_2 re-vaporization can be coupled with the liquefaction of the GH2 or another refrigerant streams that participle at the pre-cooling stage of the liquefaction process. This allows the recuperation of some of the frigories produced by the vaporization of the LH_2, which otherwise would be lost with an increase even greater in the energy consumptions. The scheme of the presented process is presented in the following Figure 49

The solutions consist in a liquefaction system with a closed precooling system, three storage systems (LH_2, GH_2 and LN_2) and an evaporator in which the GH_2 is produced from the LH_2 with at the same time the liquefaction of GN_2 into LN_2.

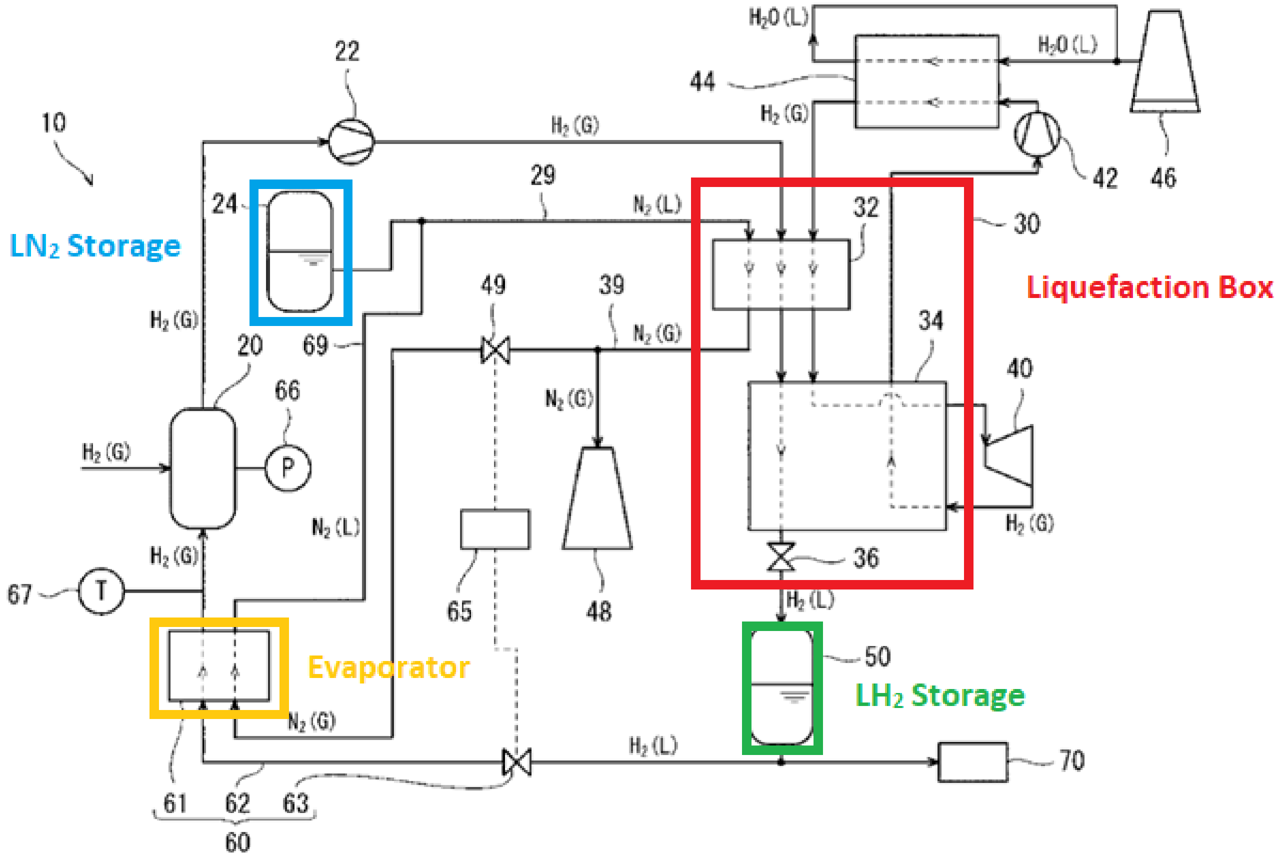

Figure 49. LH_2 re-vaporization system scheme Japan patent n° JP20200024064A, 2020

To compare the impact of such solution with the base case of the Linde Leuna with open LN_2 precooling system, simulations have been performed to evaluate the quantity of LN_2 that could be produced using the vaporized LH_2. Results showed that one ton of LH_2 re-vaporized can liquefy 6.8 tons of GN_2. In previous simulations carried internally, it has been determined that around 8 tons of LN_2 are necessary to liquefy one ton of GH_2. An energetic inefficiency can therefore be observed due to the application of this process already in the precooling stage, which results in an increase of around 15% of the SEC related to the LN_2 precooling.

The impact of this solutions has been investigated in the same range of part-load condition as in the previous Section, i.e., until 50% of the nominal liquefaction value. The case where no energy recuperation and therefore no nitrogen liquefaction has been simulated as well. Since the process will work at its nominal value, the CAPEX related costs won't change (considering the cost of the evaporator negligible compared to the other units), but only the one related to the energetic costs. The impact of the implementation of this solution on the SEC is showed in the following Figure 50 and Figure 51.

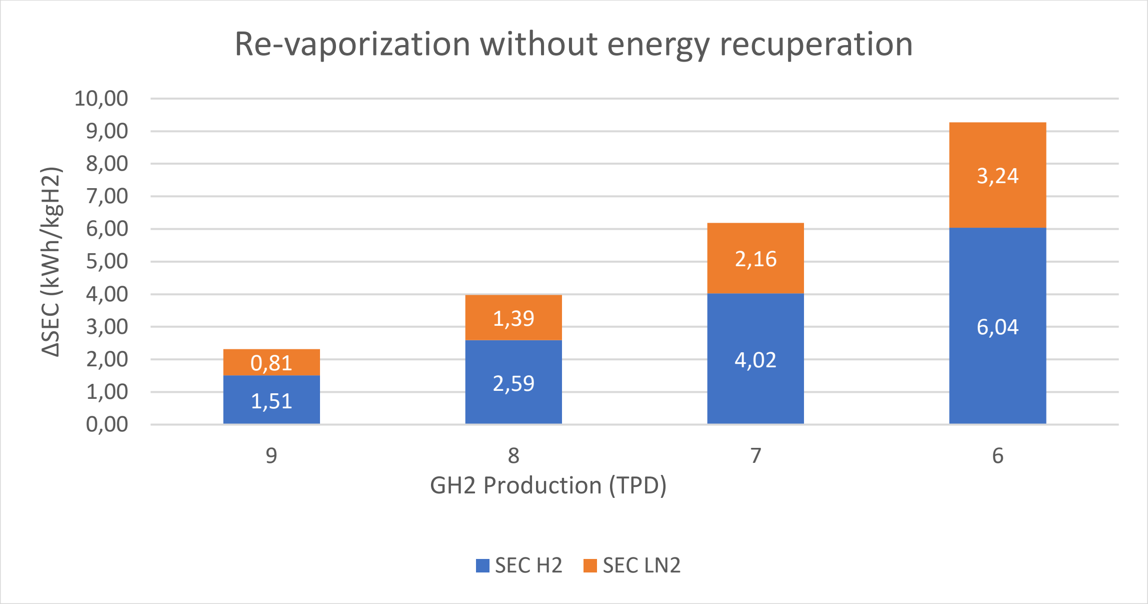

Figure 50. Re-vaporization without energy recuperation SEC evolution

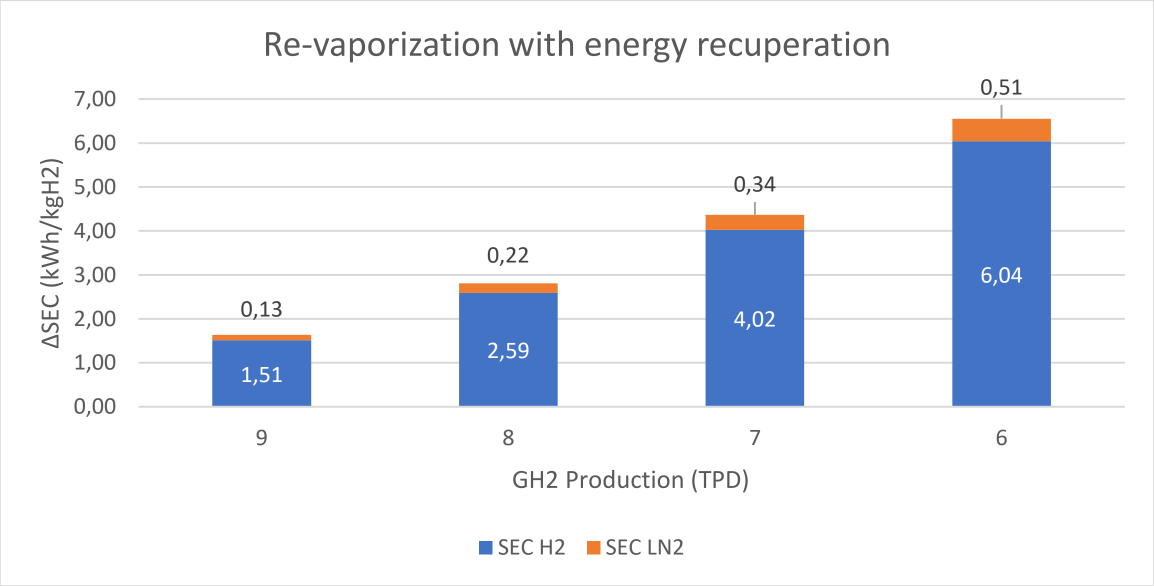

Figure 51. Re-vaporization with energy recuperation SEC evolution

It can be observed that the recuperation has a huge impact of the LN_2 related SEC, which doesn't increase greatly if compared to the no-recuperation case, where it is doubled at 50% of the production. The impact on the SLC is evaluated as a ΔSLC due to the increase of the energy consumption. The results for the two cases are presented in the following Figure 52.

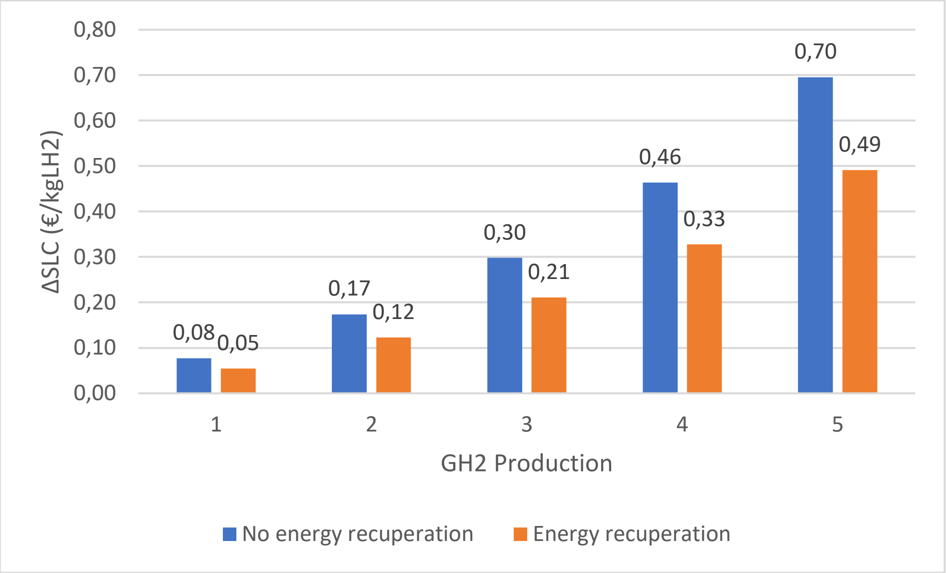

Figure 52. SLC variation from nominal with re-vaporization system

7.4. Off-design and re-vaporization coupling

If the two solutions presented are compared, it is possible to observe that for the same GH_2 produced, it is more interesting to work at off-design conditions rather than perform the re-vaporization. The interest of the latter, on the other hand, is the possibility to ensure the work of the liquefaction unit at his nominal conditions.

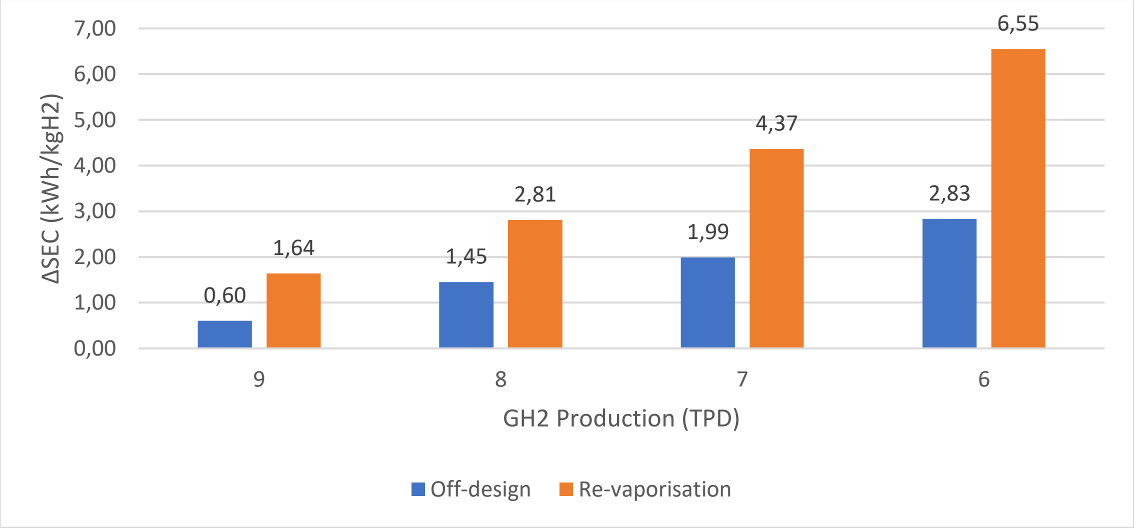

Figure 53. Off-design and re-vaporization SEC comparison

It could be interesting to allow a certain range of off-design, higher than the lowest value of production, to avoid a too high level of part load condition and perform the re-vaporization to reach the allowed minimum off-design condition. This would reduce the energetic consumption if compared to the full re-vaporization solution but with the upside of allowing the process to work with a tighter range of operability that could be beneficial for the units and their correct functioning.

In the next Figure 54 and Figure 55 are showed the evolution of the SECs when considering partial re-vaporization and partial off-design conditions for the cases with a load equal to 80%-70%-60% of the nominal liquefaction value.

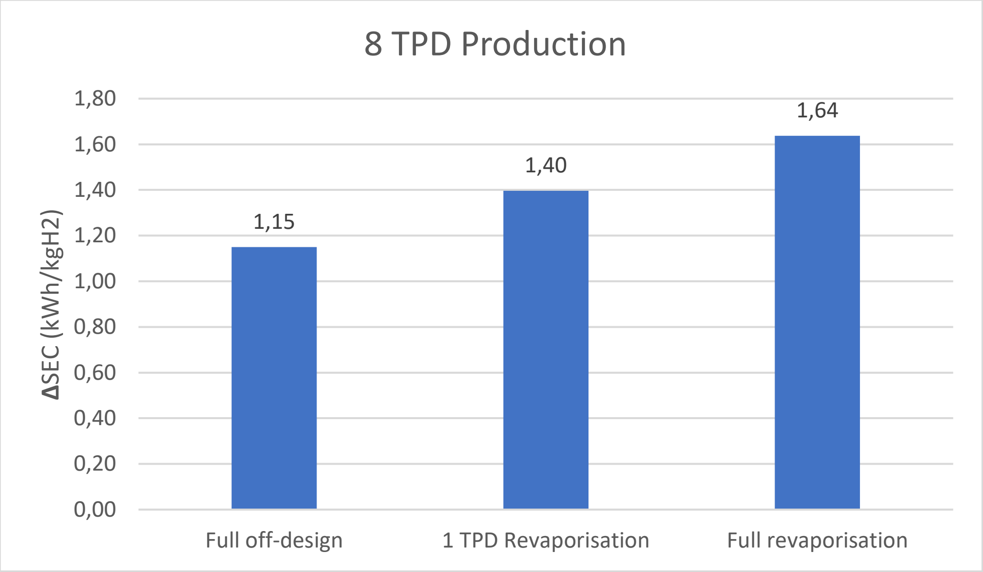

Figure 54. 8 TPD solutions mix impact

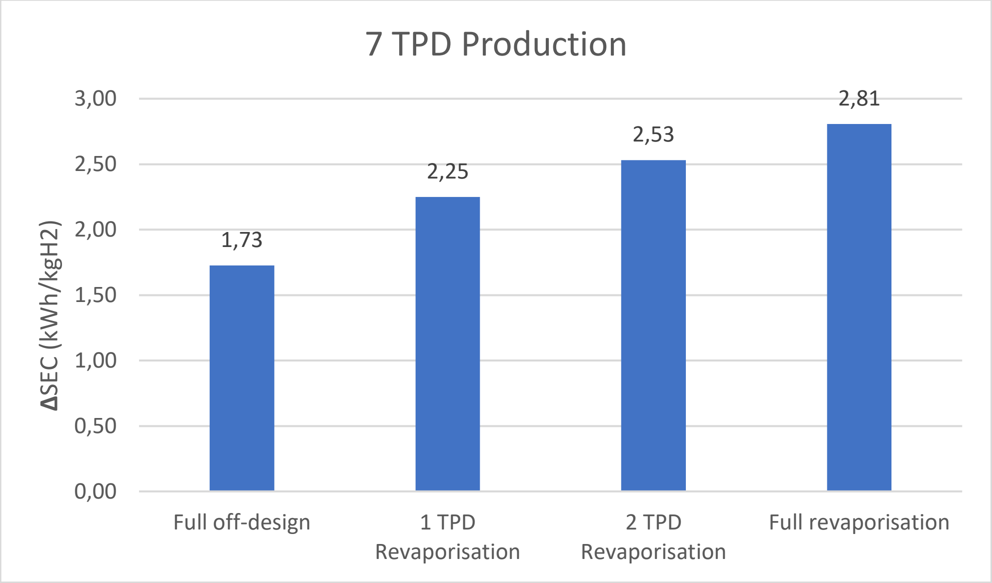

Figure 55. 7 TPD solutions mix impact

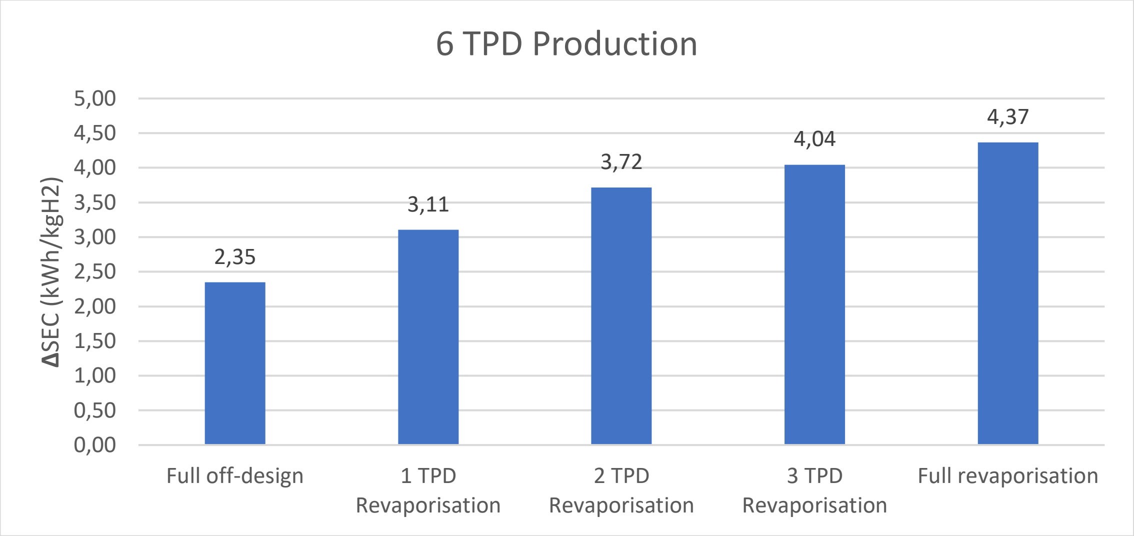

Figure 56. 6 TPD solutions mix impact

Results showed a beneficial effect of considering off-design conditions rather than a full re-vaporization, decreasing the total SEC necessary to perform the liquefaction. The optimal solution can therefore be chosen considering the maximum allowed operating range of the process.

7.5. External Compressed H_2 storage

Since the implementation of an external CGH_2 storage able to absorb the totality of the GH_2 production variation has already been investigated with an internal study, showing as results an unacceptable increase of the costs, the possibility of performing a storage of a lower GH_2 quantity will be explored.

The objective of this solution is not the complete absorption of possible feed variation, but rather the tightening of the working load ranges required by a specific production profile by lowering the days at which the liquefaction unit would work far from its nominal value.

The overproduced GH_2 is compressed to 250 bar and stored in the buffer tank. When the production of GH_2 is under the allowed operative range, the stored CGH_2 is expanded and sent to the liquefaction unit, allowing to maintain the LH_2 process at its nominal value. The characteristics of the buffer tanks are listed in the next Table 9

Table 9. CGH_2 tank characteristics

Tank characteristics	Value
Volume (m^3)	45
Maximum allowed pressure (bar)	500
Cost ($)	570 000
Capacity (tons of H_2)	1.5

The impact of the implementation of this solution with a given profile is presented in Section 8.

As a first simulation, a constant symmetric profile is considered: the GH_2 overproduction is followed by an underproduction of the same value. The storage is therefore filled and emptied regularly, hence its profile over time does not require any special attention. Two different configurations, with 3 tons and a 1.5 tons storage (two or one tanks), have been investigated.

The GH_2 production profile varies between 13 and 7 TPD for the first case and between 11.5 and 8.5 TPD for the second case. In the former study, the overload condition is higher than the assumed limit of +20% and therefore the only possibility is to use an additional train of compressors. In the latter case, the two possibilities presented in section 7.2.2 are possible.

7.5.1. 1.5 Tons storage

Table 10. 1.5 tons CGH_2 storage results

Case	ΔSEC (kWh/kg_{H2})	ΔSLC (€/kg_{LH2})	ΔCAPEX (k€)	Installed Power (MW)
With Storage	0.77	0.33	3137	4.19
Without Storage Two trains	0.73	0.70	7526	4.98
Without Storage Single train	1.08	0.08	0	4.85

7.5.2. 3 Tons storage

Table 11. 3 tons CGH_2 storage results

Case	SEC (kWh/kg_{H2})	SLC (€/kg_{LH2})	ΔCAPEX (k€)	Installed Power (MW)
With Storage	0.93	0.43	4174	4.25
Without Storage	1.01	1.04	11500	6

For both the cases, the use of the CGH_2 storage reveals to be more economic rather than the use of an additional compressor train due to the CAPEX difference between the two solutions, while the energetic consumption is quite similar. The use of a single compressor, on the other hand, is less expensive even if it produces a slightly increase of the SEC.

8. Application case: GH_2 variable production profile

The solutions presented in the previous sections to improve process flexibility have been applied to a practical case considering a variable GH_2 production profile over a year. This profile will be associated to a liquefaction process designed to have a nominal production of 10 TPD.

The profile is presented in the following Figure 57.

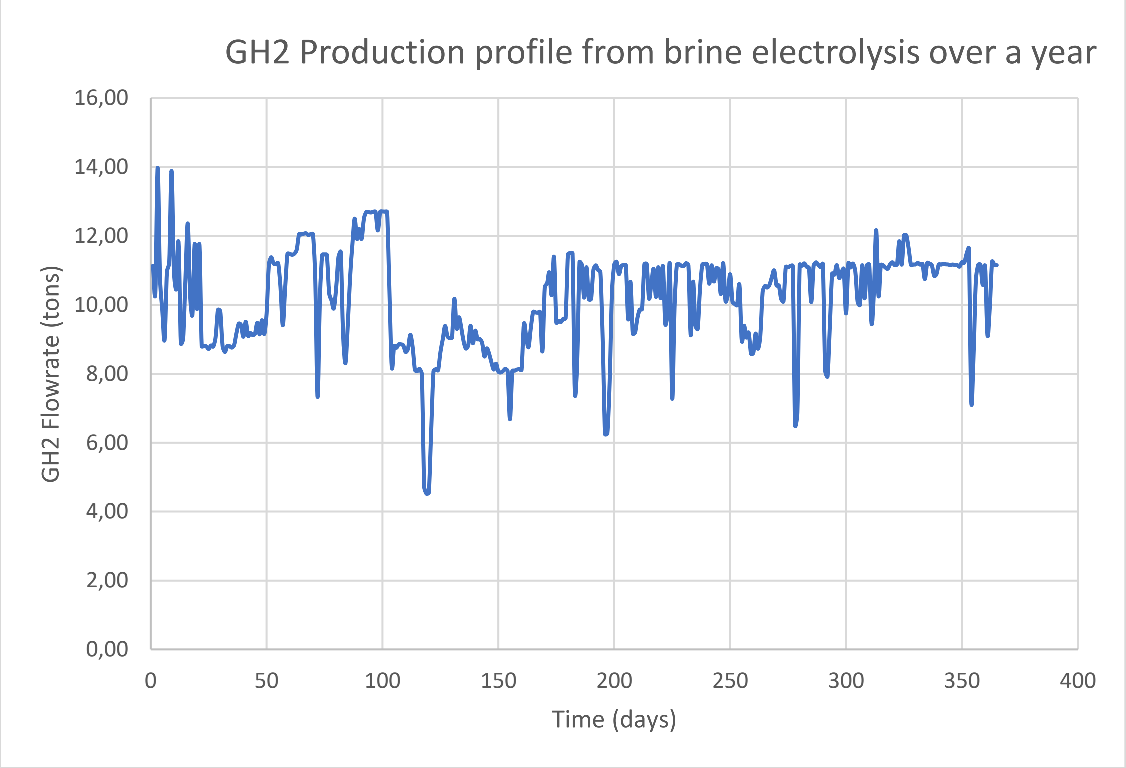

Figure 57. GH_2 production profile

Primary statistics are executed to get basic information from provided data. The following Figure 58 and Table 12 represent respectively the distribution of the average daily production rates and the statistical features.

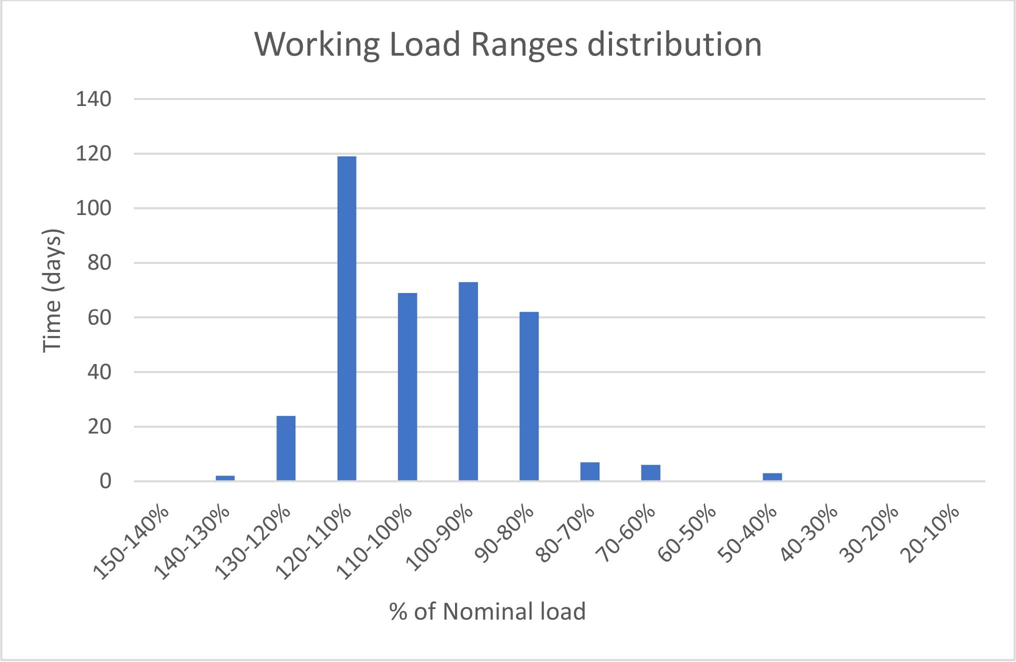

Figure 58. Working load ranges distribution

Table 12. GH_2 production profile characteristics

Average (TPD)	10.16
Standard Deviation	1.43
Maximum value (TPD)	13.98
Minimum value (TPD)	4.52

As can be observed by the presented data, this profile provides a wide range of value of H_2, between 140% and 40% of the nominal value. Most of the days, though, are in the range +-20% from the nominal. An internal study on the implementation of an external buffer, with the objective of store the surplus of GH_2 in the periods where the production is over the nominal value, and to provide GH_2 to the liquefaction unit when the production is lower than the nominal liquefaction value has already been conducted on this profile. This solution has for objective to avoid wasting a great amount of GH_2 overproduced and to avoid the shut-down of the plant in the low-production periods, increasing therefore the overall LH_2 production.

The objective of this section is to evaluate the impact of a theoretical flexible plant, able to withstand the variations of the profile. The economical and the energetic impact will be investigated. Besides, the various solutions investigated in section 7 will be applied to this application case to evaluate the best solution to manage such profile.

8.1. CGH_2 storage impact

The implementation of a CGH_2 storage has an impact on the working ranges of the liquefaction process. It increases the number of days where the process works at a value comprised between +-20% of the nominal value, reducing the days outside this value. In this first analysis, the process has been considered capable to work at any load, and the management of the storage is based on the following algorithm.

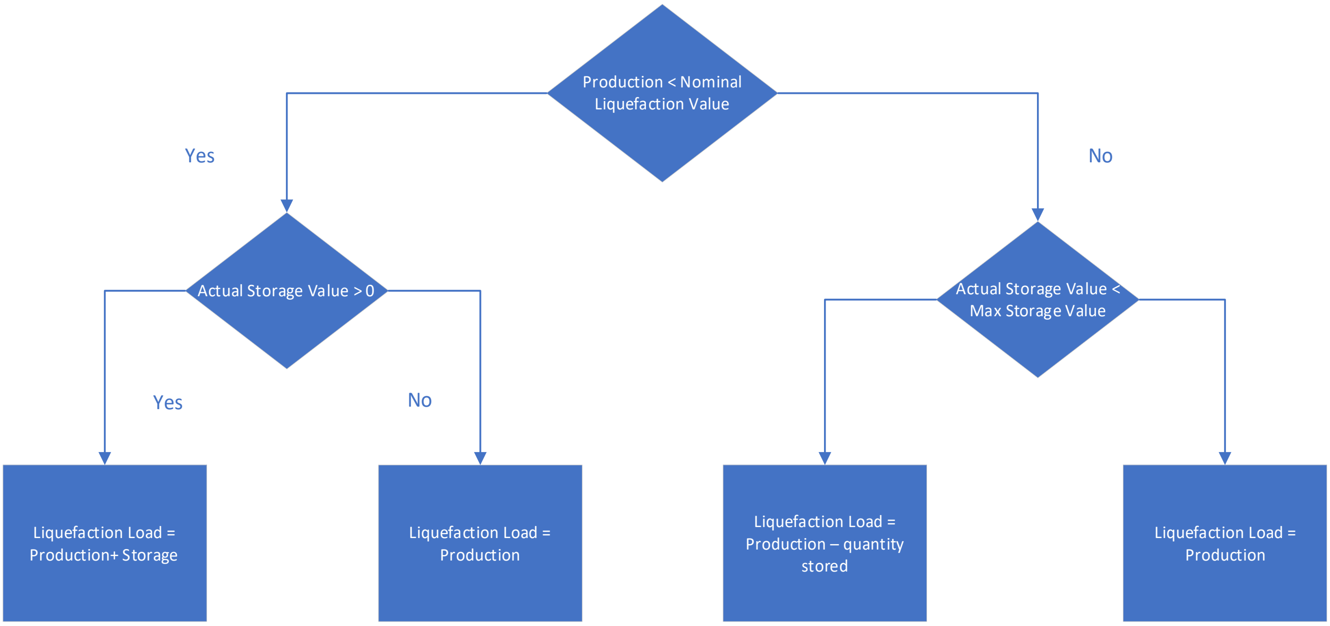

Figure 59. CGH2 storage implementation algorithm

This algorithm, without considering losses and with a perfect filling and discharge of the storage, allows to obtain the liquefaction profile from the production profile, i.e., the quantity that is effectively liquefied in a certain day. The liquefaction profile, compared to the production profile, is presented in the following Figure 60.

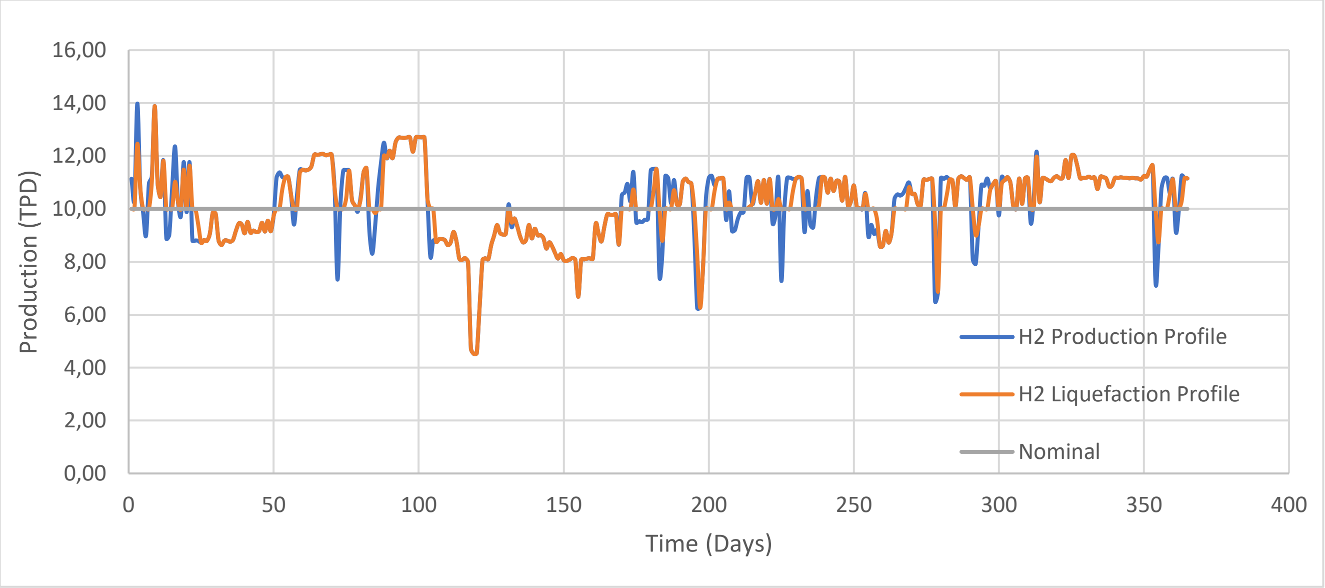

Figure 60. Profiles comparison

The storage profile over the year and the impact on the working load ranges can be obtained by the analysis of the liquefaction profile.

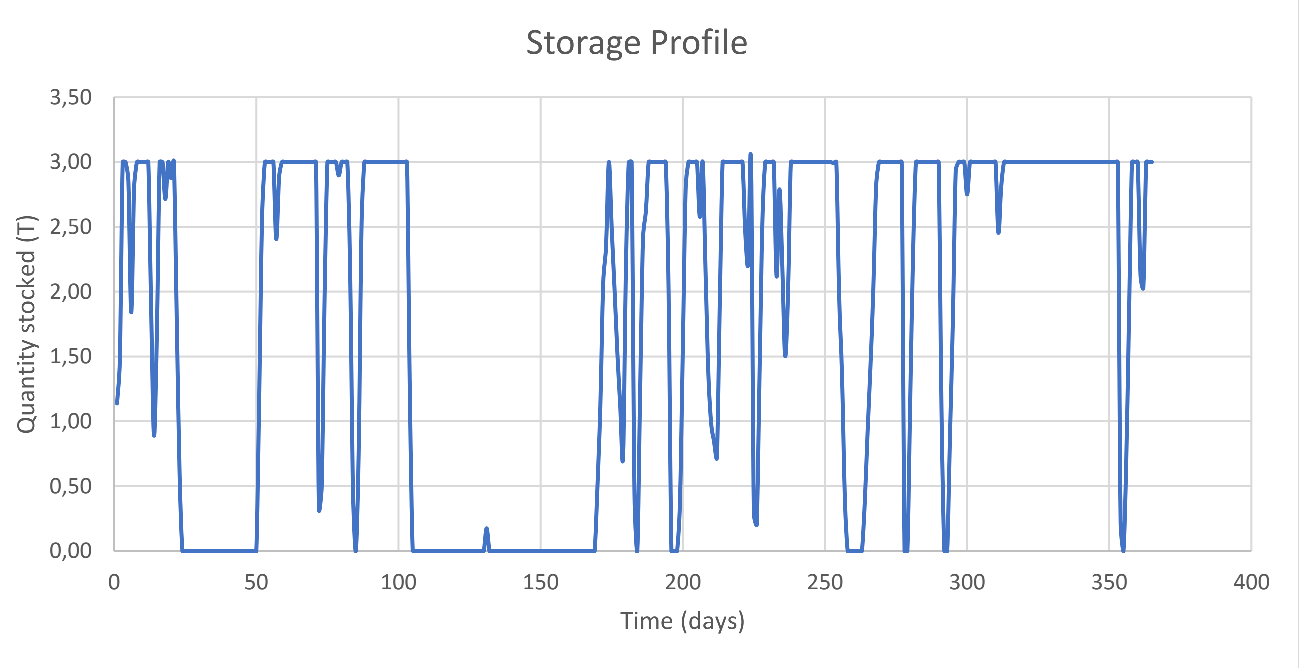

Figure 62. CGH$_2$ storage profile

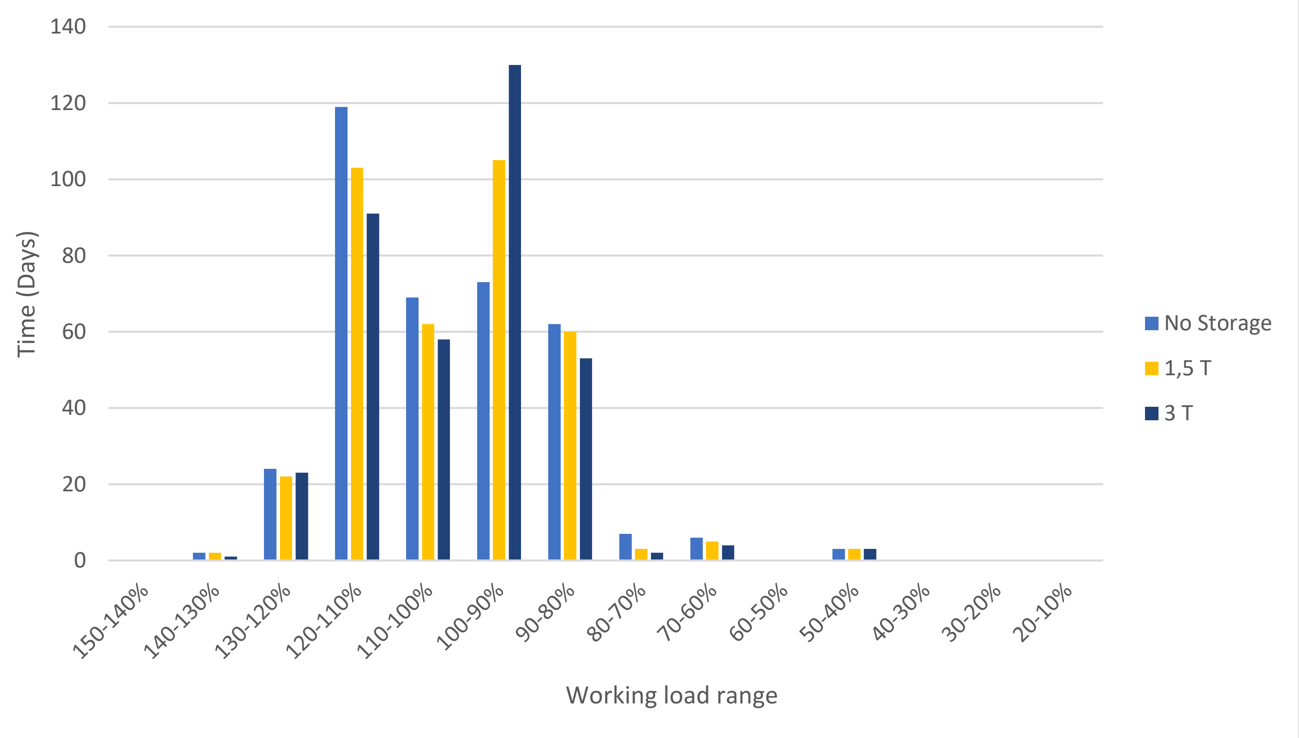

Figure 61. Working load ranges impact

Even if the two profiles seem to be very similar, the impact of the addition of the buffer storage has positive results in the shift of the working load ranges. Indeed, the small variations that don't persist for very long periods are absorbed by the presence of the storage, even if it's small and able to manage only daily variations. A bigger storage allows to have more flexibility over a longer period. It is possible to notice how the implementation of the buffering storage reduces the number of days out of the 90-100% load range, allowing the system to work for longer periods closer to the nominal conditions and therefore at a higher efficiency. One of the main problems is represented mainly by the fact that the number of days at which it doesn't work (consecutive days full or empty) is quite high (around 1/3 of the year).

8.2. Allowed Flexibility and re-vaporization impact

In addition to the CGH_2 storage, also the re-vaporization it has been implemented in the process, considering the coupling of this solution with the storage. In this case, a maximum range of flexibility of the process has been fixed. Over the upper bound and under the lower bound the process is not capable to perform the liquefaction, and if the daily GH_2 production is out of these boundaries, the H_2 will be lost. The implementation of the CGH_2 is in this case related to the recuperation of the H_2 those exceed above-mentioned boundaries, and it is used to reach the lower bound during the days of underproduction. During these days, also the re-vaporization is used to allow the liquefaction. For what concerns this last solution, two approaches are defined: use of the re-vaporization until the reach of the nominal liquefaction value or use of the re-vaporization only until the attaint of the lower chosen bound. The former solution, counterintuitive, is proposed because also the LH_2 storage is limited, by size and by quantity of LH_2 stocked. Considering a constant sale of 10 TPD of LH_2, i.e., the nominal value of the designed plant, if the liquid storage is full during an overproduction period, that surplus of hydrogen couldn't be stocked, and it will be lost. With the same idea, if all the LH_2 produced will be sold without storing a part, the re-vaporization solution couldn't be applied because the storage will be rapidly emptied and therefore there will not be any possibility to perform a re-vaporization.

The two version of the re-vaporization are resumed in the algorithms in the two following sections. Different cases have been simulated for both the algorithms presented, considering the coupling and the non-coupling of the presented solution. For what concerns the liquefaction process, a value of +20% was allowed as overload for the single compressor. If the allowed flexibility was higher than this value, an additional compressor train was considered. As remarked in section 7.2.2 for simplicity a train of variable compressor and a train of fixed speed compressor was considered, with the latter with a fixed working load equal to the considered allowed overload. The choice of a two train of variable speed compressor would lead to a more optimized process with an average energy saving of around 2-5%.

For both the chosen algorithms, the following cases have been simulated: use of re-vaporization technology for the process with an allowed flexibility of 20% and 30% difference from the nominal, and integration with the CGH_2 storage to the 20% allowed flexibility process considering a storage of 1.5 and 3 tons. The chosen value for the liquid hydrogen storage is 45 tons, with a minimum quantity of 1 ton stocked to maintain in temperature the unit.

Simulations have been performed through the following process: using the following algorithms it is possible to obtain the liquefaction profile, i.e., the daily GH_2 quantity that is sent to liquefaction from the production profile. Using the relations to obtain the optimal refrigerants flowrates corresponding to a certain GH_2 feed is then possible to perform the simulation on Hysys and obtain the energetic consumption and therefore the daily SEC of the process.

8.2.1. Re-vaporization to nominal value (Algorithm V_1)

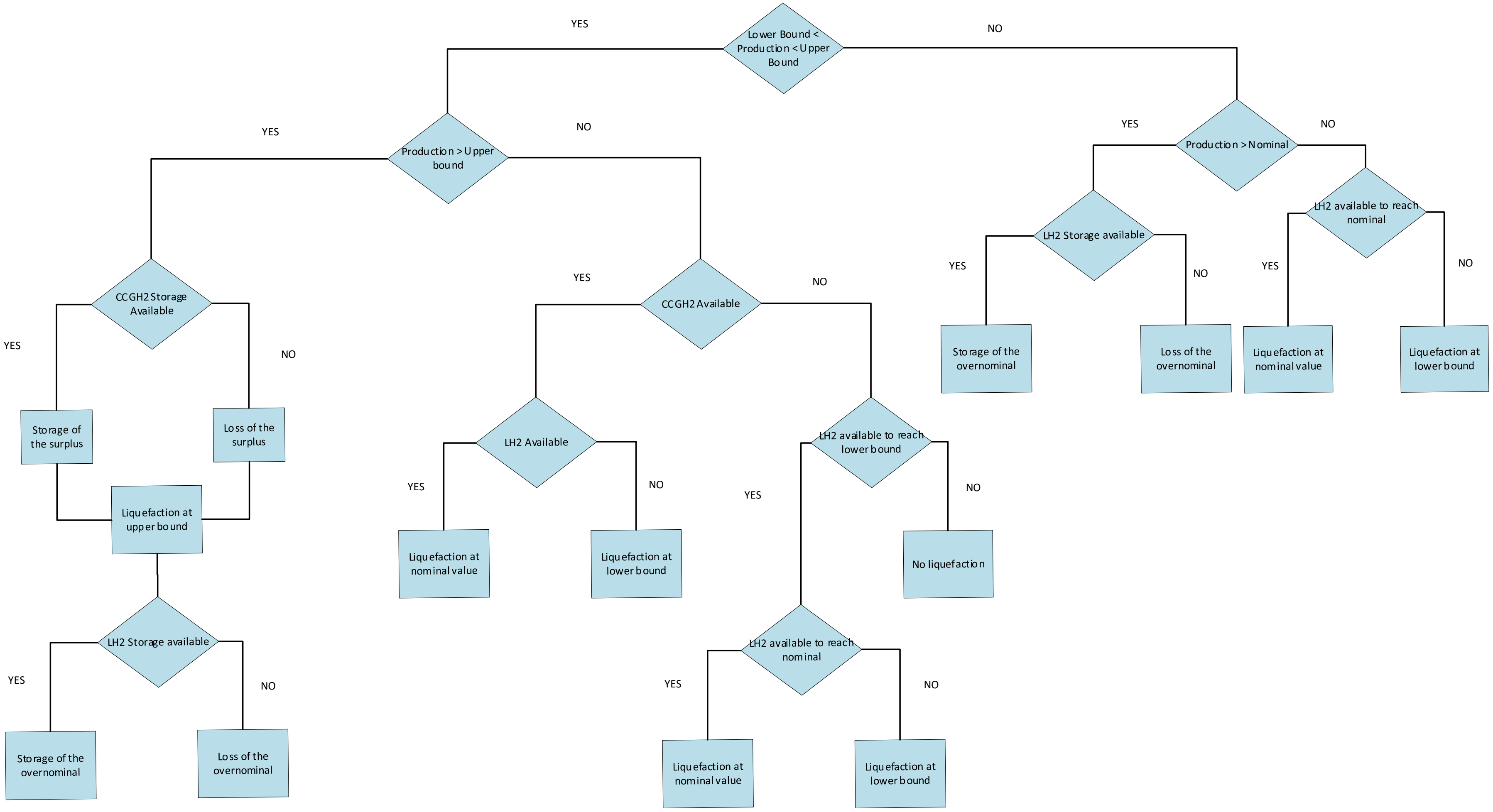

Figure 63. Algorithm V_1

8.2.2. Re-vaporization to lower bound (Algorithm V_2)

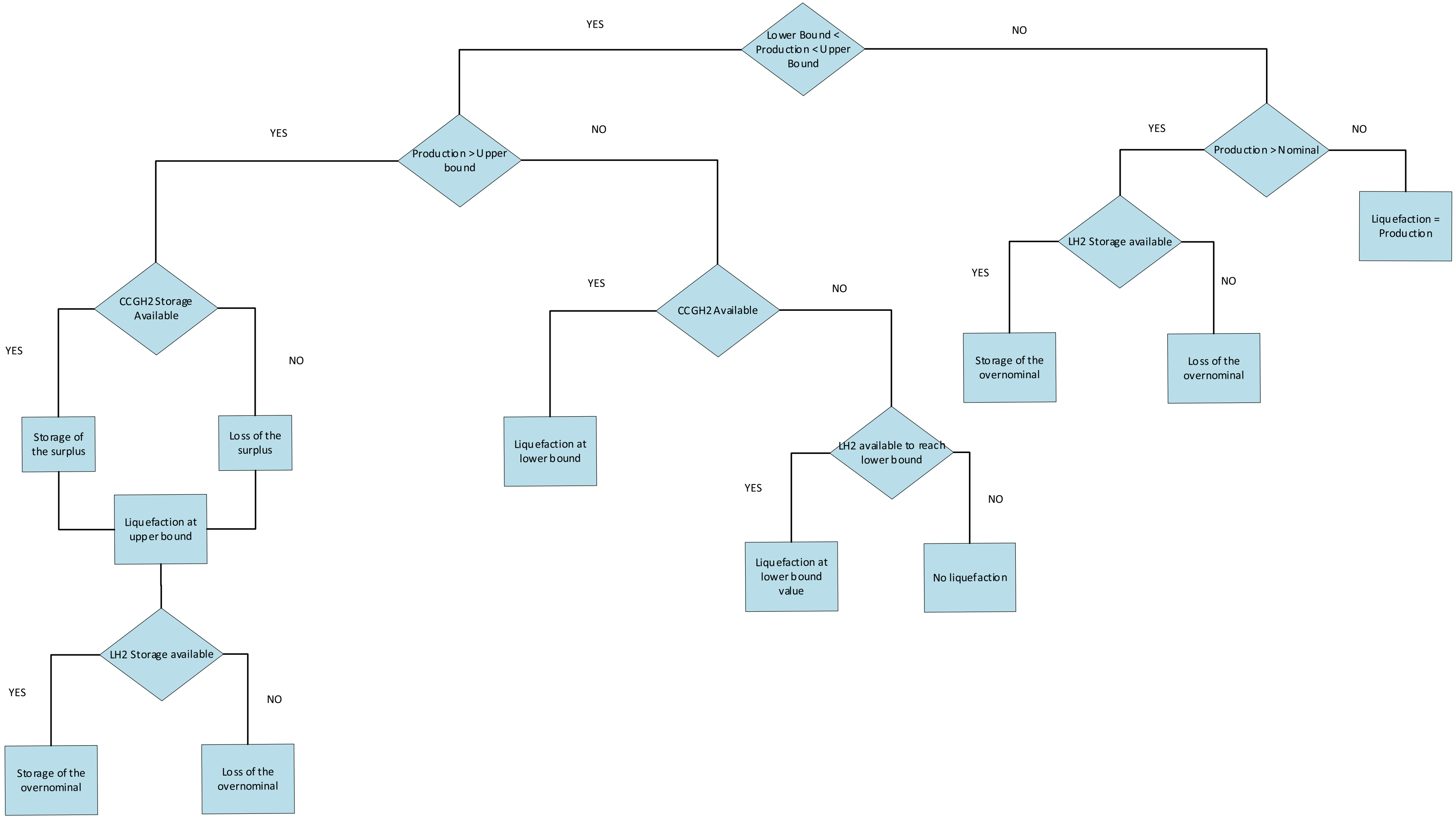

Figure 64. Algorithm V_2

8.2.3. Simulation results

8.2.3.1. Profiles evolution

As it has already been done to evaluate the implementation of the CGH_2 impact, also in this case the production and the liquefaction profile will be compared for some of the simulated cases, in addition to the profile describing the evolution of the liquid storage and the CGH_2 if considered in the simulation.

8.2.3.1.1. 20% Allowed Flexibility and re-vaporization

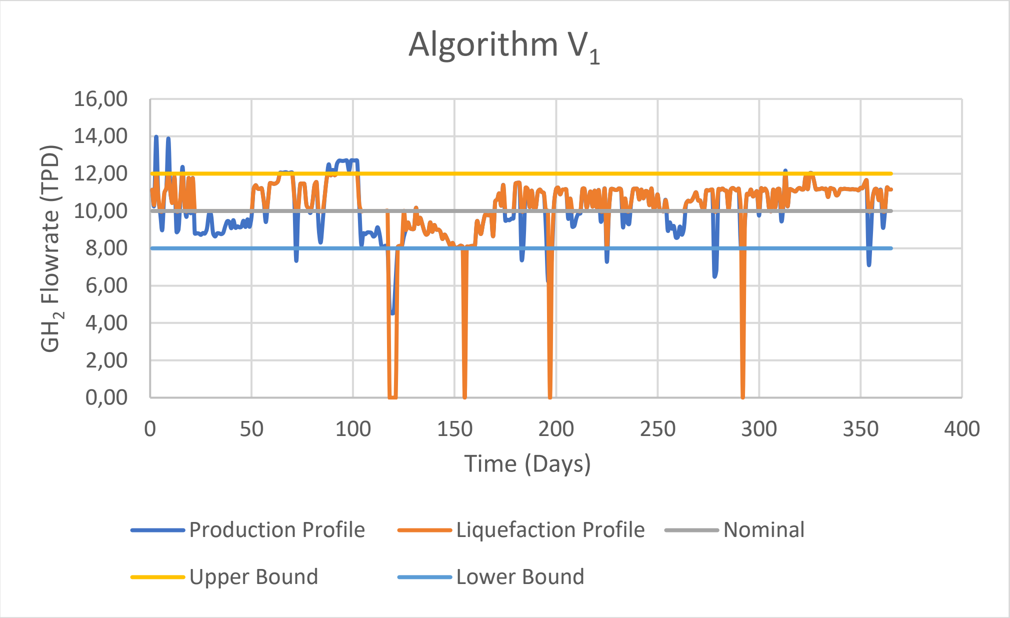

Figure 65. Algorithm V1 20% Flexibility profiles comparison

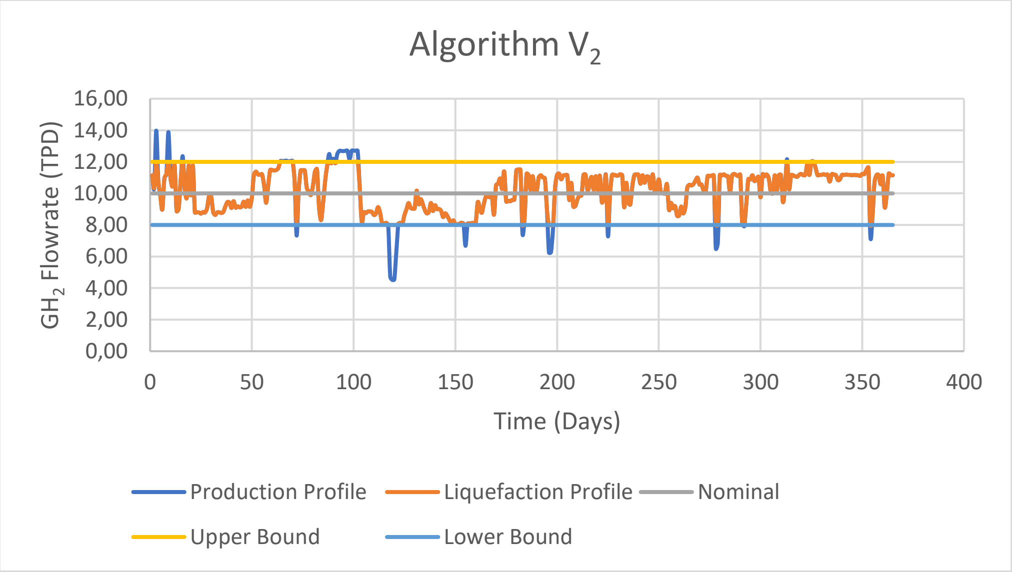

Figure 66. Algorithm V2 20% Flexibility profiles comparison

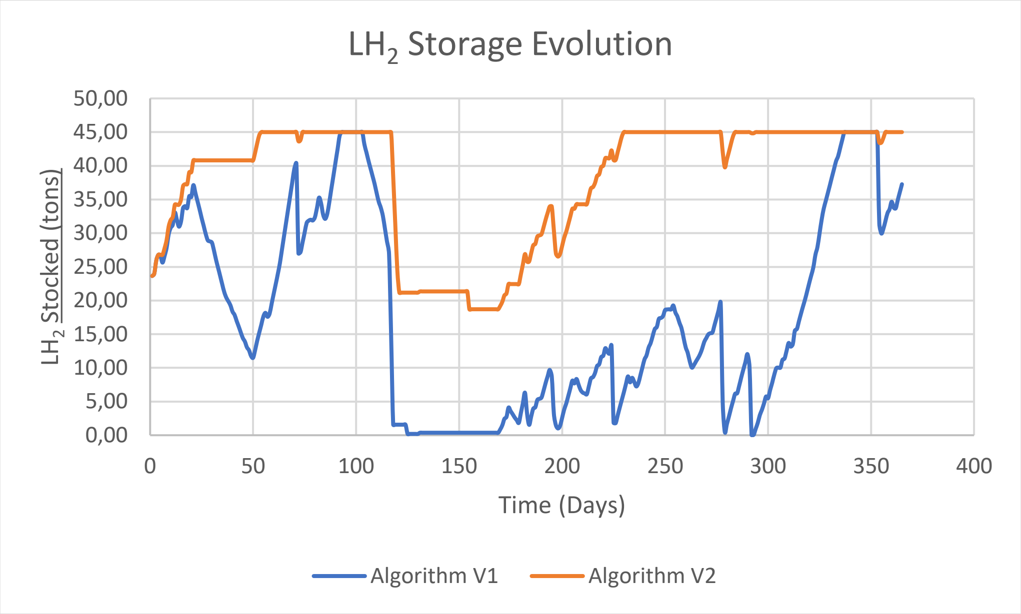

Figure 67. LH$_2$ storage evolution (20% allowed flexibility)

8.2.3.1.2. 30% Allowed Flexibility and re-vaporization

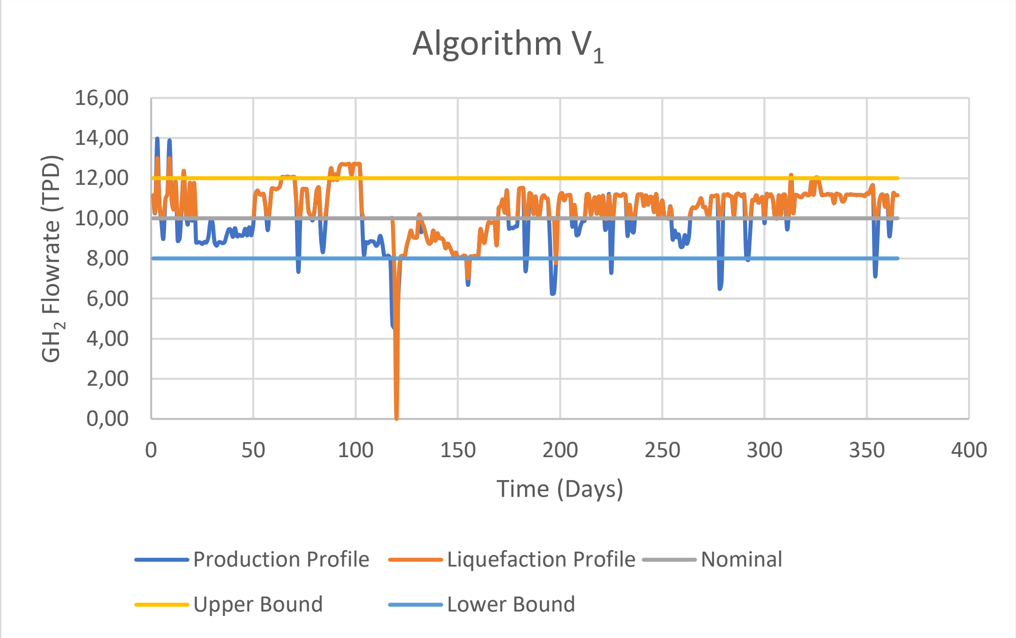

Figure 68. Algorithm V1 30% Flexibility profiles comparison

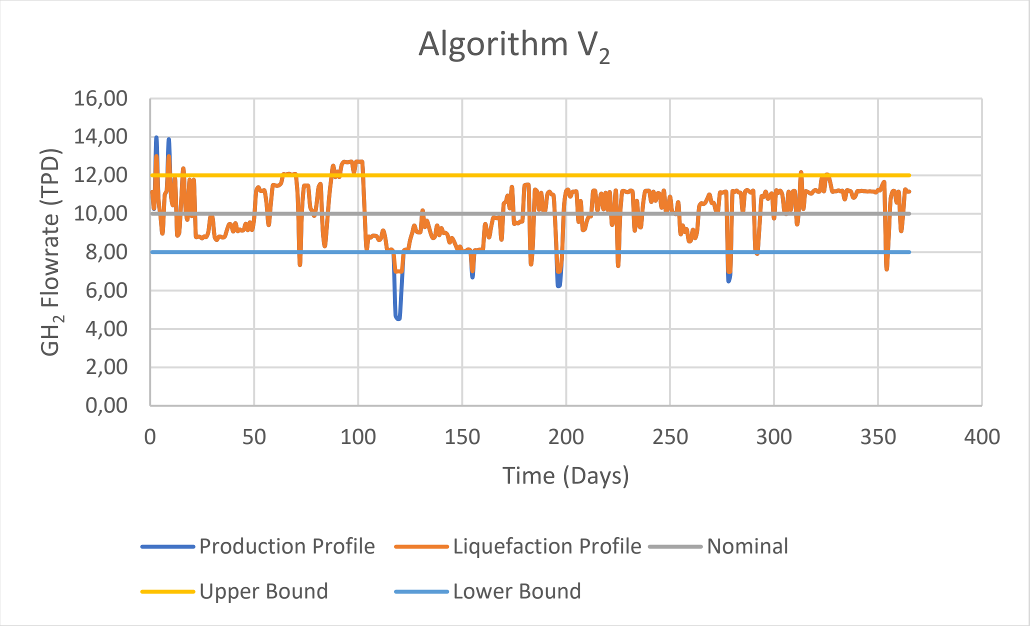

Figure 69. Algorithm V2 30% Flexibility profiles comparison

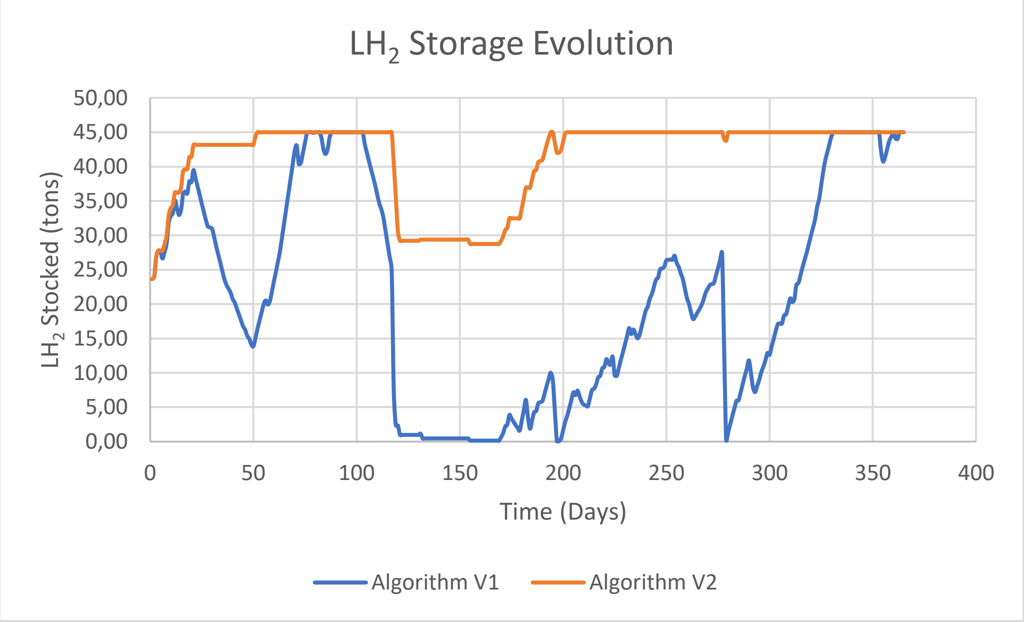

Figure 70. LH_2 storage evolution (30% allowed flexibility)

8.2.3.1.3. 20% Allowed Flexibility, re-vaporization and CGH_2 Storage

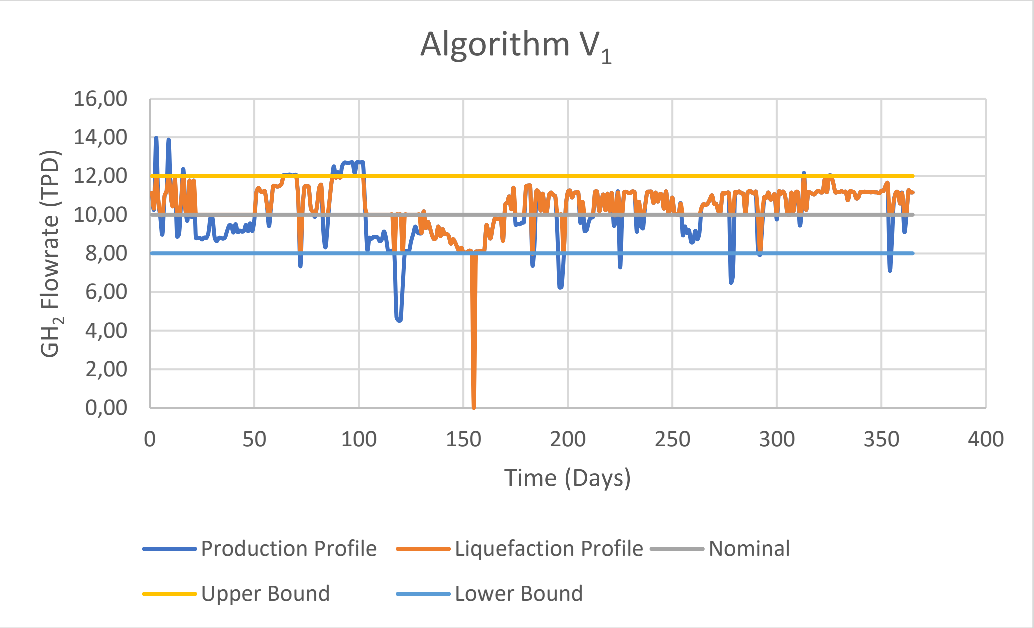

Figure 71.Algorithm V1 20% Flexibility and CGH_2 profiles comparison

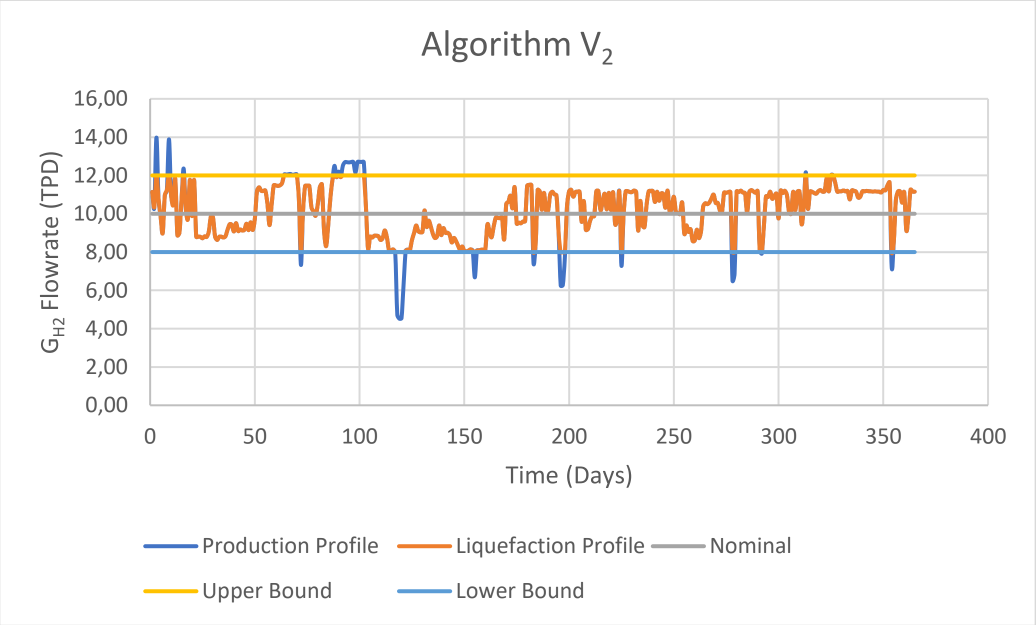

Figure 72. Algorithm V2 20% Flexibility and CGH_2 profiles comparison

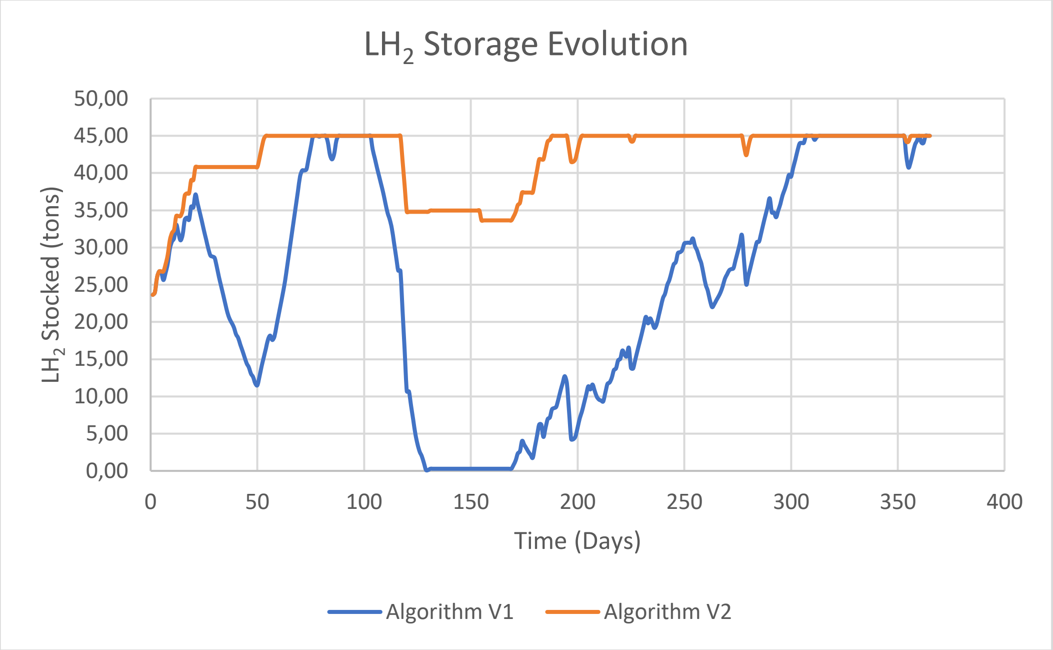

Figure 73. 20% Flexibility and CGH$_2$ storage LH$_2$ storage profile comparison

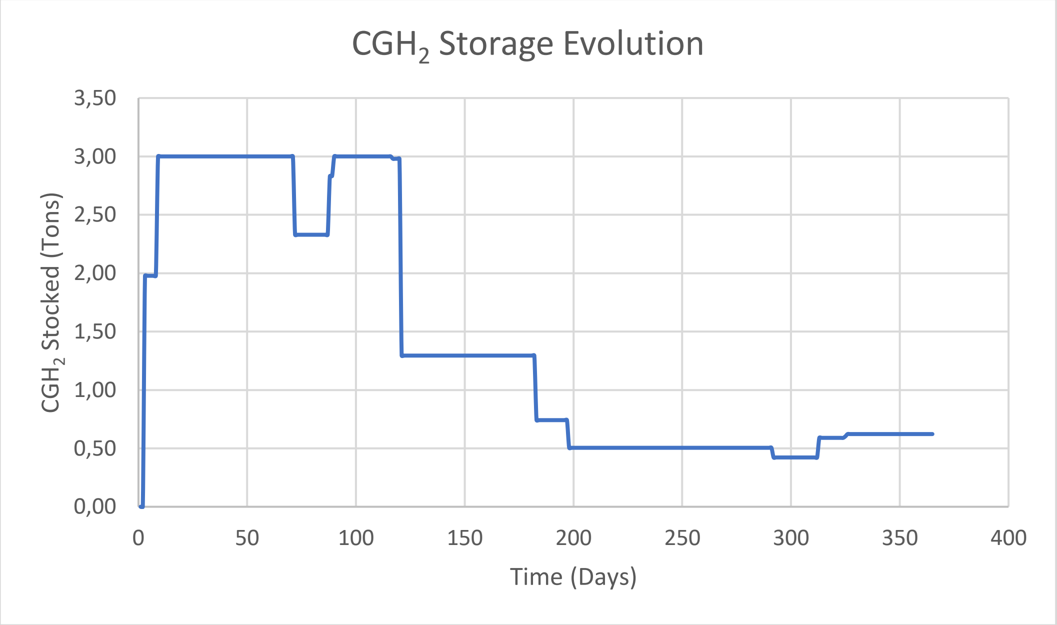

Figure 74. CGH$_2$ Storage profile

As can be observed by the obtained results, the two algorithms allow to have two different liquefaction profile and two different LH$_2$ storage evolution through the year. The main difference is represented by the fact that the second algorithm, allows to decrease to zero the number of days at which the liquefaction is not possible due to the not attaint of the lower allowed bound of liquefaction. This is possible since this solution allows to have a higher content of LH$_2$ in the liquid storage, which is almost always full and over its half value. On the other hand, if it is not possible to deliver more LH$_2$ than the planned nominal, having a full storage does not allow to store more LH$_2$ which therefore will be lost. Considering a flexible delivery allows to increase the total LH_2 produced avoiding the loss of part of it due to the impossibility to stock it in the liquid storage.

For what concerns the use of the CGH_2 storage as a temporary stockage for the GH_2 overproduction, its impact on the profile is not significant, and therefore its utilization could be avoided since the gains are not quite high to justify its implementation. This becomes clearer also considering the energetic and economic results showed in the next section.

8.2.3.2. Energetic and economic results

In the following Table 13 and are resumed the SECs and SLCs obtained for the different proposed solutions.

Table 13. Energetic and economic parameters for the simulated cases

CASE	Average ΔSEC (kWh/kg_{H2})	Average ΔSEC with flexible delivering (kWh/kg_{H2})	Average ΔSLC (€/kg_{H2})	Average ΔSLC with flexible delivery (€/kg_{H2})
20% Allowed Flexibility (2 compressors)	0.42	0.2	-0.10	-0.26
30% Allowed Flexibility (2 compressors)	0.41	0.03	0.10	-0.06
20% Allowed Flexibility (1 Compressor)	0.5	0.11	-0.90	-1.03
'20% Allowed Flexibility + 1.5 tons storage	0.54	0.36	0.21	0.11
'20% Allowed Flexibility + 3 tons storage	0.77	0.57	0.32	0.22

While the energetic consumptions of the different proposed solutions are quite similar, the SLC showed great differences, especially due to the CAPEX impact. It can be observed that the use of a single compressor (limited to +20% load) results in a much lower SLC because of the high costs of the installation of a parallel compressors train. The implementation of the CGH_2 has a quite high cost, which does not have a significant impact on the functioning of the process as showed in the previous section. The possibility of also having a flexible distribution results in a further decrease of the SLC. As for what concerns the two different algorithms used to manage the re-vaporization, the second one offer better results in terms of SLC, thanks to the overall higher content of LH_2 in the liquid storage, which allows to reduce the number of days where the minimum production is not attained. This difference is especially true when considering a flexible LH_2 delivery since the main losses in the second algorithm are due to the full LH_2 storage and therefore the impossibility to stock the LH_2 produced.

The relative comparison between the different cases using the second algorithm is presented in the following 75 and Figure 76.

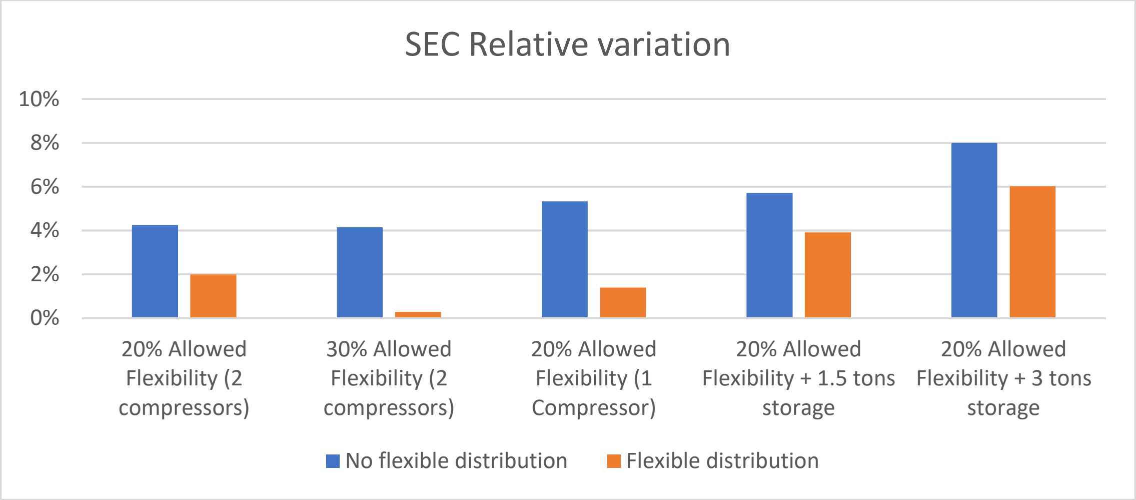

Figure 75. Relative SEC variation for different solutions

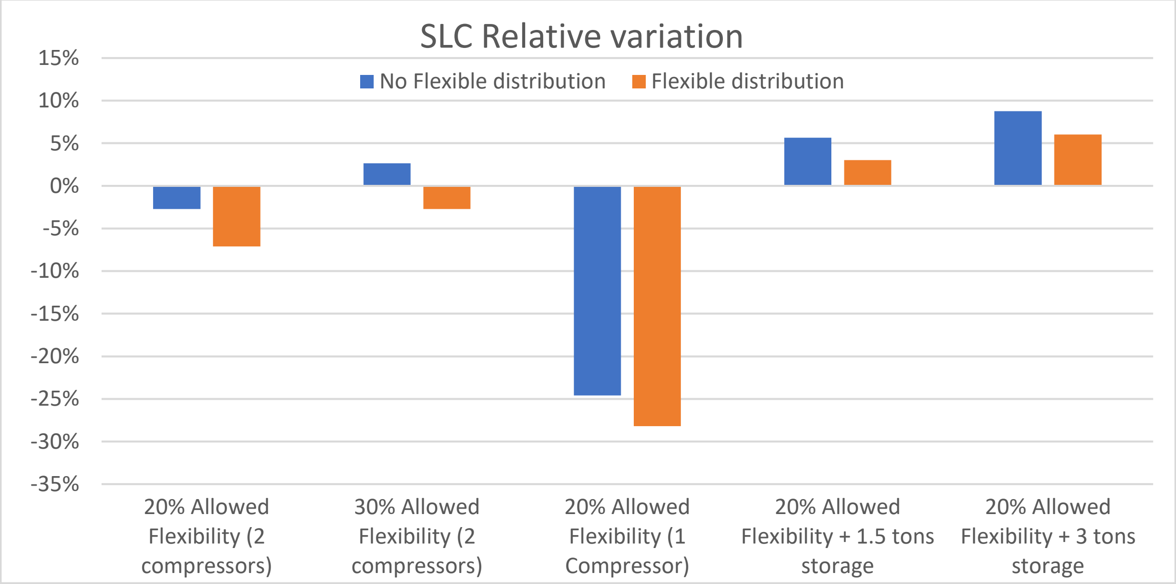

Figure 76. Relative SLC variation for different solutions

As can be observed by the presented results, the best solutions are represented using a single compressor with an allowed flexibility of 20% and with the possibility to have a flexible delivery of the LH_2 thus reducing its loss. This solution allows a decrease in the SLC if compared to the base case of around 27%. Solutions using two parallel trains of compressors allow a slight improvement of the SEC, while the use of the CGH_2 storage in this case does not allow to have a decrease in the costs, but on the contrary an increase of them. The increase related to the use of the CGH_2 storage can be observed also in the case where only one compressor is used.

Thereby, by comparing the different cases using the SLC value, it is possible to observe that, compared to the base case of a constant 10 TPD production, the costs related to the liquefaction of the overall profile are quite high. This increase is equal to 41% of the SLC, due mostly to the installation of an additional compression line which allows to process the overproduced hydrogen throughout the year. These costs can be reduced by "limiting" the maximum allowed liquefaction load and therefore having the possibility to use only one compressor with a speed variability technology that allows to increase the range of operability in the allowed liquefaction load range. In this way the cost increase related to this liquefaction profile is equal to 6.5%, which is a reasonable and acceptable increase. Nevertheless, it should be noted that no CAPEX increase has been considered for the use of variable speed compressors due to the unavailability of data, which could result in an increase of the SLC of the process. The SLC results are showed in the following 77.

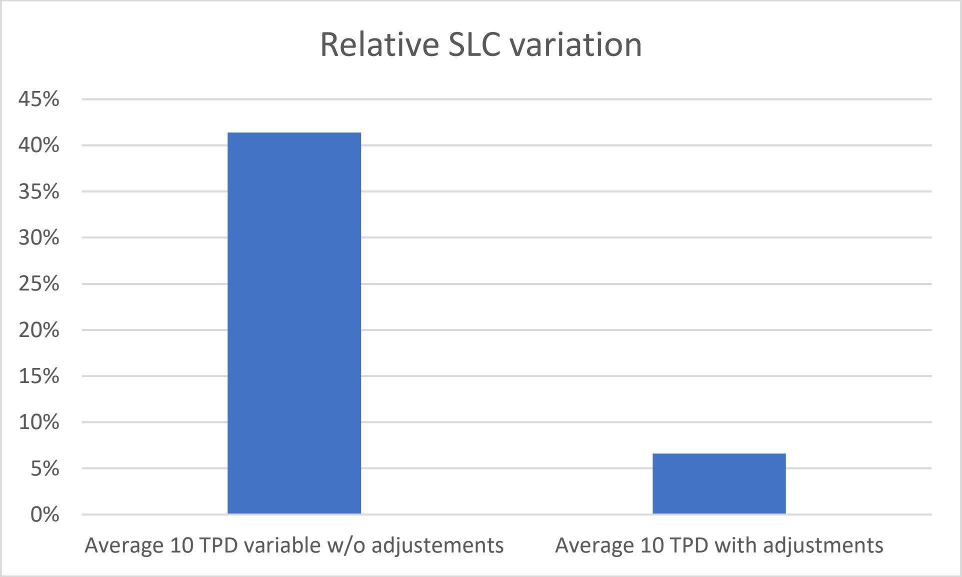

Figure 77. SLC values for the different scenarii simulated

9. Conclusion and future works

As a conclusion of the presented study, it is possible to state, from the literature, the technical feasibility of the flexibilization of the hydrogen liquefaction plant. The use of a variable speed technology in the compression system and the management of the flowrates of the streams involved in the process allowed to assure an acceptable operability of the plant over a range of loads. On an energetic and economic point of view, it has been showed by the performed simulations and the following analysis that a variability higher than +-20% of the nominal liquefaction load has a huge impact. For what concerns the part-load conditions, loads lower than 20% result in a higher deterioration of the compressors efficiency which results in an increase of the energetic costs of the plant. On the other hand, an overload condition higher than 20% of the nominal load requires an installation of an additional compression line due to the exceeding of the maximum allowed load that a single compressor can handle.
The best solution is therefore to perform a liquefaction between +-20% of the liquefaction load, using the overproduced hydrogen elsewhere and by performing a re-vaporization of the LH_2 in under-production periods to reach the minimum liquefaction load hence reducing the losses of hydrogen on the liquefaction chain.

A more detailed work is nevertheless needed to validate the obtained results. Indeed, the presented results are only numerical obtained by simulation but has not been validated due to the impossibility to perform experiences on real units. In this perspective, the study of the off-design conditions of the two major units, the heat exchanger, and the compressor, must be further explored and investigated in order to validate the simulation. Other possibilities could be studied in regard to the problematic of the H_2 liquefaction flexibility. For instance, the development of alternative liquefaction cycles which use non-mechanical compression, such as metal hydride compression (see section 3.5.3) or electrolysis compressor could open new possibilities to this work. Indeed, the mechanical compressor, with its high cost and narrow range of operability represent the main obstacle to the development of a completely flexible process.

10. Bibliographic references

[1] D. Stolten and B. Emonts, *Hydrogen Science and Engineering: Materials, Processes, Systems and Technology*. 2016, p. 1138. doi: 10.1002/9783527674268.

[2] J. Gallarda, 'Liquéfaction de l'hydrogène', p. 15, 2001.

[3] U. F. Cardella, 'Large-scale hydrogen liquefaction', p. 192.

[4] D. O. Berstad, J. H. Stang, and P. Nekså, 'Large-scale hydrogen liquefier utilising mixed-refrigerant pre-cooling', *Int. J. Hydrog. Energy*, vol. 35, no. 10, pp. 4512–4523, May 2010, doi: 10.1016/j.ijhydene.2010.02.001.

[5] A. Cornell, 'Hydrogen production by electrolysis', p. 19.

[6] 'Hydrogen: A renewable energy perspective', p. 52.

[7] D. Stolten and T. Grube, Eds., *18th World Hydrogen Energy Conference 2010 - WHEC 2010: proceedings. 3 part 2: Hydrogen production technologies Parallel sessions book*. Jülich: Forschungszentrum, IEF-3, 2010.

[8] D. Ferrero, M. Gamba, A. Lanzini, and M. Santarelli, 'Power-to-Gas Hydrogen: Techno-economic Assessment of Processes towards a Multi-purpose Energy Carrier', *Energy Procedia*, vol. 101, pp. 50–57, Nov. 2016, doi: 10.1016/j.egypro.2016.11.007.

[9] B. Zohuri, 'Hydrogen-Powered Fuel Cell and Hybrid Automobiles of the Near Future', in *Hydrogen Energy*, Cham: Springer International Publishing, 2019, pp. 37–59. doi: 10.1007/978-3-319-93461-7_2.

[10] D. Berstad, J. Stang, and P. Nekså, 'A future energy chain based on liquefied hydrogen', p. 18.

[11] M. Reuß, T. Grube, M. Robinius, P. Preuster, P. Wasserscheid, and D. Stolten, 'Seasonal storage and alternative carriers: A flexible hydrogen supply chain model', *Appl. Energy*, vol. 200, pp. 290–302, Aug. 2017, doi: 10.1016/j.apenergy.2017.05.050.

[12] M. Asadnia and M. Mehrpooya, 'Conceptual design and analysis of a novel process for hydrogen liquefaction assisted by absorption precooling system', *J. Clean. Prod.*, vol. 205, Sep. 2018, doi: 10.1016/j.jclepro.2018.09.001.

[13] C. Windmeier and R. Barron, 'Ullmann's Encyclopedia of Industrial Chemistry: Cryogenic Technology', 2013, pp. 1–71. doi: 10.1002/14356007.b03_20.pub2.

[14] 'Aasadnia et Mehrpooya - 2018 - Large-scale liquid hydrogen production methods and.pdf'.

[15] J. Eckroll, 'Concepts for Large Scale Hydrogen Liquefaction Plants', 2017.

[16] 'Cardella - Large-scale hydrogen liquefaction.pdf'.

[17] 'Sun et Ding - 2014 - Plant simulation and operation optimisation of SMR.pdf'.

[18] E. Stamatakis *et al.*, 'Metal hydride hydrogen compressors: Current developments & early markets', *Renew. Energy*, vol. 127, pp. 850–862, 2018, doi: https://doi.org/10.1016/j.renene.2018.04.073.

[19] D. Berstad, J. Stang, and P. Nekså, 'Comparison Criteria for Large-Scale Hydrogen Liquefaction Processes', *Int. J. Hydrog. Energy - INT J Hydrog. ENERG*, vol. 34, pp. 1560–1568, février 2009, doi: 10.1016/j.ijhydene.2008.11.058.

[20] S. Krasae-in, J. H. Stang, and P. Neksa, 'Simulation on a proposed large-scale liquid hydrogen plant using a multi-component refrigerant refrigeration system', *Int. J. Hydrog. Energy*, vol. 35, no. 22, pp. 12531–12544, Nov. 2010, doi: 10.1016/j.ijhydene.2010.08.062.

[21] H. Quack, 'Conceptual Design of a High Efficiency Large Capacity Hydrogen Liquefier', *AIP Conf Proc*, vol. 613, mai 2002, doi: 10.1063/1.1472029.

[22] S. Krasae-in, ‘Optimal operation of a large-scale liquid hydrogen plant utilizing mixed fluid refrigeration system’, *Int. J. Hydrog. Energy*, vol. 39, no. 13, pp. 7015–7029, Apr. 2014, doi: 10.1016/j.ijhydene.2014.02.046.

[23] C. Chen and A. Yang, ‘Power-to-methanol: The role of process flexibility in the integration of variable renewable energy into chemical production’, *Energy Convers. Manag.*, vol. 228, p. 113673, Jan. 2021, doi: 10.1016/j.enconman.2020.113673.

[24] J. Armijo and C. Philibert, ‘Flexible production of green hydrogen and ammonia from variable solar and wind energy: Case study of Chile and Argentina’, *Int. J. Hydrog. Energy*, vol. 45, no. 3, pp. 1541–1558, Jan. 2020, doi: 10.1016/j.ijhydene.2019.11.028.

[25] R. E. Swaney and I. E. Grossmann, ‘An index for operational flexibility in chemical process design. Part I’, p. 48.

[26] V. Bansal, J. D. Perkins, and E. N. Pistikopoulos, ‘Flexibility analysis and design of dynamic processes with stochastic parameters’, *Comput. Chem. Eng.*, vol. 22, pp. S817–S820, Mar. 1998, doi: 10.1016/S0098-1354(98)00156-2.

[27] K. Zirngast, ‘A Robust Decomposition Methodology for Synthesis of Flexible Processes with Many Uncertainty Parameters – Application to HEN Synthesis’, *Chem. Biochem. Eng. Q.*, vol. 32, no. 4, pp. 401–411, Jan. 2019, doi: 10.15255/CABEQ.2018.1400.

[28] C. Chen, A. Yang, and R. Bañares-Alcántara, ‘Renewable methanol production: Understanding the interplay between storage sizing, renewable mix and dispatchable energy price’, *Adv. Appl. Energy*, vol. 2, p. 100021, May 2021, doi: 10.1016/j.adapen.2021.100021.

[29] R. Nayak-Luke, R. Bañares-Alcántara, and I. Wilkinson, ‘“Green” Ammonia: Impact of Renewable Energy Intermittency on Plant Sizing and Levelized Cost of Ammonia’, *Ind. Eng. Chem. Res.*, vol. 57, no. 43, pp. 14607–14616, Oct. 2018, doi: 10.1021/acs.iecr.8b02447.

[30] S. Lusson, ‘Hydrogen liquefaction chain: Co-product hydrogen and upstream study’, p. 47.

[31] T. He, Z. Liu, Y. Ju, and A. M. Parvez, ‘A comprehensive optimization and comparison of modified single mixed refrigerant and parallel nitrogen expansion liquefaction process for small-scale mobile LNG plant’, *Energy*, vol. 167, pp. 1–12, Jan. 2019, doi: 10.1016/j.energy.2018.10.169.

[32] S. Eini, G. M. Kontogeorgis, and D. Rashtchian, ‘Cost Optimization and Flexibility Analysis for the Liquefaction of an Associated Natural Gas Stream’, *J. Energy Resour. Technol.*, vol. 142, no. 6, p. 062801, Jun. 2020, doi: 10.1115/1.4045459.

[33] H. Sun and H. Ding, ‘Plant simulation and operation optimisation of SMR plant with different adjustment methods under part-load conditions’, *Comput. Chem. Eng.*, vol. 68, pp. 107–113, Sep. 2014, doi: 10.1016/j.compchemeng.2014.05.011.

[34] J. Berg, W. Schmidt, D. F. Chen, and C. Ott, ‘DESIGNING FLEXIBLE LNG PLANTS FOR MARKET ADAPTATION’, p. 15.

[35] W. Lee, J. An, J. M. Lee, and Y. Lim, ‘Design of single mixed refrigerant natural gas liquefaction process considering load variation’, *Chem. Eng. Res. Des.*, vol. 139, pp. 89–103, Nov. 2018, doi: 10.1016/j.cherd.2018.09.017.

[36] H.-M. Chang, B. H. Kim, and B. Choi, ‘Hydrogen liquefaction process with Brayton refrigeration cycle to utilize the cold energy of LNG’, *Cryogenics*, vol. 108, p. 103093, Jun. 2020, doi: 10.1016/j.cryogenics.2020.103093.

[37] ‘Aspen HYSYS Unit Operations Reference Guide’, p. 1193.

[38] ‘Aspen HYSYS Dynamic Modeling’, p. 224.

[39] J. M. Sorokes, H. F. Miller, and J. M. Koch, ‘THE CONSEQUENCES OF COMPRESSOR OPERATION IN OVERLOAD’, p. 10, 2006.

[40] T. Q. Qureshi and S. A. Tassou, ‘Variable-speed capacity control in refrigeration systems’, *Appl. Therm. Eng.*, vol. 16, no. 2, pp. 103–113, Feb. 1996, doi: 10.1016/1359-4311(95)00051-E.

[41] S. Jain and C. W. Bullard, ‘Capacity and Efficiency in Variable Speed, Vapor Injection and Multi-Compressor Systems’, p. 51.

[42] J. J. J. Brasz, ‘Comparison of Part-Load Efficiency Characteristics of Screw and Centrifugal Compressors’, p. 8, 2006.

[43] Z. Wang, Z. Wang, J. Wang, W. Jiang, and Q. Feng, ‘Research of thermal dynamic characteristics for variable load single screw refrigeration compressor with different capacity control mechanism’, *Appl. Therm. Eng.*, vol. 110, pp. 1172–1182, Jan. 2017, doi: 10.1016/j.applthermaleng.2016.08.189.